PATH PLANNING MODELS FOR MOBILE ANCHOR-ASSISTED LOCALIZATION IN WIRELESS SENSOR NETWORKS

by

Abdullah Alomari

Submitted in partial fulfillment of the requirements
for the degree of Doctor of Philosophy

at

Dalhousie University
Halifax, Nova Scotia
February 2018

إلى والديّ الحبيبين ..

أهديكما نتاج جهدكما .. لا جهدي ،،

To my beloved parents,

I dedicate the harvest of what you planted.

Table of Contents

List of Tables

List of Figures

Abstract

As event detection is one of the main purposes of using wireless sensor networks (WSNs), the location of nodes is essential to determine the location of an event when it occurs. Many localization models have been proposed in the literature, one of which is to deploy a set of static location-aware nodes, called anchors, to exchange information with the other nodes to determine their location. Another promising proposal involves replacing these sets of static anchors with only one mobile anchor (MA). While this method seems to produce favorable results, it also brings new challenges. The primary challenge is to find an optimal path for the mobile anchor to follow while taking into account the need to provide highly accurate data and more localizable nodes in less time and with less energy. This thesis proposes techniques for mobility-assisted localization in WSNs. In this research work, four main contributions are achieved in the design of such models.

Firstly, we introduce a new static path planning model for mobile anchor-assisted localization in WSNs. Our proposed model guarantees that, when the resolution is equal or greater than one, all nodes can receive the localization information and thus estimate their location with higher localization accuracy in comparison to similar static models. Moreover, this model overcomes the problem of collinearity and considers the metrics of precision and energy consumption as well as accuracy, localization ratio and the path length of the mobile anchor.

Secondly, although some path planning models in two-dimensional (2D) regions have been proposed in recent years, many WSNs' practical applications are applied in three-dimensional (3D) regions. We also introduce a three-dimensional path planning model for mobile anchor-assisted localization in WSNs. Our proposed model offers higher performance regarding localization accuracy with a lower error rate in comparison to other proposed models.

Thirdly, we propose a novel distributed range-free movement mechanism for mobility-assisted localization in WSNs when the mobile anchor's movement is limited. The designed movement is formed in a real-time pattern using a fuzzy-logic approach based on the information received from the network and the nodes' deployment. The novelty of this model lies in employing multiple individual inputs in a fuzzy-logic approach for path planning that are important to minimizing the localization error and maximizing the localization ratio. Our proposed model offers superior results in several metrics including both localization accuracy and localization ratio in comparison to other similar works.

Finally, we design two novel dynamic movement techniques that offer obstacle avoidance path planning for mobility-assisted localization in WSNs. The movement planning is designed in real-time using two swarm intelligence-based algorithms: the Grey Wolf Optimizer (GWO) and Whale Optimization Algorithm (WOA). The novelty of our proposed models is the use of optimization algorithms to direct the path formation of the MA, which helps to maximize the localization ratio and minimize the localization error. Both of our proposed models provide better outcomes in comparison to other existing works in several metrics including both localization ratio and localization error rate.

List of Abbreviations Used

AoA	Angle of Arrival
APIT	Approximate Point in Triangle
BRF	Breadth-First
BS	Base Station
BTG	Backtracking Greedy
CH	Cluster Head
DFT	Depth-First Traversal
DPMB	Dynamic Path of Mobile Beacon algorithm
DREAMS	Deterministic Dynamic Beacon Mobility Scheduling
DV-Hop	Distance-Vector Hop
FIS	Fuzzy Logic Inference System
FL	Fuzzy Logic
FLC	Fuzzy Logic Controller
FLCFP	Fuzzy Logic Cluster Formation Protocol
FLPPL	Fuzzy-Logic based Path Planning for mobile anchor-assisted Localization
GM	Gauss-Markov Model
GPS	Global Positioning System
GWO	Grey Wolf Optimizer
GWPP	Grey Wolf optimizer based obstacle-avoidance Path Planning
HiRLoc	High-Resolution Robust Localization
IoT	Internet of Things
LCB	Localizable Collaborative Body
LMAT	Localization algorithm with a Mobile Anchor node based on Trilateration
LMST	ocal Minimum Spanning Tree
MA	Mobile Anchor
MAALRH	Mobile Anchor-Assisted Localization algorithm based on a Regular Hexagon
NLA_MB	Node Localization Algorithm with Mobile Beacon node

PIT	Point In Triangle
PNT	Positioning, Navigation, and Timing System
PSO	Particle Swarm Optimization
QN	Quantity of Neighbors
RD	Random Direct
RN	Reference Node
RSSI	Received Signal Strength Indicator
RWP	Random WayPoint
TDoA	Time Difference of Arrival
ToA	Time of Arrival
WCL	Weighted Centroid Localization algorithm
WCWCL	Weight-Compensated Weighted Centroid Localization
WSN	Wireless Sensor Network
WOA	Whale Optimization Algorithm
WOPP	Whale Optimization algorithm based obstacle-avoidance Path Planning
UAV	Unmanned Aerial Vehicle
UN	Unknown Node

List of Symbols Used

α	Standard deviation
$\vec{a}$	Linearly decreased value from 2 to 0 over the iterations course in GWO and WOA
$\vec{A}$	Coefficient vector used in GWO and WOA
b	Constant value that defines the logarithmic spiral in WOA
β	Path loss exponent
$\vec{C}$	Coefficient vector used in GWO and WOA
c	Signal propagation speed
CI	Confidence interval
$\vec{D}'$	Distance of the ith whale to the prey in WOA
$\vec{D}_{\alpha}$	Updated distance vectors between the position of α wolf and the other wolves
$\vec{D}_{\beta}$	Updated distance vectors between the position of β wolf and the other wolves
$\vec{D}_{\delta}$	Updated distance vectors between the position of δ wolf and the other wolves
$d0$	Reference point
d_{ij}	Euclidean distance between two given nodes i and j
d_{max}	Maximum movement distance
$error_{avg}$	Average localization error
$error_{(i)}$	Localization error for a localized node i
$error_{std}$	Standard deviation of the localization error
hop_{ij}	Number of hops between two nodes i and j
I_{max}	Maximum number of iterations
l	Random number in the range [-1, 1] in WOA
L_{avg}	Localization ratio
M	Number of mobile anchors
N	Number of unknown nodes
N_{α}	Zero-mean Gaussian random variable
O	Number of obstacles
O_{size}	Obstacles dimensions

p	Random value in [0, 1] used in WOA
$PL(d0)$	Power loss at d_0
$\vec{r}_{1,2}$	Vectors chosen randomly in the range of [0, 1] in GWO and WOA
R	Resolutions
RN	Total number of reference nodes
R_{Tx}	Communication range
S	Network size
t_{ij}	Estimated time for a signal traveling from a node i to another node j
w_{ij}	Weight function of two nodes i and j
$\vec{X}$	TPosition vector of a grey wolf in GWO
$\vec{X}^*$	Best solution of position vector in WOA
X_α	Best search agent in GWO
X_β	Second best search agent in GWO
X_δ	Third best search agent in GWO
X_i	Number of movement steps
$\vec{X}_P$	Position vector of the prey in WOA
$\vec{X}_{rand}$	Random value representing a random position vector (a random whale) in WOA
σ	Standard deviation of noise

Acknowledgements

O, Allah! Yours is the Hamd that is suitable for the grace of Your Face and the greatness of Your Supreme Authority.

I would like to express my sincere gratitude to my supervisors, Dr. William Phillips and Dr. Nauman Aslam, for their help, support, guidance, valuable advice, and friendship. I also wish to extend my appreciation to Dr. Frank Comeau, who has been working with us since the beginning of my PhD program. Without their inspirational guidance, encouragement, and selfless help, I would have never reached this achievement.

My special thanks go to the committee members, Dr. Srinivas Sampalli and Dr. Thomas Kunz, for agreeing to be a part of the examining committee and taking the time to read my thesis.

Despite being separated by oceans and continents, my beloved parents have always inspired me through their courage, strength, and love. I would like to thank them for helping me to realize my potential. The support they have provided me over the years has been the greatest gift I could ever have asked for. I would like to give my heartfelt acknowledgment and dedicate the achievement of this study to them for their prayer, wisdom, love, and care.

I am deeply grateful to my wife, Fatimah, for every single moment of her love, care, patience, and unfailing faith in me. Her tolerance of my occasional difficult moods is a testament to her unyielding devotion and love.

God's gift, my children, Ahmad, Mohammed, and Saud, have been my source of inspiration during this work. They have made our life in Canada enjoyable and rewarding. Ahmad, Mohammed, and Saud are the pride and joy of our lives. I am very thankful to Allah for having them.

I have no words to express my gratitude to my wonderful siblings, Halimah, Yousef, Manal, Ahmed, Wafa, and Layla. I will be in debt for the rest of my life to them for their unlimited support and love. I will love and appreciate you forever. I pray to God to save, protect, and bless all of you.

My wholehearted love to my nieces and nephews; Hassan, Yousef, Elaf, Ghala, Khalid, Wafa, Jenan, Mary, Sara, Shahad, Mohammed, Yousef, Wa'ad, Abdullah, Hesan, Ayman, Sema, Abdulaziz, Albara, Ward, Sana, Kadi, Ghina, Yasmine and our new guest, the 3-weeks-old Hanay. Happy for having all of you.

My thanks also go to many people around me including my aunts and uncles, my cousins, my brothers-in-law and many of friends. Finally, I would like to acknowledge the generous financial support and scholarship provided by the Ministry of Education and Albaha University in Saudi Arabia.

Chapter 1

Introduction

1.1 Motivation and Background

Over the last few years, wireless sensor networks (WSNs) have been introduced as a new and simple technology for data gathering in many different physical environments [1]. A WSN typically consists of a large set of small nodes deployed in an area of interest to collect, store, and forward data and deliver it where it is needed. These nodes are usually low-cost, low-power, limited in terms of memory, and programmable [1, 2]. WSNs' simple components and sizes allow them to be implemented for many purposes in health, security, the military, and in tracking and monitoring applications [3]. In many applications of WSNs, the location of the sensor node (i.e., the location of the gathered data) is highly important. A useful example is the location of the fire source or the exact position of pollution in some underwater applications.

Node deployment in WSNs is typically done in an arbitrary form, where these nodes are distributed randomly, especially when many nodes are used or a wide area is being monitored. Several approaches to providing nodes with information on their location have been proposed. A straightforward approach is to provide each node with a global positioning system (GPS) device. However, such a solution is impractical for many reasons including the cost of the devices, the limited energy of each node and the small size of the nodes [4, 5]. Another solution is to inform certain nodes of their locations and let those location-aware nodes, called anchors or beacons, help the rest of the nodes in determining their locations. These anchor nodes can be either static nodes such as those in [6–8], or mobile nodes such as in [9–11]. MAs have shown a better performance in terms of cost, coverage,

and accuracy [4]. In this method, the many static anchors in the network are replaced with a smaller number of MAs (one in many studies). The MA traverses the network to inform the nodes that are not location-aware, called unknown nodes (UNs), of their current location. Based on the planned path and the ability to receive the MA's signals, some UNs can estimate their location. However, adopting mobility comes with many challenges such as finding the way with minimum distance, the impact of the path on both the accuracy and rate of localization, energy efficiency issues and others.

Optimizing the traveling path of a mobile element is an active area of research in other fields including unmanned aerial vehicles (UAVs) such as those in [12–14], robotics as in [15, 16], and data collection as in [17, 18]. In such areas, the mobile element begins its journey from a starting point (a) and aims to reach an ending point (b) while traversing the shortest possible distance. There may be some obstacles in the area that the mobile element has to avoid. However, the objective of localization in WSNs is different from those in UAVs, robotics, or data collection. The aim is to make the mobility path as short and efficient as possible by having as many localized nodes as possible with the highest possible localization accuracy. Accuracy is represented through the localization error rate; the lower the error rate is, the higher the accuracy.

In mobility-assisted localization models, research mainly concentrates on exploring two fundamental areas: proposing a sufficient static localization algorithm and designing an efficient path model for the MA. The primary issue in developing path models is designing a traversing path that guarantees that a significant number of the UNs can receive the localization information with a high accuracy and low energy consumption and time. The path strategy should be as short as possible while also being comprehensive in order to reach all the UNs inside the monitored area.

1.2 Contributions

This thesis aims to contribute to this area of research by proposing new path planning models for mobile anchor-assisted localization in WSNs following four different network scenarios and assumptions. A number of contributions in mobility-assisted localization in WSNs are proposed. These contributions are summarized as follows:

1. In the first scenario, a two-dimensional flat network is assumed with no obstacles, and the MA can traverse the network without any constraints. The research proposes a path planning model that ensures that all of the UNs in the network can receive the localization information. All the UNs will be able to estimate their current locations if they receive this data. The proposed path model is designed to increase the localization accuracy and ratio of the successfully localized nodes. Moreover, we suggested considering the precision metric in designing the path. To the best of our knowledge, we are the first to consider the precision metric in mobility-assisted localization in WSNs. We also noted that most of the current works do not take into account wireless channel specifications; thus, realistic wireless specifications are used in evaluating the different models in this work.

2. In the second scenario, similar assumptions are considered with a three-dimensional flat network. A new path planning model for mobile anchor-assisted localization in WSNs is designed where nodes deployment occurs in 3D areas. The results show that the proposed model offers a lower localization error in comparison to other existing models.

3. The third scenario is assumed to exist when the maximum movement distance of the MA is limited, where a dynamic path planning model is needed to deal with such conditions. We present a dynamic fuzzy-logic-based path planning model for mobility-assisted localization that applies various criteria for the movement decision to form the path of the MA. The novelty of this

model lies in the employment of multiple individual inputs in a fuzzy-logic approach for path planning that are important to minimizing the localization error and maximizing the localization ratio. By using a fuzzy-logic approach, an improved movement path will be designed to achieve the objectives of the process while taking into account the limited movement of the MA. To the best of our knowledge, we are the first to use a fuzzy-logic-based model in path planning for localization in WSNs. The proposed model offers superior results in many metrics in comparison to existing models.

4. Finally, a more constrained environment is assumed where the network area has a set of obstacles, and the MA has a limited movement distance. The task for the MA is not only to take into account the limitation of the movement but also to avoid the obstacles in its way in a real-time dynamic fashion. For this scenario, we introduce two novel dynamic meta-heuristic optimization techniques for mobility-assisted localization in WSNs. The suggested path planning models are based on two new optimization algorithms: the Grey Wolf Optimizer (GWO) [19] and the Whale Optimization Algorithm (WOA) [20]. The proposed models are respectively called Grey Wolf optimizer-based obstacle-avoidance Path Planning (GWPP) and Whale Optimization algorithm-based obstacle-avoidance Path Planning (WOPP). The novelty of our proposed models lies in employing optimization algorithms to direct the path formation of the MA, which helps maximize the localization ratio and minimize the localization error. By using the optimization algorithms, the MA movement is formed in real-time; it also avoids the obstacles, takes into account the maximum distance constraint, and simultaneously achieves the objectives of the entire localization process. To the best of our knowledge, we are the first to use swarm-based optimization techniques assuming such scenarios in path planning for localization in WSNs. The proposed models provide outstanding results in several metrics in comparison to existing works.

Table 1.1 below summarizes the different scenarios of the four thesis contributions.

Table 1.1: An overview of the mobility-assisted movement models proposed in this thesis

#	Model	Movement type	Area	Movement constraints	Obstacles	Decision base
1	[9]	Static	2-D	No	No	Trilateration
2	[10]	Static	3-D	No	No	Quadlateration
3	[21]	Dynamic	2-D	Yes	No	Fuzzy-logic system
4	[22]	Dynamic	2-D	Yes	Yes	SI optimization

As a result, parts of this thesis have been published in the following publications:

[J-3] **A. Alomari**, W. Phillips, N. Aslam, & F. Comeau, "Swarm Intelligence Optimization Techniques for Obstacle-Avoidance Mobility-Assisted Localization in Wireless Sensor Networks," *IEEE Access*, 2017. [Online]. Available: https://doi.org/10.1109/ACCESS.2017.2787140

[J-2] **A. Alomari**, W. Phillips, N. Aslam, & F. Comeau, "Dynamic Fuzzy-Logic Based Path Planning for Mobility-Assisted Localization in Wireless Sensor Networks," *Sensors*, vol. 17, no. 8, 2017

[J-1] **A. Alomari**, F. Comeau, W. Phillips, & N. Aslam, "New Path Planning Model for Mobile Anchor Assisted Localization in Wireless Sensor Networks," *Wireless Networks*, pp. 1-19, 2017. [Online]. Available: https://doi.org/10.1007/s11276-017-1493-2

[C-3] **A. Alomari**, N. Aslam, W. Phillips, & F. Comeau, "Three-Dimensional Path Planning Model for Mobile Anchor-Assisted Localization in Wireless Sensor Networks," in *2017 IEEE 30th Canadian Conference on Electrical and Computer Engineering (CCECE)*, April 2017, pp. 1-5.

[C-2] **A. Alomari**, N. Aslam, W. Phillips, & F. Comeau, "Using DV-Hop Technique to Increase Localization Ratio in Static Path Planning Models in Wireless Sensor Network," in *2016 10th International Symposium on Communication Systems, Networks and Digital Signal Processing (CSNDSP)*, July 2016, pp. 1–6..

[C-1] **A. Alomari**, N. Aslam, W. Phillips, & F. Comeau, "A Scheme for Using Closest Rendezvous Points and Mobile Elements for Data Gathering in Wireless Sensor Networks," in *IFIP Wireless Days (WD)* , November 2014, pp. 1-6

1.3 Thesis Outline

This thesis consists of seven chapters, organized as follows:

- **Chapter 2:** discusses some of the applications of WSNs along with their current challenges and investigates in detail some of the localization approaches and techniques described in the literature. Then, a survey of the usage of mobility in localization in WSNs, and the different mobility path models and their concepts are presented.

- **Chapter 3:** introduces a new static path planning model for mobile anchor-assisted localization in WSNs. The proposed model guarantees that, when the relationship between the transmission range and the distance between every two points is equal or greater than one, all nodes can receive the localization information and thus estimate their location with higher localization accuracy in comparison to similar static models. Moreover, this model overcomes the problem of collinearity and takes into account the metrics of precision and energy consumption as well as accuracy, localization ratio and the path length of the MA.

- **Chapter 4:** presents a three-dimensional path planning model for mobile

anchor-assisted localization in WSNs. Our proposed model offers higher performance in terms of localization accuracy with a lower error rate in comparison to other proposed models.

- **Chapter 5:** presents Fuzzy-Logic-based Path Planning for mobile anchor-assisted Localization (FLPPL). FLPPL is a novel distributed range-free movement mechanism for mobility-assisted localization in WSNs when the MA's movement is limited. The designed movement is formed in a real-time pattern using a fuzzy-logic approach based on the information received from the network and the nodes' deployment.

- **Chapter 6:** introduces the Grey Wolf optimizer-based Path Planning model (GWPP) and Whale Optimization algorithm-based Path Planning model (WOPP). GWPP and WOPP are two novel dynamic movement techniques that offer obstacle-avoidance path planning for mobility-assisted localization in WSNs when the MA's maximum movement distance is constrained. The movement planning is designed in a real-time fashion using two swarm intelligence-based algorithms. The optimized movement decision achieves superior outcomes in comparison to other existing works in several metrics including both localization ratio and localization error rate.

- **Chapter 7:** summarizes the main topics of this thesis and discusses potential future work.

Chapter 2

Literature Review and Background

This chapter provides an overview of WSNs and their applications. Some present challenges are also discussed. There is a discussion of a literature survey consisting of two parts: the first part explains localization approaches and algorithms, and the second part explains path planning models and their classifications.

2.1 Wireless Sensor Networks (WSNs)

Recent advances in wireless technologies have helped to popularize the use of WSNs in many applications. A typical WSN consists of a large number of sensor nodes that are densely deployed around an area of interest to sense, monitor, and measure specific events via wireless communication [23]. A simple WSN node is formed of a microprocessor, a radio chip, and a power source. The characteristics of these nodes differ based on the demands and applications. Ordinarily, the nodes are low-cost, require little power, are limited in terms of memory, and are programmable [24]. The sensor nodes can exchange their data through a single or multi-hop approach to deliver it to a gateway or base station (BS) for further processing. The role of the BS is to gather the sensed data into a database. The BS communicates with the sensor nodes in the network and may provide a gateway connection to other networks. It can be connected to the Internet, which allows remote systems and third parties to monitor the required collected data. Thus, the BS's database can be accessed through the Internet or locally using the BS itself [23]. WSNs typically are controlled by single or multiple protocols that are operated to accommodate the features and specifications of the network including

their nodes' deployment, network environment, self-configuration, energy consumption and fault tolerance [3,23,25]. Knowing the location of the collected data is mandatory in many applications to take further action. For example, tracking applications are highly dependent on the location of the nodes, making it difficult to work without knowing the location of each entity [4]. In conventional WSNs' localization techniques, a set of static location-aware nodes, (called anchors, beacons, etc.), are distributed around the network. Their task is to provide their location to the location-unaware sensor nodes, the UNs, in their transmission range and to assist them in computing and estimating their location according to the individually designed algorithm [3,4]. The more extensive the network, the more anchors are needed; however, using these fixed anchors brings many challenges in cost, energy, and accuracy. Instead, a promising method to localize UNs is to use an MA equipped with a Global Positioning System (GPS) device moving among UNs and periodically broadcasting its current location (anchor point) to help nearby UNs with localization. This approach can be useful in terms cost and energy consumption [4]. We will first present some of the sensor network applications in the following section, then discuss the current sensor network challenges in Section 2.1.2.

2.1.1 Sensor Network Applications Types

Many WSN applications share some general characteristics. There is a clear distinction between the source of data represented by the sensor nodes and the sinks represented by the BS to which data will be delivered; however, there is a need to include both of them in most WSN applications [3]. Here, we list a set of types of applications that are used in WSNs.

A. Event detection

Once a specified event has occurred, the sensor node that detects the event should report directly or indirectly to the BS. The monitored events can be detected using a single node (for example, detecting a temperature change),

or the collaboration of multiple nodes located in a specific area (for example, detecting the spread of a fire). In cases where different event types exist, there might be a need for event classification. Examples of this type of application are forest fire or flood detection in environmental applications, and battlefield surveillance in security and military applications [3, 23, 25].

B. Periodic measurements

In some applications, sensor nodes are assumed to measure a physical phenomenon and report its measured values periodically. Examples of this type of application include remote monitoring of physiological data in health applications, traffic flow surveillance in some commercial applications, reporting weather status during the day and measuring the level of gas in some environmental applications [3, 23, 25].

C. Tracking

When the source of the event is mobile, the WSN is used to collect and update data regarding that source. The WSN can also provide an estimate of its location, speed, and movement direction. In such applications, sensor nodes collaborate to exchange the required data and report it to where it is needed. Examples of tracking applications in WSNs include but are not limited to tracking and monitoring doctors and patients inside a hospital in healthcare and medical applications, vehicle tracking and detection in commercial applications and habitat tracking in environmental applications [3, 23, 25].

D. Mapping and edge detection

WSNs can be used to draw a map of the spread of specific circumstances. For example, the spread and the perimeter of a forest fire can be mapped using data gathered from a WSN to help firefighters locate the source of the fire.

E. Other applications

Some applications of WSNs can be classified under one or more type based on the requirement of the sensed data. These applications include military, environment monitoring, habitat Monitoring, health, commercial and home applications.

2.1.2 Sensor Network Challenges

Although there is wide diversity in WSNs' applications, each WSN requires specific attention regarding deployment options, maintenance options, and the options for the energy supply source [3]. For example, the deployment process can be done randomly using an aircraft to drop a large number of sensor nodes into a particular area, or can be well-planned and use fixed deployment in some small areas of interest. The energy supply issue is important to consider, especially in applications where sensor nodes have to be in transmission mode for a long time. Other notable design factors that arise in the application of WSNs include the type of service, quality of service, fault tolerance, network lifetime, and scalability.

2.2 Survey of Localization Algorithms

Localization in WSNs has become an active area of research, resulting in the development of several models and algorithms in the last few years [4]. Localization is defined as the process of finding the positions of the WSN nodes in respect to some absolute or relative reference [3, 4, 9, 23]. In many WSN applications, the location where data has been gathered is important for locating the monitored events of interest and reacting accordingly [26]. For example, in the case of a wildfire, knowing the location of the fire source and the area to which the fire has spread is critical for firefighters to start planning their response [1, 3]. Localization is also critically important in other applications such as target tracking and monitoring disaster areas [1, 27]. The node can be localized using a physical position represented through a numeric coordinate system, or symbolic position such as "computer lab" or "building A" or both systems "Store A located in x,y coordinates." For example, if a sensor

node is located at the point (44.637369, -63.591231) of the Earth's latitude and longitude coordinates as an absolute reference, it can also be represented by "located in the Killam Library at Dalhousie University" as a relative reference. In [3,4,25], a number of node localization advantages are identified, including:

1. The requirement of the location in some applications, such as those for tracking, is mandatory to have readable and valid data.
2. Many location-based routing protocols need the location of the nodes to run their operations.
3. Knowledge of the node location is helpful to enhance network security.
4. Knowledge of the node location can improve network monitoring and management.
5. Knowing location information is necessary when sensor nodes are mobile.

Since WSN is considered as one of the primary components of IoT, they both share the same problems. Localization in IoT is important similar to WSN. Since the action in IoT networks, such as fire alarm, energy transfer, emergency request, is performed originally on the data center, a way to identify the location information of entire nodes at the data center is of significance [28]. One of the potential applications of our models is the target tracking. Target tracking is one of the significant purposes of WSN in which sensor nodes monitor and report the locations of moving objects to the end user. Indeed, target tracking has many practical applications such as battlefield surveillance, detection of illegal borders crossing, gas leakage, fire spread, and wildlife monitoring [29].

A. Global Positioning System (GPS)

The Global Positioning System (GPS) is a global navigation satellite system owned by the U.S. government that provides users with positioning, navigation, and timing (PNT) services [30]. The GPS system consists of 24-31

satellites that orbit the Earth. Only four of these satellites are required to obtain location information; three are needed to determine a position and one to resolve local clock uncertainty and synchronization [31]. Each satellite receiver continually transmits data about its current position, time and other vital statistics. Based on lateration and other statistical concepts, the receivers on the ground can estimate their own location. Due to its easy installation and precise localization estimation, GPS is considered an easy approach for node localization; however, this solution is also impractical for many reasons including:

1. GPS devices require a line-of-sight communication with multiple satellites, which means it is difficult to use them in certain deployment environments. Examples of these environments include indoor applications, underground, underwater, urban areas between buildings, forests, mountains and others [23, 31].
2. Although GPS devices are available on the market, they are still relatively expensive. The cost of the network will increase if a GPS device is attached to every single node.
3. Sensor nodes are energy-constrained. Attaching a GPS to each sensor limits the energy source which will lead to a network failure.

Similar to GPS, there are also global navigation satellite systems: GLONASS, which is owned by the Russian government; Galileo, which is owned by the European Union; and BeiDou, which is owned by China.

2.2.1 Localization Categorization and Models

In general, localization models differ based on their objectives in several ways such as localization method, localization processing, deployment area, application area, or anchor type [21]. Figure 2.1 summarizes the objectives of the localization models. Some of these classifications will be discussed in the next several sections.

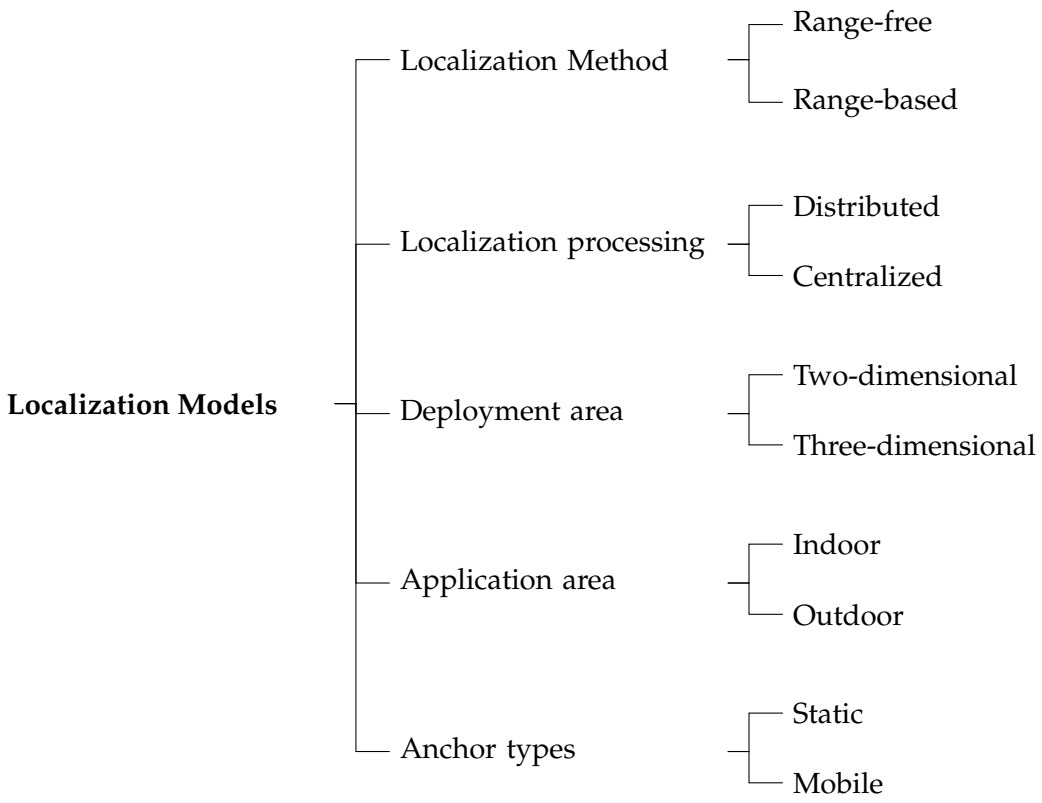

Figure 2.1: Classification of localization models in WSNs based on their objectives

A. Localization method (Range-Based vs. Range-Free)

Generally, the classification of localization methods in WSNs consists of two categories: range-based models and range-free models [27]. Range-based techniques estimate the nodes' locations by taking advantage of the angle or the distance of their communication connection. Examples of such information include Received Signal Strength Indicator (RSSI), Time of Arrival (TOA), Time Difference of Arrival (TDoA), and Angle of Arrival (AoA) [32, 33]. On the other hand, range-free techniques depend only on the connection between the nodes and some location-aware nodes, the anchors [1,26,27]. By exchanging location information and making calculations, the UN can estimate its own location [32].

B. Localization Processing (Centralized vs. Distributed)

In the distributed algorithms, the UN localizes itself by exchanging messages with its neighbors located within its communication range in a single-hop, or even through multi-hop communication. In the centralized algorithm, the localization estimation will be treated at the BS after data is exchanged between nodes [4].

C. Deployment Area (Two-Dimensional vs. Three-Dimensional)

A large number of studies on localization in WSNs have been proposed, but these studies focus on two-dimensional (2D) areas. In most real-world applications, sensor nodes are deployed on planar surfaces where three-dimensional (3D) areas are found [34, 35]. Examples of these surfaces include indoor applications, such as floors, walls, tables and doors, and outdoor applications such as mountains, valleys, hills, and forests [34, 35].

D. Application Area (Indoor vs. Outdoor)

In indoor environments, physical obstructions like walls can decrease the localization measurements and accuracy. Such obstacles can exist in outdoor environments as well; therefore, careful consideration should be given to the application area when applying a localization method.

E. Anchor and Node Type (Static vs. Mobile)

Localization models using anchor nodes are classified under one of the following types: (static nodes and static anchors), (mobile nodes and static anchors), (static nodes and mobile anchors) and (mobile nodes and mobile anchors) [9, 36].

2.2.2 Evaluation Criteria

As the primary work on mobility-assisted localization focuses on designing a path planning model to assist UNs in their localization process, the results are measured in both path planning and localization metrics. While localization accuracy and

ratio seem to be the most important metrics, other metrics are chosen based on their significance to improve the overall framework. A number of them has been already discussed in some similar works such as these in [5, 11, 36–38]. Here are the main metrics that are evaluated:

A. Localization Accuracy

In path planning for mobility-assisted localization in WSNs, localization accuracy is one of the most important performance metrics. Higher accuracy gives more confidence about the localization estimation of one model over another; hence, it is considered the main factor in many works in this research field. Accuracy is computed using the localization error. The lower the estimation of error, the higher the localization accuracy.

i. Average Localization Error

The average localization error is indicated as the calculated distance between the real location and the estimated location of the localized node. It is used to determine the degree to which the localization estimation is accurate. The node localization error is formulated as

$$error_{(i)} = \sqrt{(x_i - u_i)^2 + (y_i - v_i)^2} \tag{2.1}$$

where (x_i, y_i) are the true coordinates of the node i, and (u_i, v_i) are the estimated coordinates of the same node i. Therefore, the average localization error, $error_{avg}$, is calculated as:

$$error_{avg} = \Big(\sum_{i=1}^{N} error_{(i)} \Big) / RN \tag{2.2}$$

where RN is the total number of localized sensor nodes (reference nodes).

ii. Standard Deviation of the Localization Error

A low standard deviation in localization error is desired, since it means a high percentage of error values are close to the mean of all errors. The

standard deviation of the localization error for the entire population is calculated as

$$error_{std} = \sqrt{\frac{\sum_{i=1}^{N}(error_{(i)} - error_{avg})^2}{RN}} \tag{2.3}$$

Where RN is the total number of localized nodes, $error_i$ is the node i's localization error, and $error_{avg}$ is the average localization error.

iii. Confidence Interval of the Localization Error

Confidence interval (CI) is the chance that a specific value falls between an upper and lower bound of a probability distribution [39]. It is a simple way to explain the significance of uncertainty in a sample estimate of a population [40]. While 95% and 99% are the most common, the CI can take any number of probabilities [39]. A smaller CI indicates that there is less chance of getting an observation within that interval, thus, the accuracy is higher.

In general, the CI is calculated as follows:

$$\bar{X} \pm Z\frac{S}{\sqrt{n}} \tag{2.4}$$

Where $\bar{X}$ is the mean, Z is the chosen Z-value, s is the standard deviation and n is the number of samples.

After replacing the symbols with the ones in our models, the CI is represented as follows:

$$error_{avg} \pm Z\frac{error_{std}}{\sqrt{RN}} \tag{2.5}$$

Where Z is the chosen Z-value, $error_{std}$ is the standard deviation of the localization error and RN is the total number of localized nodes. For simplicity, a table of pre-calculated Z values for various confidence levels is used.

B. Localization Precision

The accuracy of the location of each node in a network is determined by the localization error, which is the distance between the actual location of the node and its location as calculated by the localization algorithm. The proportion of localization errors smaller than a certain threshold error value is known as localization precision. For example, if 80% of the nodes have a localization error of less than 3 m, the precision is 0.8 at < 3 m, which we can write as P_3 =0.8.

Precision can be formulated as

$$P_k = \frac{\sum_{i=1}^{N}(b_i)}{RN} \qquad \begin{cases} b_i = 1, & \text{if } LE(i) <= k \\ 0, & \text{otherwise} \end{cases} \tag{2.6}$$

Where P_k is the precision values achieved under the k threshold of distance in m, LE is the localization error, and RN is the set of all localized nodes in the network.

C. Localization Ratio

The localization ratio, or coverage, indicates the number of localized nodes (reference nodes) divided by the total number of nodes. A high localization ratio gives an impression of how successful the path planning is. The localization ratio is represented as

$$L_{avg} = \frac{RN}{N} \tag{2.7}$$

Where RN is the total number of reference nodes, and N is the total number of deployed nodes.

D. Path Length

Although path length does not affect the localization error rate or the number

of localized nodes directly, it helps determine the time needed for the localization process to be completed and may affect other critical metrics such as energy consumption.

E. Energy Consumption

Energy consumption is another metric that is considered in this work. Since sensor nodes depend highly on a limited source of energy, respecting this condition requires a model that is efficient in terms of energy consumption. Nonetheless, the number of path planning models that consider energy consumption is limited [41]. The energy is consumed from two sides, the nodes' side and the MAs' side. For sensor nodes, most of the energy is spent during communication between the sensors and the MAs. On the MAs' side, the energy is spent in the communication process as well, but most of the consumed energy is spent on traveling around the network.

F. Obstacles Consideration

The obstacle-resistant trajectory is considered to handle obstacles that may block the MA trajectory.

2.2.3 Range-Based Localization

As mentioned before, the range-based models estimate their locations based on wireless characteristics such as the power and direction of the signal. Here, a discussion about the essential range-based methods is presented.

A. Distance Measurement Approaches

To estimate the location of a given UN, the real distance between this UN and its neighbor MAs or localized nodes is needed. In range-based localization, the distance measurement is based on four central concepts:

i. Received Signal Strength Indicator (RSSI)

RSSI is an indicator available in most modern WSNs and Internet of Things (IoT) motes that measures the power of the received radio signal [42]. It is principally used for the measurement of the distance between the transmitter and the receiver [43]. The relationship between the RSSI and the actual distance is a core idea in many WSNs localization approaches [44]. If the power of the signal at the sender node is known, it is possible to estimate the distance at the receiver node. RSSI is a desirable method since it requires no dedicated hardware. In other words, the node needs wireless characteristics for distance estimation. Many RSSI modules exist in the literature. Considering the module in [45] and assuming $d_0 = 1$, the distance between two nodes i and j extracted from the RSSI values is estimated as

$$d_{ij} = 10^{(-RSSI+P_L(d_0)+N_\alpha)/(10\beta)} \tag{2.8}$$

Where $P_L(d_0)$ is the power loss at the reference point (d_0) in dB, N_α is the zero-mean Gaussian random variable with a standard deviation α (i.e. $N(0, \alpha)$) and β is a constant path loss exponent.

However, RSSI has some drawbacks. For example, RSSI is affected by physical obstacles such as walls, which can impact the estimation accuracy. In practice, the real estimation rarely matches theoretical estimations.

ii. Time of Arrival (ToA)

ToA (also known as the time of flight) is another simple method of distance estimation between the sender and the receiver in wireless technologies [3, 23]. The core idea of ToA is to measure the time taken for a signal traveling from one node to another. The sender and the receiver have synchronized clocks. Once a signal arrives at the receiver side, the receiver registers the time of transmitting (at the sender) and the time of arrival and computes the distance between both of them based on the

difference between those two sessions. However, the propagation speed must be known. The time estimated for a signal traveling from a node i to another node j is modelled as [46]

$$t_{ij} = \frac{||x_i - x_j||}{c} + N_\alpha \tag{2.9}$$

Where c is the signal propagation speed, and N_α is the zero-mean Gaussian random variable with a standard deviation α. The distance estimation is formed

$$d_{ij} = ct_{ij} = ||x_i - x_j|| + c.N_\alpha \tag{2.10}$$

Figure 2.2 presents an example of the ToA estimation concept.

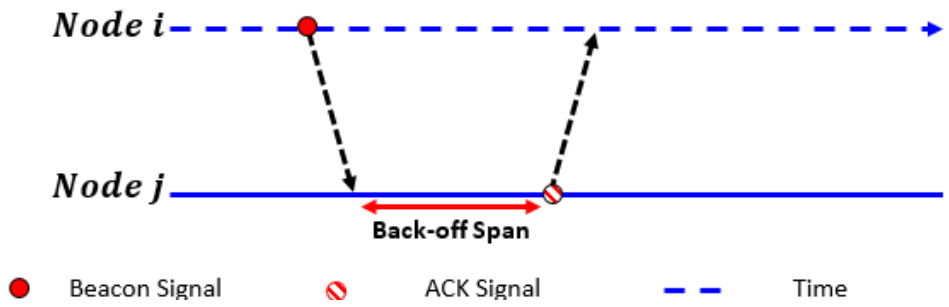

Figure 2.2: An example of the essential ToA ranging concept (redrawn from [4])

Similar to RSSI, ToA suffers from several drawbacks. First, ToA requires very high-resolution clocks for acceptable accuracy [3]. Second, it is difficult to determine the propagation speed since it depends on other external factors such as temperature or humidity [3]. As radio signals travel at the speed of light, it is a challenge to estimate their time of arrival precisely [23].

iii. Time Difference of Arrival (TDoA)

TDoA exists to overcome the need for the explicit synchronization required in ToA [3]. It calculates the distance between two given nodes by computing the different times of arrival of two different signals [47]. The two signals have to be produced by two transmission mediums of very different propagation speeds, typically radio waves and ultrasound [3,23]. Usually, a sender node i starts sending an ultrasound and a radio transmission at the same time to another node j. Radio waves typically travel at the speed of light. Hence, they are much faster in comparison to ultrasound. When the receiver node j receives the first signal, it will start measuring the time until the next message arrives, thus, it ignores the propagation time of the radio communication [3,25,47]. Figure 2.3 shows an example of the TDoA estimation concept.

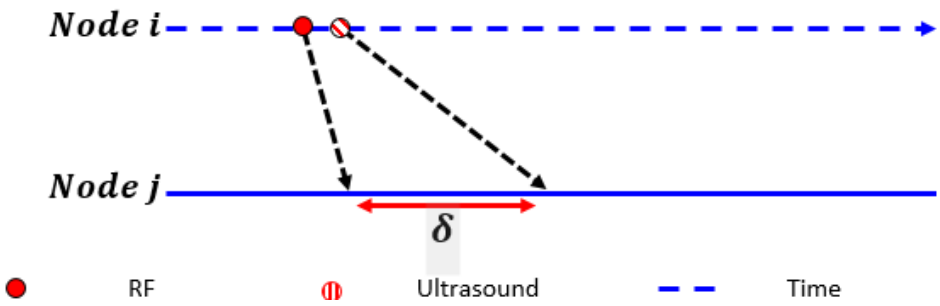

Figure 2.3: An example of the essential TDoA ranging concept (redrawn from [4])

The main disadvantage of TDoA is the need for more than one type of sender and receiver on each node, which increases the energy consumption. On the other hand, this method provides better estimation accuracy compared to those used in RSSI-based approaches.

iv. Angle of Arrival (AoA)

This method determines the direction of the radio-frequency waves propagation using an antenna array [3]. The antenna array is a set of connected antennas that combine together as a single antenna to transmit

or receive radio waves. AoA defines the direction of a signal using the TDoA at one antenna and measures the delay between them.

B. Discussion

There is a trade-off between the ranging error, and the complexity and the cost of the measurement method. While RSSI-based approaches are simple and require no additional hardware, the deployment environment has an impact on the accuracy of the estimation. On the other hand, TDoA provides more accurate prediction in comparison to RSSI, though it also requires more complicated and additional hardware which consumes more energy. Studying the application requirement needed to determine which approach is more suitable to use is mandatory.

C. Computing Locations Using Ranging-Based Measurement

Lateration and angulation are two methods that use the geometric information extracted from the communication between two nodes [3].

i. Lateration

Lateration is used when the distance between nodes is known. In the case where a node has accurate distance measurements to three noncolinear anchors, it is called trilateration, which is required in most 2D applications. In the 3D case, four noncolinear anchors are required, which is called quadlateration. Figure 2.4 illustrates an example of trilateration using three intersecting anchors. The UN will estimate its location based on the determined distance between itself and the other three anchors.

ii. Angulation

On the other hand, when angles between nodes are known, the node location can be derived using angulation. Similar to trilateration and

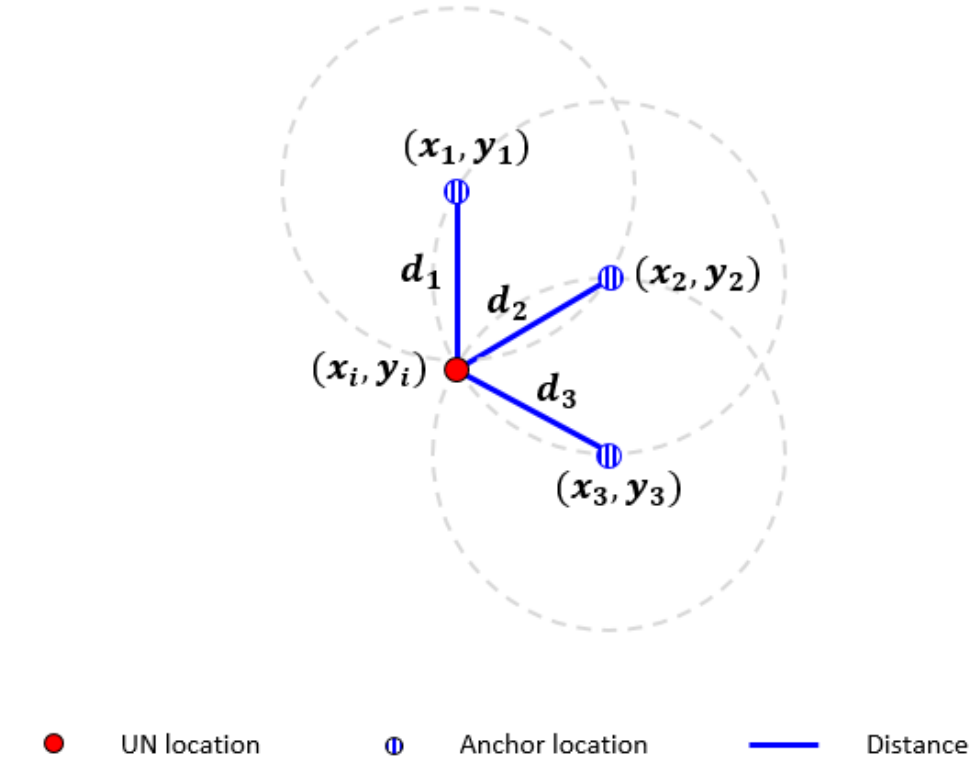

Figure 2.4: Illustration of triangulation using three intersecting anchors (redrawn from [3])

quadlateration, triangulation and quadrangulation exist in 2D and 3D estimation. Figure 2.5 depicts another example of triangulation based on the locations of two anchors.

iii. Distance Determination

In both lateration and angulation, the distance between the UN and the anchors is required. To determine the distance between each anchor node and the UN, the radio communication characteristics between both of them can be helpful. In particular, the RSSI, the ToA, and the TDoA can provide a distance estimation based on the communication between the sender and the receiver.

Now, assume that there are three location-aware anchors with the positions (x_j, y_j), where j = 1, ...,3, and a UN is located at (x_i, y_i). Using the

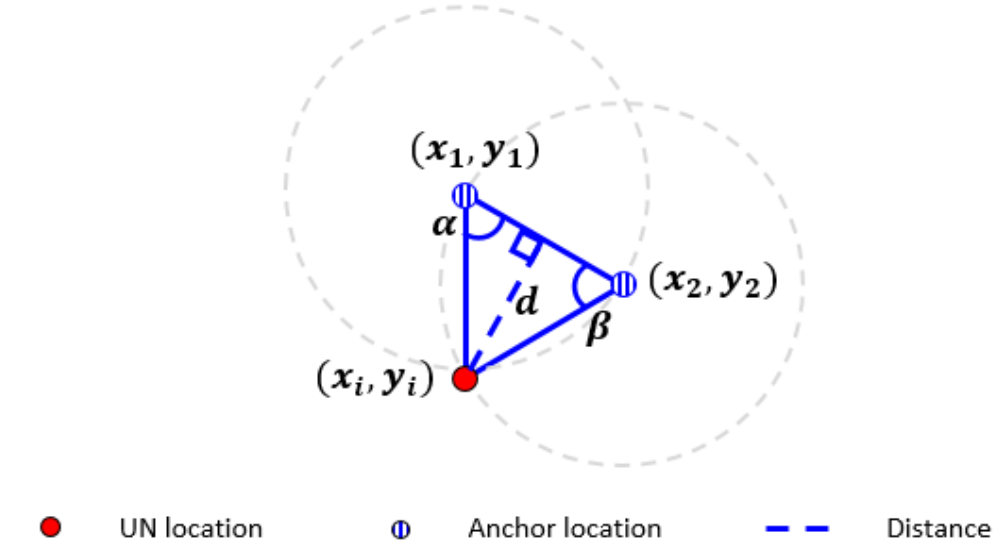

Figure 2.5: Illustration of angulation based on two anchors (redrawn from [23])

Pythagorean theorem, the distance relation between every anchor and the UN will be expressed as

$$\sqrt{(x_j - x_i)^2 + (y_j - y_i)^2} = d_{ij} \qquad \text{for } j = 1, 2, 3 \tag{2.11}$$

Where d_{ij} is the distance between the UN i and the anchor j.

Now the location of the UN can be estimated as

$$\begin{bmatrix} x_i \\ y_i \end{bmatrix} = \begin{bmatrix} 2(x_1 - x_3) & 2(y_1 - y_3) \\ 2(x_2 - x_3) & 2(y_2 - y_3) \end{bmatrix}^{-1} \begin{bmatrix} (x_1^2 - x_3^2) + (y_1^2 - y_3^2) + (d_{i3}^2 - d_{i1}^2) \\ (x_2^2 - x_3^2) + (y_2^2 - y_3^2) + (d_{i3}^2 - d_{i2}^2) \end{bmatrix} \tag{2.12}$$

2.2.4 Range-Free Localization

Unlike the former models (range-based), range-free localization algorithms estimate their UNs' locations using the connectivity information between the UNs and anchor nodes. Next, the main principles used in this connectivity information are displayed.

A. Proximity-Based Methods

These methods are simple and cost-efficient. They work based on whether a given UN is located within the range of another node or not. Based on the communication technology used: radio, infrared or sound, the information exchanges between every two nodes can be used to estimate their locations [3, 23, 48]. One of the most straightforward approaches that utilizes this concept is the Centroid method [45, 49]. In this method, a given UN can estimate its own location by gaining an advantage from the overlapping signals of multiple location-aware nodes (anchors). The location of a UN can be calculated using the following generic formula

$$(x_i, y_i) = \left(\frac{\sum_{j=1}^{n} x_j}{n}, \frac{\sum_{j=1}^{n} y_j}{n} \right) \tag{2.13}$$

Where (x_i, y_i) are the estimated coordinates of a given node i, and n is the total number of received anchors [48]. The proximity-based method requires a network with a large number of anchors to minimize the localization error and maximize the localization rate.

i. Approximate Point in Triangle (APIT)

This model is one of the most well-studied methods in localization in WSNs, and is proposed in [50]. APIT's basic idea is to divide the network area into portions of triangular regions so that their vertices indicate the locations of anchor nodes. The UN estimates its location based on the three vertices around it. APIT works in three phases where in the first phase, Message Exchange, all nodes will receive locations information from anchors around them. In the second phase, Point In Triangle (PIT) Testing, each node will select three anchors and test whether they form a triangle around it or not. This procedure will be repeated until all UNs belong to at least one triangle. In the third phase, APIT Aggregation, a centroid calculation is performed to estimate the location of the

node.

ii. High-Resolution Robust Localization (HiRLoc)

HiRLoc is another proximity-based localization algorithm proposed in [51]. Its concept is similar to APIT; however, HiRLoc aims to reduce the overlapping regions using the transmission power and directional antennas of UNs. The localized nodes will share their information as well, which helps to maximize the localization coverage. The communication cost of HiRlLoc increases as the network region increases [52].

iii. Weighted Centroid Localization (WCL)

WCL is a localization method that was first proposed in [49]. The idea behind it was to design an algorithm that would be able to achieve a small amount of computation, with a lower communication consumption and cost. The nodes' positions in WCL can be estimated after calculating the weights of anchors based on their estimated distance. The weight function can be calculated as

$$w_{ij} = \frac{1}{(d_{ij})^g} \tag{2.14}$$

Where g is a default degree based on different scenarios. Thus, the node position can be estimated as

$$p_i = \frac{\sum_{j=1}^{n} \left(w_{ij}.a_j\right)}{\sum_{j=1}^{n} w_{ij}} \tag{2.15}$$

Where P_i is the (x_i, y_i) coordinates of the UN i, and $a_j = (x_j, y_j)$ is the anchor's j position.

After replacing the w_{ij} with the $RSSI$ in equation 2.17, the final p_i can be estimated as

$$p_i = \frac{\sum_{j=1}^{n} \left(RSSI_{ij}.a_j\right)}{\sum_{j=1}^{n} RSSI_{ij}} \tag{2.16}$$

iv. Weight-Compensated Weighted Centroid Localization (WCWCL)

WCWCL is another localization model that is based on the idea of WCL [45]. However, WCWCL allows for more impact from the nearby anchors when calculating the weights. In other words, the estimation of the node location will be based on the minimum number of closest anchor locations, in case of receiving more. For this reason, WCWCL modifies the weight function to a new one that can be calculated depending on the RSSI model. A simple RSSI model is shown in the following

$$RSSI = P_L(d_0)^{dB} \; + \; 10\,\beta \log_{10} \; (\frac{d}{d_0}) \; + \; N_{\alpha}^{dB} \tag{2.17}$$

Where $P_L(d_0)$ is the power loss at the reference point (d_0), β is a constant path loss exponent, d is the real distance, and N_α is the zero-mean Gaussian random variable with a standard deviation α. The improved weights function proposed in WCWCL can be shown as

$$W_i = \frac{w_{ij}}{\sum_{j=1}^{n} w_{ij}} = \frac{\sqrt{\left(10^{\frac{RSSI_{ij}}{10}}\right)^{g}}}{\sum_{j=1}^{n} \sqrt{\left(10^{\frac{RSSI_{ij}}{10}}\right)^{g}}} \tag{2.18}$$

The WCWCL model works in three simple steps:

i. Recording the RSSI value and the anchor's location, a_j, in each UN after receiving the signals.

ii. Computing the weight function as

$$Wn_{ij} = \frac{W_{ij}.n^{2.W_{ij}}}{\sum_{j=1}^{n} W_{ij}.n^{2.W_{ij}}} \tag{2.19}$$

iii. Estimating the node's position using the following equation

$$p_j = \sum_{i=1}^{n} W_i.a_j \tag{2.20}$$

Where p_i is the (x_i, y_i) coordinates of the UN i, and $a_j = (x_j, y_j)$ is the position of anchor j.

B. Connectivity-Based Methods

Connectivity-based localization algorithms use the connectivity information for the entire network [23]. They employ the concept of graph theory for node localization [52]. Distance-Vector Hop (DV-Hop) [53] and Localizable Collaborative Body (LCB) [54] are two well-known algorithms that fall under this approach.

i. Distance-Vector Hop (DV-Hop)

DV-Hop is a range-free algorithm, proposed by the authors of [53]. It is a simple distributed technique that provides approximations of locations at a low cost, and no extra hardware is needed. DV-Hop assumes that the WSN is composed of a set of randomly distributed UNs along with another set of reference nodes, namely anchors. All anchor nodes are aware of each others locations as well. DV-Hop has received extensive attention because of its simplicity and localization capability. In [55], the authors propose using DV-Hop to increase the coverage and localization ratio in mobility trajectories models.

The DV-Hop algorithm is divided into three main stages:

Stage 1: Hop count

In this stage, each anchor node sends its location to all UNs located in its communication range. Following the information flooding approach, each of these UNs that receives the anchor's information will broadcast

it again to the other UNs in their communication range. Initialized originally to 0 in each anchor node, with each set of data sent, the number of hops between each anchor and each UN increases by a value of 1. In the end, each UN will have an information table that includes the location information of all anchors and the number of hops to each anchor.

Stage 2: Distance calculation

This stage consists of two steps:

(a) Calculation of average Hop-Size:

Once an anchor node, say $\imath$, receives the hop count information from other anchor nodes, it can estimate the average hop-size using the following formula [56],

$$HopSize_i = \frac{\sum \sqrt{(x_i - x_j)^2 + (x_i - x_j)^2}}{\sum hop_{ij}} \tag{2.21}$$

Where $\imath \neq \jmath$ and, (x_i, y_i) and (x_j, y_j) are the location coordinates for the anchors $\imath$ and $\jmath$, and hop_{ij} is the number of hops between them. Lastly, each anchor will flood its hop-size to all network nodes.

(b) Sensor-anchor distance estimation:

This step is a chance for the UNs to estimate their distance to each known anchor. Based on the information in step (a), the distance estimation between each UN s and anchor $\imath$ can be calculated as

$$d_{si} = CountHop_{si} * HopSize_i \tag{2.22}$$

Stage 3: Location estimation

Once three different distance estimations are performed, the UNs can estimate their locations using the trilateration method as described before.

ii. Localizable Collaborative Body (LCB)

LCB is a localization algorithm that estimates UN locations based on the graph theory [54]. Similar to DV-Hop, LCB also uses the connection of multi-hop anchors for location estimation, allowing it to overcome the problem of having three direct neighbor anchors. A tree structure called BN-tree is formed to construct a localizable collaborative body of the network. An advantage of using LCB is that it decreases computation and communication costs since the localized nodes can share their information with their neighbors. On the other hand, the localization error in one node has a significant impact on the localization error of another node, thus increasing the localization error in general [52].

C. Event-Driven Methods

This is an emerging range-free localization approach that aims to reduce the computation overload on the UN's side [57]. This is done by applying an asymmetric system design where the sensor nodes only need to conduct simple operations of event detection and reporting. Most of the localization procedures follow a centralized approach where the localization process will be conducted on another device. Some of the notable works under this method are: the Lighthouse model proposed in [58], the Spotlight model proposed in [59] and the laser Scan model proposed in [60]. While event-based methods are now drawing more attention, there are some disadvantages of using this method such as the need for expensive localization devices and its sensitivity to the environment in which it is deployed [57].

2.3 Survey of Path Planning Models

With the increased number of localization proposals, the classification of localization models has been extended. Based on the nature of the mobility, and according

to [36], localization models are grouped into four main categories as shown in Figure 2.6. The first category (Static Node – Static Anchor), where both nodes and anchors are static, represents the original area of localization research. An extensive body of work has been conducted on this category, and this work continues. This category is classified into two types that were discussed above, the range-based and range-free models. It is important to mention that in one way or another, most of the other types of models depend somewhat on this type. Examples of this type can be found in [45, 49, 50, 53]. The second category (Mobile Node – Static Anchor) contains the algorithms in which the mobility exists in nodes, not the anchors. This type usually includes scenarios where a sensor node is attached to a monitored body, such as an animal, and the static anchors provide each node with an updated location with each movement. Examples of this category are proposed in [61, 62]. In the third category (Static Node – Mobile Anchor), which we are interested in, the sensor nodes remain static at the time, while the MA is responsible for traversing the network and assisting these sensor nodes in estimating their locations. This type of localization model is further subdivided into two categories: random mobility and planned mobility. Since our proposed models are located under the (Static Node – Mobile Anchor) category, more details about these models are provided in this section. The last category (Mobile Node – Mobile Anchor) includes scenarios where both sensor nodes and anchors are mobile. Examples of this category are more likely to be found in robotics applications, like those in [63, 64].

2.3.1 Random Path Planning

As indicated by its name, the direction of movement and steps are chosen randomly. Nonetheless, more parameters may also be determined randomly, such as the velocity and length of each movement. This kind of mobility is used in cases where no accurate locations or localization ratios are required. Consequently, there is no guarantee that all UNs will receive enough localization information; hence,

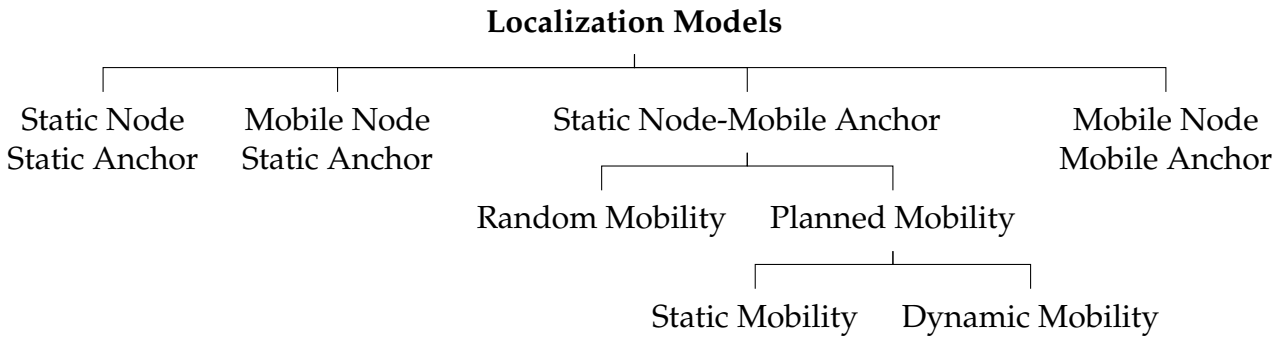

Figure 2.6: Classification of localization models in WSNs

many UNs will not be able to estimate their locations.

A. Random Waypoint (RWP) Model

It was first proposed for routing purposes in ad hoc networks, then was extended to be used in localization assistance models. RWP randomly changes the MA's direction and velocity. Each velocity is chosen as a value between the minimum and maximum velocity in m/s. RWP highly depends on the waves that represent the clustering sensors located in the center of the monitored area. As with most random mobility models, RWP does not solve the coverage problem of having all UNs receive localization information, nor does it provide a reasonable error rate. An example of RWP is shown in Figure 2.7. Other random mobility models were proposed and used in [65, 66].

B. Random Direct (RD) Model

The Random direct model (RD) was proposed to overcome the weakness of RWP [66]. It is similar to RWP, except that the MA moves along the border of the monitoring area. Thus, the MA can travel through the whole area instead of restricting itself to the center of the area, which helps to reach a more substantial number of nodes.

C. Gauss-Markov(GM) Mobility Model

The Gauss-Markov(GM) mobility model is an adaptive localization approach for WSNs based on the Gauss-Markov mobility model proposed in [67]. It

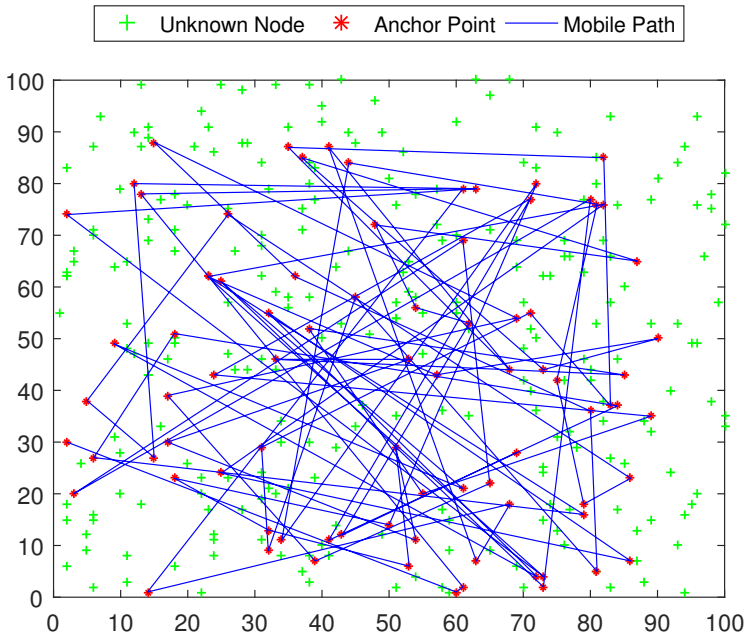

Figure 2.7: Mobile path movements models in RWP

consists of three main phases: the perpendicular bisector phase, the virtual repulsive phase and the velocity adjustment phase. The three phases work simultaneously to enhance the localization efficiency. The perpendicular bisector phase aims to adjust the path of the MA to avoid collinearity. The virtual repulsive phase ensures the MA movement is within the boundary of the network, and the velocity adjustment phase changes the MA velocity based on the network topology. Based on these three phases, the MA adaptively adjusts its velocity and direction. In comparison to RWP, GM shows better performance in terms of accuracy and ratio [4].

2.3.2 Static Path Planning

The main difference between static mobility paths and other mobility types is that the movement trajectory is set in advance and cannot be changed or modified after deployment, except in some models where obstacles are considered. Thus, most

static path proposals are in some way based on triangulation or trilateration concepts. In general, static path models show high localization ratios, since one of their primary goals is to guarantee that all UNs receive localization information. Nonetheless, in comparison to other types of mobility, static models offer a low localization error, which means the UNs will be able to estimate their locations more accurately and precisely. However, proposing a static path requires giving more attention to the details of the anchor points and the designed trajectory to avoid other problems, such as collinearity and path length. The collinearity problem exists when a UN receives only one localization message from one direction or when it receives multiple messages from one line and different directions. Another issue is that since the static mobility models depend highly on trilateration concepts, the designed path should ensure that all UNs can receive at least three different anchor locations so they can determine their own locations. Examples of static mobility models for sensor localization are presented in [11, 36–38].

A. SCAN

The SCAN and Hilbert models are considered the first mobility assisted-localization path models and were proposed in [36]. SCAN is a simple model that allows the MA to move in straight lines in one dimension, x or y. The distance between every two lines is defined as the *resolution*. At the same time, the resolution represents the distance between every two anchor points in each line. Figure 2.8 shows the path model of SCAN.

The main advantage of the SCAN model is its simplicity to implement; however, it suffers from the collinearity problem, which significantly affects its accuracy.

B. Double-SCAN

To overcome the collinearity problem in SCAN, another model called Double-Scan, or D-SCAN for short, was designed similarly to SCAN, but with an

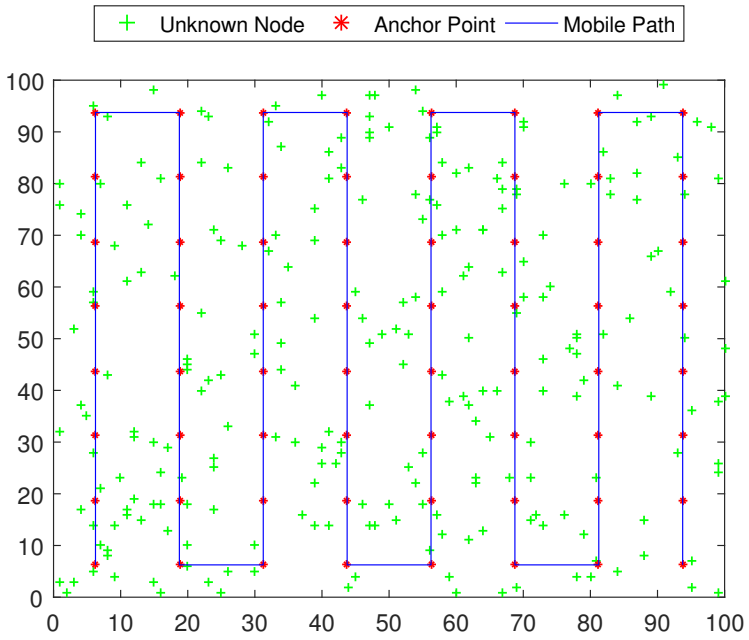

Figure 2.8: Mobile path movements model in SCAN

extension in two directions. D-SCAN works in both the horizontal and vertical vertices to increase the coverage and solve the collinearity problem [36]. However, it increases the path length of the MA, due to the nature of SCAN and D-SCAN regarding moving in straight lines.

C. Hilbert

To avoid the weaknesses of SCAN, Hilbert, which is shown in Figure 2.9, was proposed to make more turns and avoid collinearity. Hilbert works by dividing the area into four equal squares and connecting the points between these squares. With the localization information from different non-collinear positions, the UNs are able to estimate their location more accurately than in SCAN. One of the significant issues in Hilbert is the coverage problem because the UNs that are located at the border of the area are unable to receive enough information to estimate their locations, which then affects the localization ratio and increases the localization error [52].

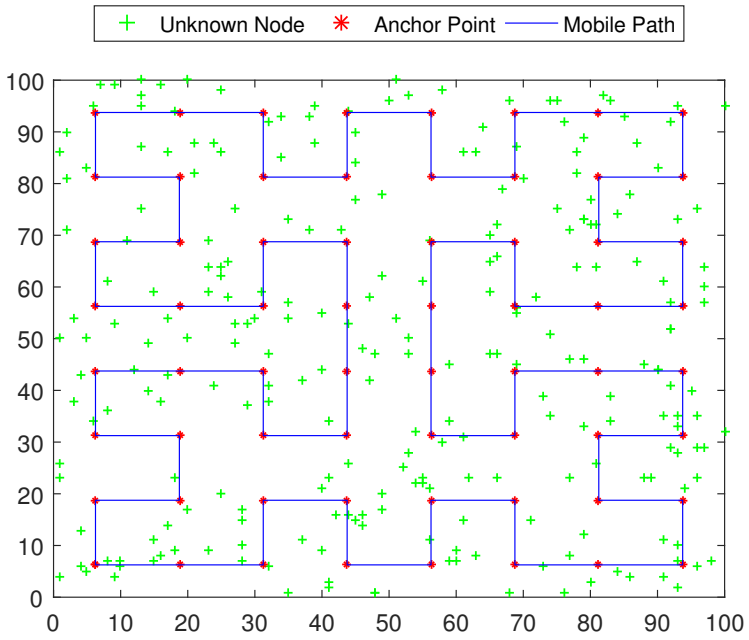

Figure 2.9: Mobile path movements model in Hilbert

D. CIRCLES

Along with S-Curves, CIRCLES is one of the earliest and most well-known path planning models for MA-assisted localization [68]. CIRCLES is formed based on circular path movement. The primary goal of CIRCLES is to overcome the collinearity problem. However, this model is unable to reach the nodes located in the corners of the network, thus, affecting the localization ratio negatively. This problem can be solved by adding more outer circles to the path; however, this will bring another issue to the path length.

E. S-Curves

S-Curves is a static path planning model proposed in [68]. In its basic concept, the movement pattern of S-Curves is similar to that formed in SCAN, which progressively scans the deployment area vertically or horizontally. To overcome the collinearity in SCAN, the S-Curves algorithm follows an 'S' curve instead of moving in straight lines. Because the straight lines strategy

is avoided, and in comparison to SCAN and Hilbert, S-Curves offers better accuracy and a higher localization ratio. The path length in S-Curves is slightly shorter than those in SCAN and Hilbert.

F. Localization algorithm with a Mobile Anchor node based on Trilateration (LMAT)

In [11], a Localization algorithm with a Mobile Anchor node based on Trilateration (LMAT) was proposed. In LMAT, the path is formed in many symmetrical triangles. The distance between every two points in LMAT's path is defined in advance as the resolution value. The main reason for using trilateration in LMAT is to provide more accurate estimation and to avoid collinearity. Although LMAT provides a high localization ratio with fewer errors, the path length that an MA needs to travel is an issue. LMAT path model is shown in Figure 2.10.

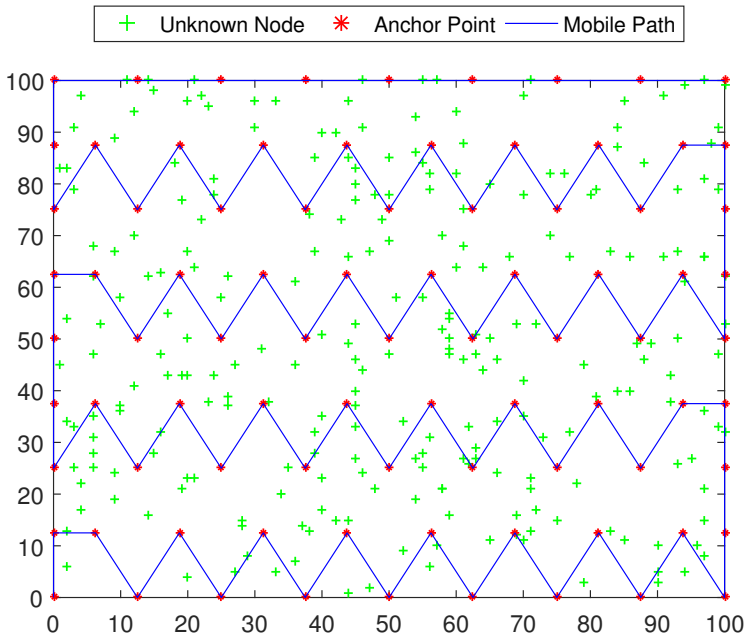

Figure 2.10: Mobile path movements model in LMAT

G. Mobile Anchor-Assisted Localization algorithm based on a Regular Hexagon (MAALRH)

Han *et al*. propose a Mobile Anchor-Assisted Localization algorithm-based on a Regular Hexagon (MAALRH) [37]. Unlike the other planning trajectories, the path in MAALRH starts from the center point and moves a hexagon-form step. Once the MA reaches the hexagon's starting point, it moves out one step in the distance of the resolution and starts forming another larger hexagon as shown in Figure 2.11.

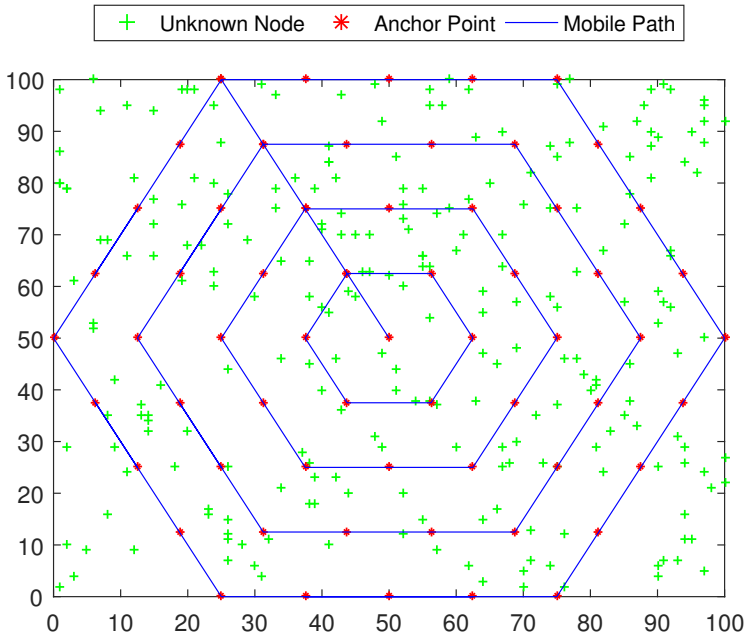

Figure 2.11: Mobile path movements model in MAALRH

While MAALRH is considered one of the newest models, it gives poor results in both its localization ratio and localization error. The MA in MAALRH is unable to reach the corners of the area, thus the UNs located in these corners are unable to determine their locations. Nonetheless, the UNs outside of the outermost hexagon will estimate their locations, if they can, with high error values.

H. Z-Curves

The Z-Curves mobile path model was proposed in [38]. As indicated by its name, the MA traverses the network forming a Z-shape. The network is divided into three levels, and the Z-shapes are connected to each other in each level. The final Z-Curves model is shown in Figure 2.12. Like the other localization-assisted mobility models in WSNs, the Z-Curves model aims to form a set of different points that are based on the trilateration concept to avoid collinearity and help the UNs receive at least three different localization messages from three different locations.

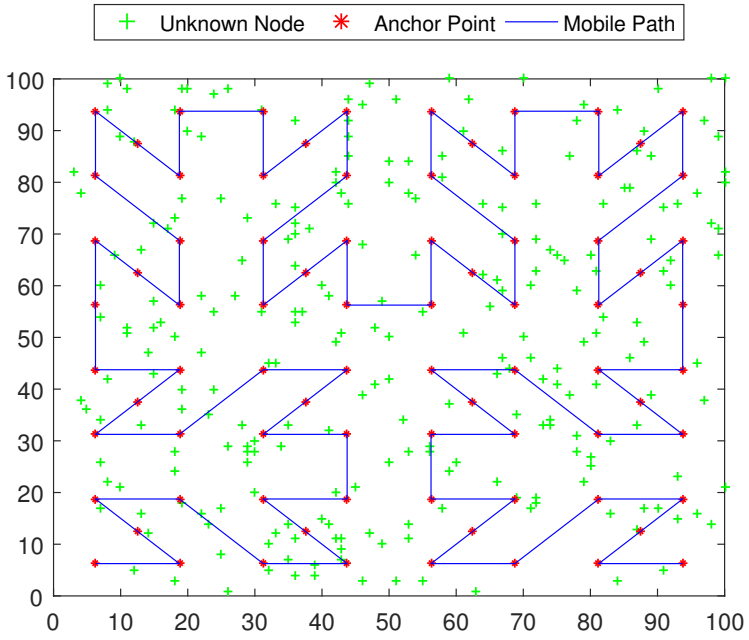

Figure 2.12: Mobile path movements model in Z-Curves

Z-Curves also proposes that when the MA faces an obstacle on its way, it simply turns around the corner of that obstacle and goes to the obverse point of the obstacle to continue the movement. However, such a solution leaves several drawbacks in terms of path length and collinearity.

2.3.3 Dynamic Path Planning

Dynamic Path Mobility is included under the second category of localization models, the planned models. In dynamic models, the direction of the MA and its movement path depend on real-time information and the demands of the initial distributed UNs. Thus, there is no specific or deterministic path in advance. Examples of this kind of mobility being used in localization-assistance are the Dynamic Path of Mobile Beacon (DPMB) algorithm in [69], Breadth-First (BRF) and Backtracking Greedy (BTG) algorithms in [70], and Deterministic Dynamic Beacon Mobility Scheduling (DREAM) in [71].

A. Dynamic Path of Mobile Beacon (DPMB)

The Dynamic Path of Mobile Beacon (DPMB) algorithm, presented in [69] divides the nodes into three classes: unknown, settled, and reference nodes. Each node contacts its neighbours that are located in its transmission range. Thus, the MA will determine its path from node to node according to the quantity of neighbours (QN) for each UN. The first triple position and other algorithms are used to determine the locations of UNs. In the first triple position, all movements are random; however, when a triangle is formed, all nodes inside it can be localized to become reference nodes.

B. Breadth-First (BRF) and Backtracking Greedy (BTG) Models

BRF and BTG are models that derive their movement design by constructing the localization problem into a graph theory [70]. The WSN is viewed as a connected undirected graph. Then, the path planning problem is translated into a spanning tree and traversing graph. Breadth-First is a searching technique that has a property in which if all of the edges in a graph are unweighted, the first time a node is visited is regarded as the shortest path to that node. On the other hand, the Backtracking Greedy Algorithm is an algorithm that continually takes the best immediate solution while attaining an answer. The MA changes its direction based on the nodes deployment. Both

BRF and BTG suffer from high localization error.

C. Deterministic Dynamic Beacon Mobility Scheduling (DREAMS)

The deterministic beacon mobility scheduling (DREAMS) model was proposed in [71]. The first MA movement in DREAMS is taken randomly. The next movements are performed based on a Depth-First Traversal (DFT) search. DFT is a searching algorithm for graph data structures that allows the graph to come to the same point, if needed. The MA performs a distance-based heuristic movement that relies on the measurement between the MA and the target UNs. A Local Minimum Spanning Tree (LMST) sub-graph is also used to minimize the path length of the MA. An advantage of DREAM is that there is no need for prior knowledge about the monitored network.

D. Snake-Like

Another dynamic model, called Snake-Like is introduced for obstacle-avoidance in [72]. The proposed movement formation is similar to that offered in SCAN; however, it follows a horizontal approach. When an obstacle is faced, identical to Z-Curves, the MA will move on the border of the obstacle and reach the other point on the same line as the last point before the obstacle and keeps its movement. The main disadvantage of the Snake-Like proposal is collinearity. Snake-Like does not provide a solution for the collinear points and how to deal with them. In addition, to avoid the repeated points in the path, some areas in the network will not be fully covered. Figure 2.13 below shows an example of a Snake-Like path when 10 obstacles exist in the network area.

E. Node Localization Algorithm with Mobile Beacon Node (NLA_MB)

A node localization algorithm with a mobile beacon node (NLA_MB) is proposed in [73] with an assumption of limited and constrained movements. In this model, the area of interest is divided into a number of hexagonal grids, and the MA moves from the centre of the hexagon to a corner and vice versa based on the proposed optimization model to form the final movement path.

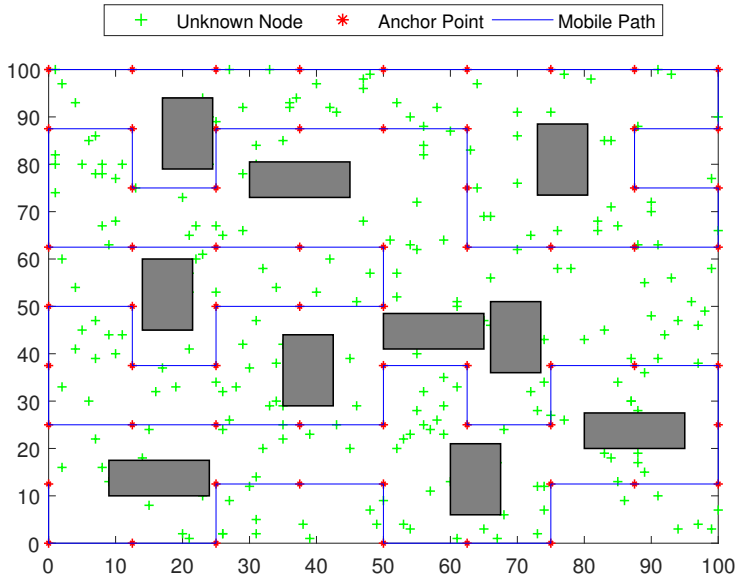

Figure 2.13: Mobile path movements model in Snake-Like when 10 obstacles exist

The area coverage of NLA_MB differs based on the available sources of time and energy (i.e., maximum path length). Figure 2.14 shows an example of an NLA_MB movement pattern when 105 m is assigned as the maximum movement of the MA.

2.3.4 Three-Dimensional Path Planning Models

As shown previously, most path planning algorithms use the concept of the trilateration path for the MA to minimize localization errors and improve localization accuracy [11]. However, in real-life scenarios, the concept of quadrilateration is vital [34]. The quadrilateration method uses distance measurements from four different non-collinear nodes to localize other nodes in 3D space. Using the quadrilateration method will overcome the coplanarity problem, where a set of nodes lie on the same straight line [34].

A. Three Dimensional Random Waypoint (3D-RWP)

A 3D-Random Waypoint (3D-RWP) model is proposed [74], which presents a

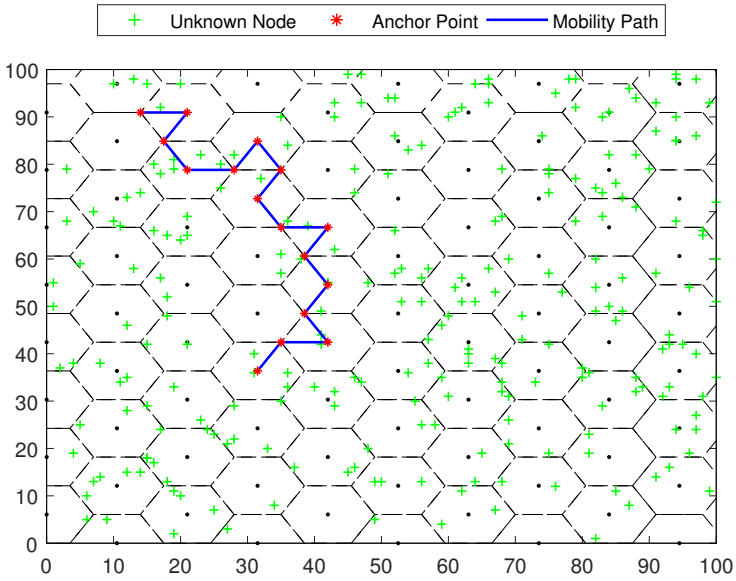

Figure 2.14: Mobile path movements model in NLA_MB with a maximum movement distance of 105 m

four-mobile-beacon assisted weighted centroid localization method in three-dimensional space. It suggests using more than a single MA for localization assistance. The main idea is to allow the MA to move freely in the network; therefore, the movement path will be similar to that shown in RWP. Figure 2.15 represents the movement pattern of the 3D-RWP.

B. Layered-SCAN

Reference [75] proposed three models: Layered-SCAN, Layered-Curve and 3D-Hilbert. In Layered-SCAN, the procedure is similar to that proposed in SCAN; however, it is applicable in a 3D area. Three coordinates (x, y and z) are considered, where Z represents a set of a 2D SCAN. Each 2D SCAN is called a layer. The distance between layers is the same as the distance between every two points in the 2D SCAN. Layered SCAN inherits the same challenges of SCAN, with both having a long movement path and coplanarity problems. Figure 2.16 shows an example of the 3D Layered SCAN.

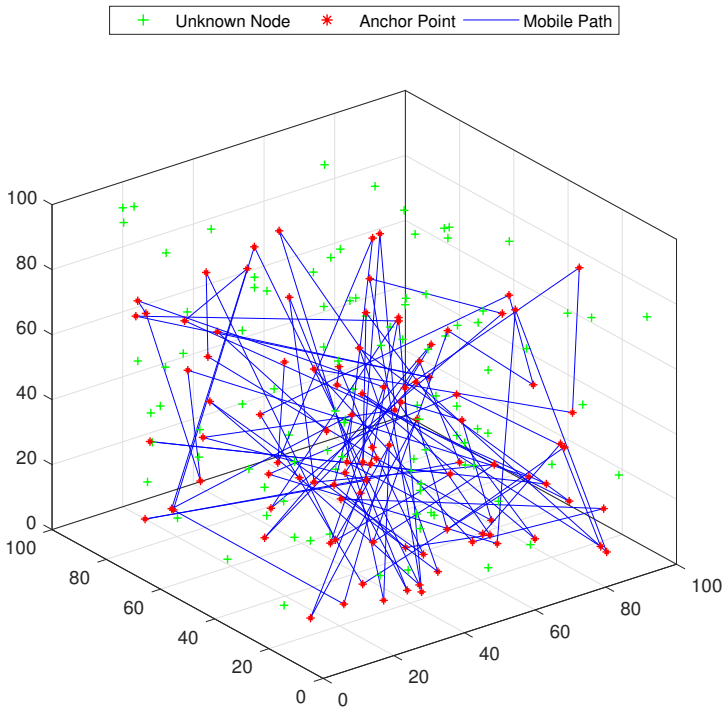

Figure 2.15: Mobile path movements models in 3D-RWP

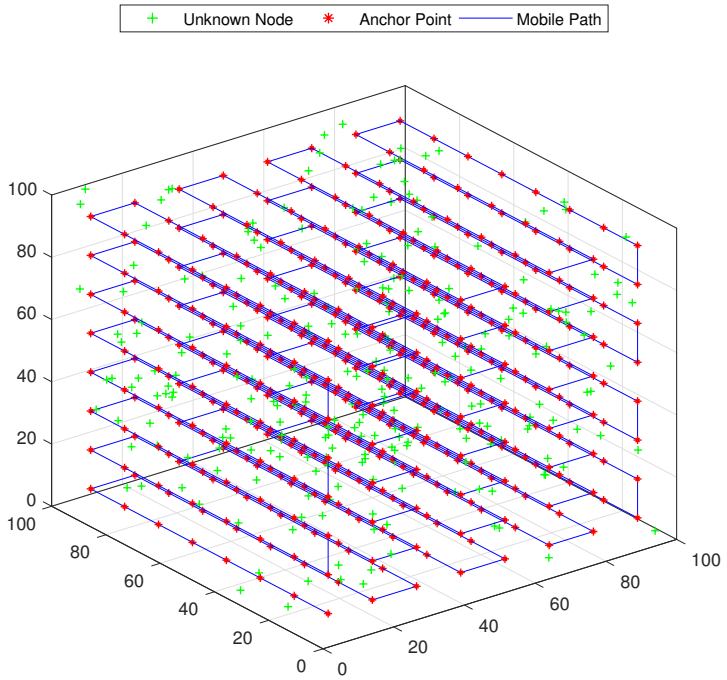

Figure 2.16: Mobile path movements models in Layered-SCAN

C. Layered-Curves

Derived from S-Curve, the Layered-Curve movement is formed using a set of layers where the distance between every two layers is constant and donated as Resolution. The MA traverses the network along one dimension using straight lines and S-Curves. While Layered-Curve overcomes collinearity, it may bring some problems associated with the path length and energy as well as some repeated points.

D. 3D-Hilbert

Since Hilbert was an improvement of SCAN that allows the MA to make turns to avoid collinearity, in Layered-Hilbert, a similar concept is employed. However, it comes with more complexity as more points are needed to localize a node in a 3D area. Figure 2.17 presents an example of a Layered-Hilbert path planning model.

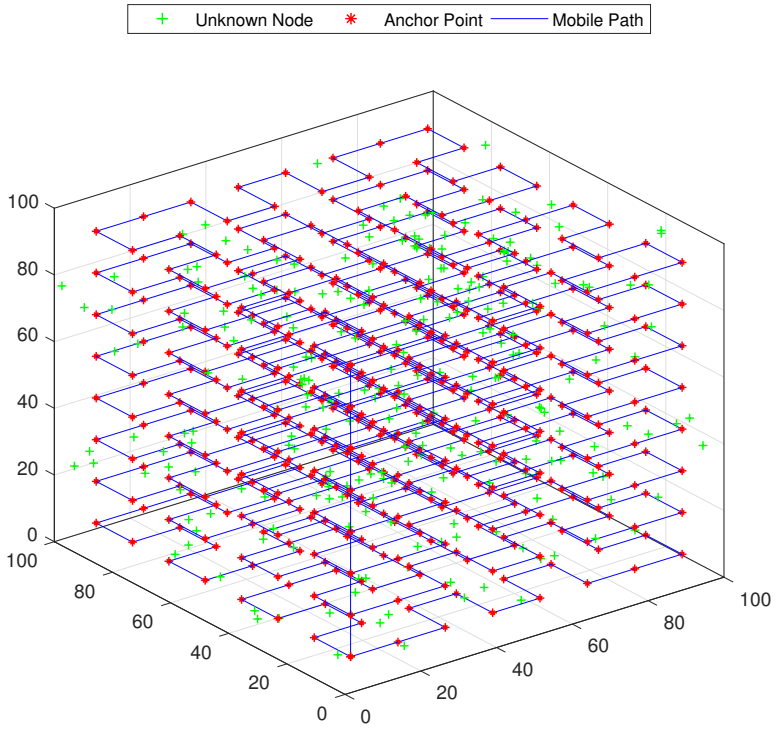

Figure 2.17: Mobile path movements models in Layered-Hilbert

E. Hexahedral Localization (HL)

A three-dimensional hexahedron localization based on MAs is proposed in [76]. The idea is essentially to divide the network space into a broad set of hexahedrons. Then, the UNs are located using the perpendicular properties of the movement path. All points inside each hexahedron should be visited so that the UNs can get their localization information. However, the authors state that the MA's path may be uncontrollable, and the path may not be the ultimate one.

2.3.5 Summary of Path Planning Models

The following Table 2.1 provides a general comparison of different path planning schemes.

Table 2.1: General comparison of mobility-assisted movement schemes in WSNs.

Mobility Protocol	Area	Movement Path	Movement Constraints	Area Covered	Collinearity Considerd	Accuracy
RWP	2-D	Random	No	No	No	Low
RD	2-D	Random	No	No	No	Low
GM	2-D	Random	No	No	No	Low
SCAN	2-D	Static	No	Yes	No	Low
Hilbert	2-D	Static	No	Yes	Yes	Medium
CIRCLES	2-D	Static	No	No	Yes	Low
MAALRH	2-D	Static	No	No	Yes	Medium
Z-Curve	2-D	Static	No/Yes	Yes	Yes	High/Medium
LMAT	2-D	Static	No	Yes	Yes	High
DPMB	2-D	Dynamic	No	No	Yes	Weak
BRF	2-D	Dynamic	No	No	No	Weak
BTG	2-D	Dynamic	No	No	No	Weak
DREAMS	2-D	Dynamic	No	No	No	Medium
Snake-Like	2-D	Dynamic	Yes	No	No	Weak
NLA_MB	2-D	Dynamic	Yes	Differs*	Yes	High
3D-RWP	3-D	Random	No	Yes	No	High
Layered-SCAN	3-D	Static	No	Yes	No	Weak
Layered-Curves	3-D	Static	No	Yes	Yes	Weak
Layered-Hilbert	3-D	Static	No	Yes	Yes	Medium
HL	3-D	Static	No	Yes	Yes	High

* Based on the maximum movement distance

As shown in Table 2.1, the random models (RWP, RD and GM) and the static models (CIRCLES and MAALRH), are not able to cover the whole area since the nodes located in the corner sides of the network are difficult to reach, while the collinearity problem affects the accuracy in RWP, RD, GM, SCAN, BRF, BTG, and DREAM. On the other hand, dependence on a single parameter leads to the weak performance of coverage and accuracy in DPMB. Thus, multiple parameters in the decision making of the movement direction are needed to improve the limitations of the static and dynamic models. This becomes more important in cases where the movement of the MA is constrained. The main aims of any proposed model are to overcome the collinearity problem that the static models suffer from as in [36], enable the MA to reach any point in the network regardless of its position unlike those in [37, 68], and to form the movement path based on various inputs to increase the performance of the optimization model, unlike the dynamic one in [69].

2.4 Conclusion

In this chapter, an overview of the WSNs and their types of applications and their current challenges were presented. In addition, a survey of the localization in WSNs was offered, which includes the localization categorization and models with more focus on both range-based and range-free localization. Then, we provided a summary of some of the existing localization models with their concepts. Another survey about the path planning models for mobility-assisted localization and their initial ideas were addressed.

Chapter 3

New Path Planning Model for Mobile Anchor-Assisted Localization in Wireless Sensor Networks

3.1 Preface

In this chapter, we introduce a new path planning model for mobile anchor-assisted localization in WSNs. Our main contribution in this chapter is providing a proposal for a competitive path planning model for mobility-assisted localization in WSNs that provides better results. The proposed path model is improved to increase the localization accuracy and ratio of the successfully localized nodes. Moreover, we suggested considering the precision metric in designing the movement path. To the best of our knowledge, our work is the first to consider the precision metric in mobility-assisted localization in WSNs. We also noticed that most of the current works do not take into account wireless channel specifications; thus, realistic wireless specifications are used in evaluating the different models in this work. We contribute a path planning model for mobile anchor-assisted localization in WSNs that

1. Ensures that all of the UNs inside the network can receive the localization information. By doing so, and in contrast with random models and some static model like Circles [68] and MAALRH [37], all UNs will be able to estimate their current locations, when the resolution is equal or greater than one, depending on the received information.

2. Provides a path model with a competitively accurate estimation with a lower localization error as compared to other static models.

3. Uses the precision metric, which is defined as the ratio of how many specific

accuracy values are reached, for evaluation in more than one area.

4. Takes into consideration the collinearity problem, as compared to the random mobility models and some static models such as SCAN, and HILBERT which do not [36].

5. Shows an average energy consumption that is related to the number of localized nodes. We consider both node and MA energy consumption in our calculations.

6. Additionally, we analyze and discuss the trade-off between the chosen localization algorithm and the designed path model. We prove that both the mobility path and the localization algorithm impact each other.

Section 3.2 shows the system model and the assumptions that are considered in the performance evaluation. In Section 3.3 we introduce our mobility-assisted path planning model and the ideas behind it. Section 3.4 presents a performance setting using the model described in Section 3.2, while Section 3.5 shows the evaluation part and the results. We discuss the trade-off between the chosen localization algorithm and the designed path in Section 3.6. We sum up this chapter in the Conclusion in Section 3.7.

3.2 System Model and Assumptions

The system model is assumed to have the following characteristics:

1. A two-dimensional network field with an area size of S in m^2.

2. A set of UNs, N, are deployed around the network following a uniform distribution.

3. At first, all UNs are not location-aware.

4. All of the distributed nodes are assumed to be static and their location will not change.

5. Each sensor node has a fixed transmission range of R_{Tx} in m.

6. An MA, or more of M number, is able to determine its location at any part of the network and is ready to traverse the whole network freely, in straight and direct lines, based on each path model. For simplicity, we assume that there are no obstacles in the deployment area to limit the MA's movement.

7. The MA is assumed to make several stops on its way, and the distance between every two stopping points is set in advance as d_m.

8. Each MA and UN are able to connect to each other only if their positions are within the same transmission range, R_{Tx}.

9. Once a UN receives three different localization messages, it can start the localization estimation using the selected localization algorithm.

10. Both UNs and MAs consume energy in their connection; however, the MA consumes a greater amount of energy during its travels around the network.

3.3 Path Planning Models for Mobile Anchor-Assisted Localization

The main contribution of this work is to design a path planning model for mobility-assisted localization in WSNs. Our proposed model is called H-Curves, because it derives its name from the multiple sloping H-Shaped paths in this design. In order to overcome the problem of collinearity and to shorten the path, the model is intended to have a winding path to ensure that each UN is located within the area of at least three different anchor points. Thus, the coverage, accuracy and localization ratio increase. Figure 3.1 shows a sketch of the mobile path for this model. The node's localization process is done in three simple steps: the mobility movement step, the localization information exchange step, and the localization estimation.

Figure 3.2 summarizes the three step process of the localization in our proposed model.

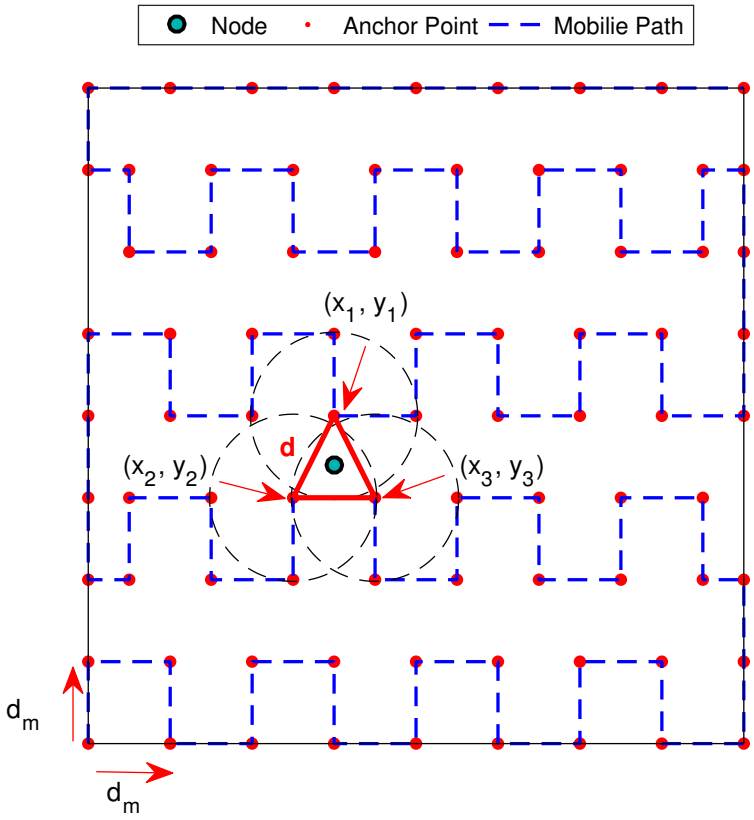

Figure 3.1: The proposed MA path in H-Curves

3.3.1 Mobility Movement

The MA will start from the beginning point at the corner of the deployment area and travel in straight lines from each anchor point to another in a fixed distance of d_m. The value of d_m will not change at any time. After completing one row of movement, upon reaching the second corner point, the MA will take a step in the other direction, or coordinate y in this example, with the same fixed d_m. However, after two movements in this direction, the MA will return to its original coordinate, x in this case, but in the reverse direction. An important point here is that the MA will travel only half of the distance d_m. This is meant to make a difference between the rows and prevents the rows from corresponding, which will help to decrease the number of points and create the triangle-like form of communication.

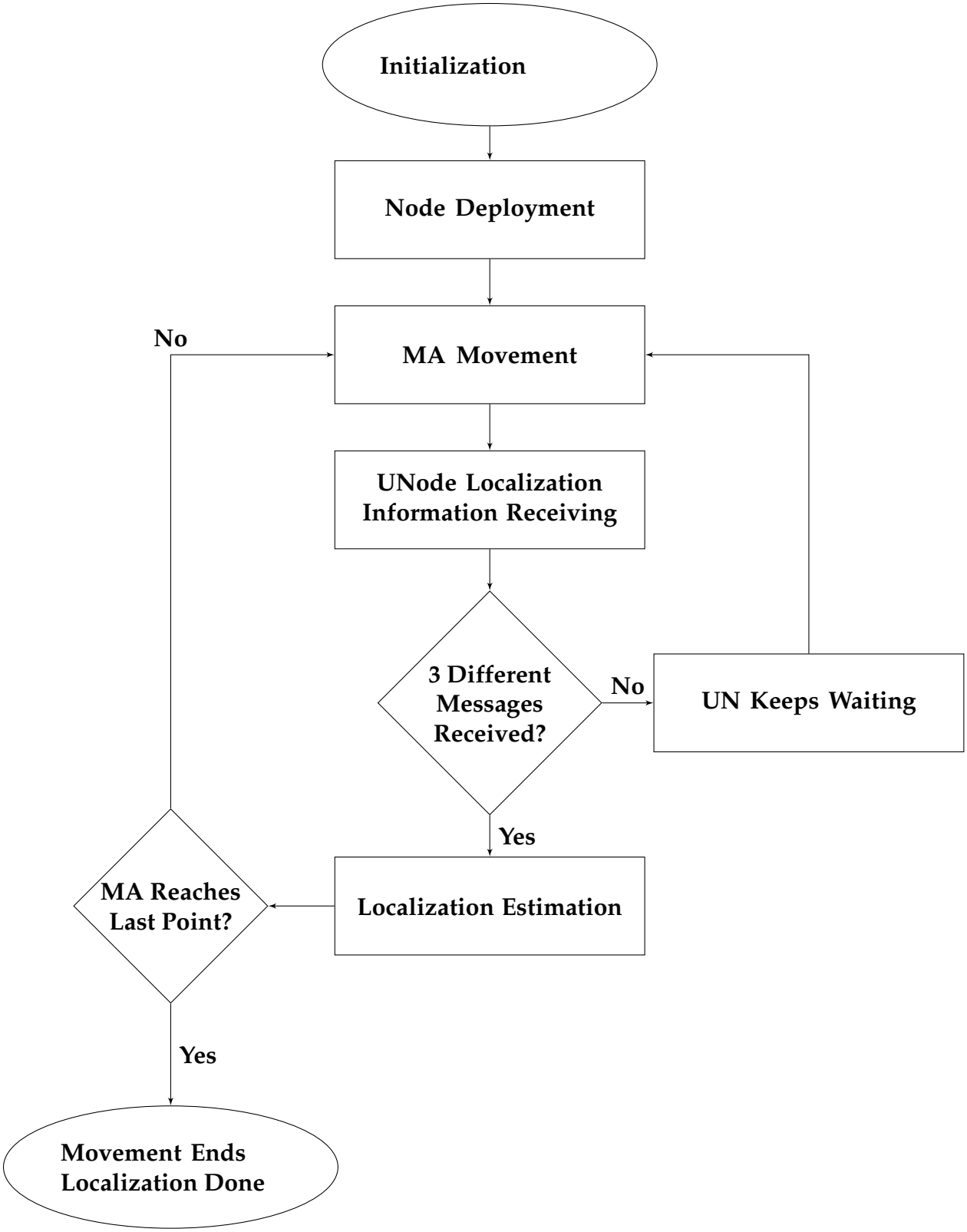

Figure 3.2: The MA movement and node localization process

3.3.2 Information Exchange

If three different points are chosen, as in Figure 3.1, (x_1, y_1), (x_2, y_2), and (x_3, y_3), then the UN located in their communication range will be able to communicate with all of them and estimate its own location. When receiving localization information from fewer than three different points, the UN will wait till the MA arrives from a different point till three points of information is provided. As mentioned earlier, our proposed model guarantees that, in most cases, each single UN will be able to receive three different localization messages.

3.3.3 Localization Estimation

Once three different localization messages are received by a UN, it becomes ready to start the location estimation. The accuracy of the localization estimation depends on the localization technique that is used. Each UN starts calculating its own coordinates in the area. The accuracy of each model will be determined as the difference between the real node's location and the estimated one.

3.4 Performance Settings

Five static path planning algorithms for mobile anchor-based localization and one random mobility model were used to assess the performance of our proposed model. The static models that were used in this work include SCAN, Hilbert, MAALRH, LMAT and Z-Curves, while the RWP model was used as a random model. Two localization algorithms, WCL and WCWCL, were used to study the efficiency of the implemented mobility models.

3.4.1 Parameters and Settings

We implemented the different models using the Matlab environment with 50 run times. The network area is assumed to be a square area with a size, S, of 100 m x 100 m. A set of 250 UNs, N, is deployed, while only one MA, M, is used. The

resolution values indicate the relationship between the transmission range, R_{Tx}, and the distance between every two points in each static model. This distance is defined as the distance metric value, d_m. Thus, the resolution is defined as:

$$R = \frac{R_{Tx}}{d_m} \tag{3.1}$$

For the wireless model, we used the specifications of a wireless node that was equipped with a Chipcon CC1100 radio module [77], which were used in [45]. The remaining parameters are shown in Table. 3.1.

Table 3.1: Simulation values and parameters in H-Curves

Parameters	**Symbol**	**Value**
Network Size (m)	S	100×100
Number of MAs	M	1
Number of UNs	N	250
Resolutions	R	0.5, 0.75, 1, 1.25, 1.5, 2
Path Loss Exponent	β	3.5
Power Loss at d_0 (dB)	$\mathrm{PL}(d_0)$	-60
Reference Point (m)	d_0	1
Standard Deviation of Noise	σ	3, 5, 7, 9
Simulation Run		50

3.5 Evaluation

To evaluate the effectiveness of the proposed model, we considered the following metrics, discussed below: accuracy, precision, localization ratio, path length, and energy consumption.

3.5.1 Accuracy

Here, we used two methods to calculate the localization error of each mode: the average localization error and the standard deviation of the localization error.

A. Average Localization Error

As described in Section 2.2.2, the average localization error is used to analyze the degree to which the estimated position is accurate. However, to compare the average localization error of each mobility model in each run, we first ran a test of 250 UNs with a communication range of 12.5 m, which is equivalent to a resolution, R, of 1, σ of 3, and 50 simulation runs. We also use the standard deviation of the localization error rate to see how different it is from the average localization error rate. A low standard deviation of error values means that a high percentage of the values are very close to the average.

Figures 3.3a and 3.4a show how the different models performed in terms of localization error when WCL and WCWCL are used, while Figures 3.3b and 3.4b show the standard deviation of the localization error for both localization techniques with each run time for the same localization techniques.

As shown in Figure 3.3a, our proposed model demonstrated higher estimated locations with a lower error rate in most of the shown results when the localization algorithm WCL was used. The LMAT model was the runner-up in many cases, while competitive with the other static models, SCAN, Hilbert and Z-Curves. However, there is a large difference in localization error between these static models and MAALRH. MAALRH showed a higher localization error rate because of the nature of its designed path. As shown in Figure 2.11, the UNs that are located in the corners of the deployment area will not be able to receive enough localization information; hence, less accurate positions will be estimated. The RWP demonstrated the highest localization error rate in every single run due to its random movement that prevents many nodes from having complete estimation information. In Figure 3.3b when WCL was used, our proposed model showed lower standard deviation values, which means they are closer to the average. The other static models, except MAALRH, move up and down with each run. However, SCAN and Hilbert showed lower values for most times in comparison to LMAT and Z-Curves.

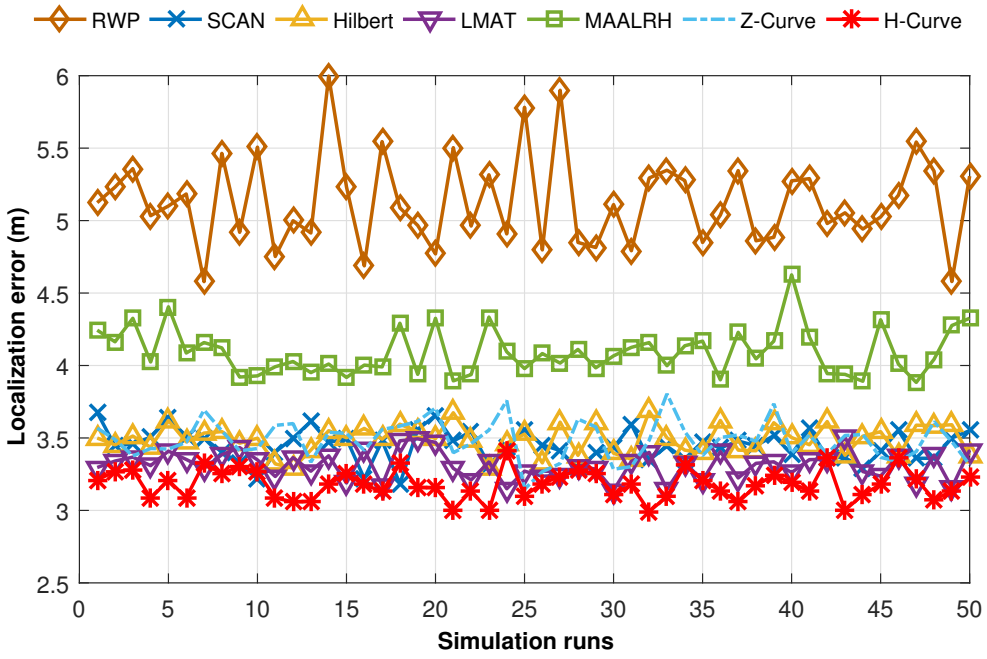

(a)

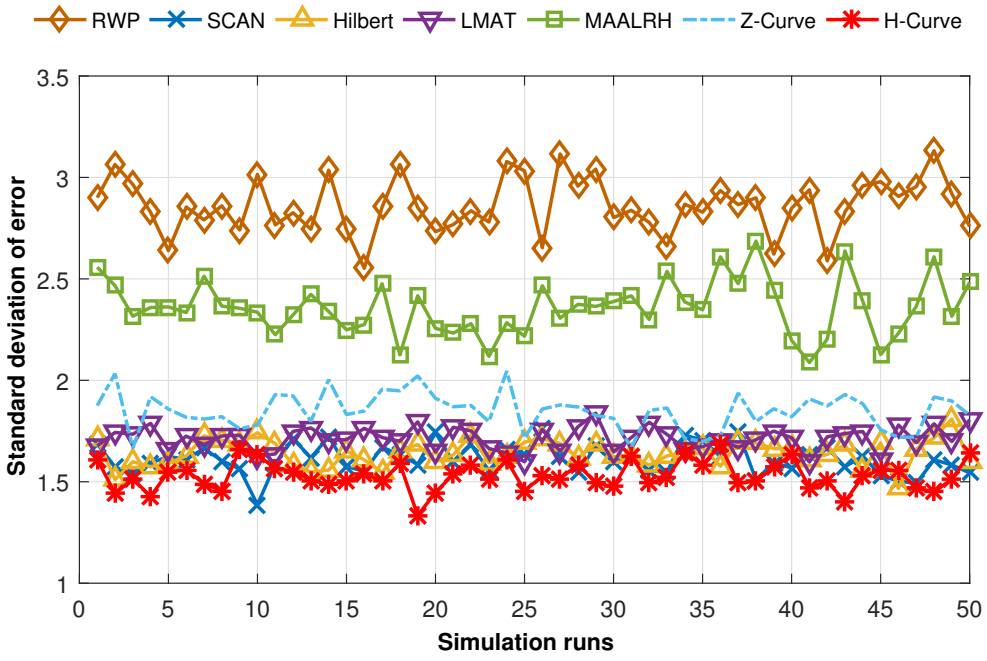

(b)

Figure 3.3: Localization errors and standard deviations of all movement strategies in WCL, ($R = 1, \sigma = 3$)

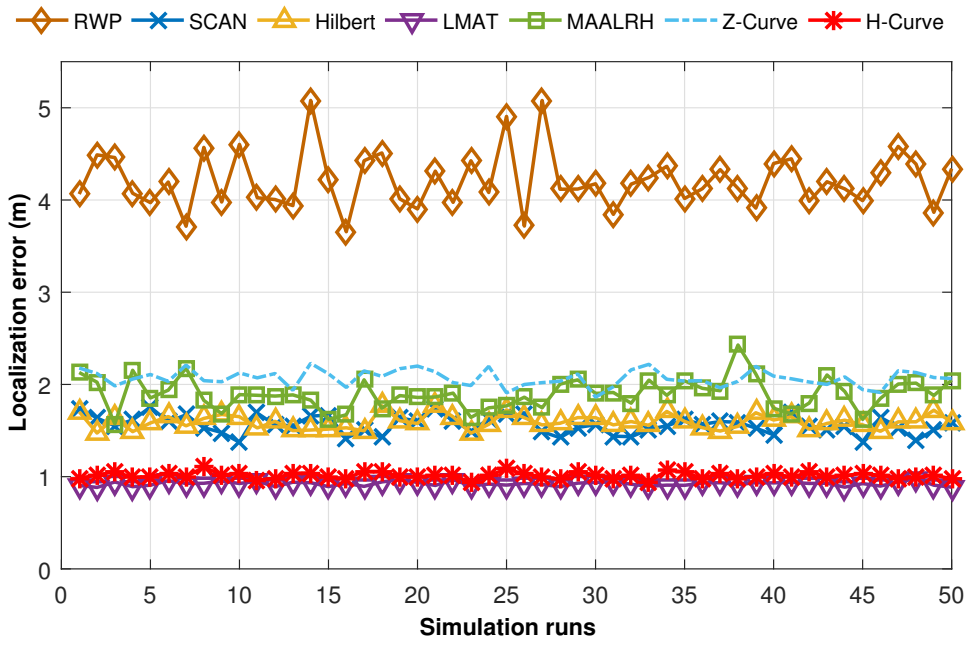

(a)

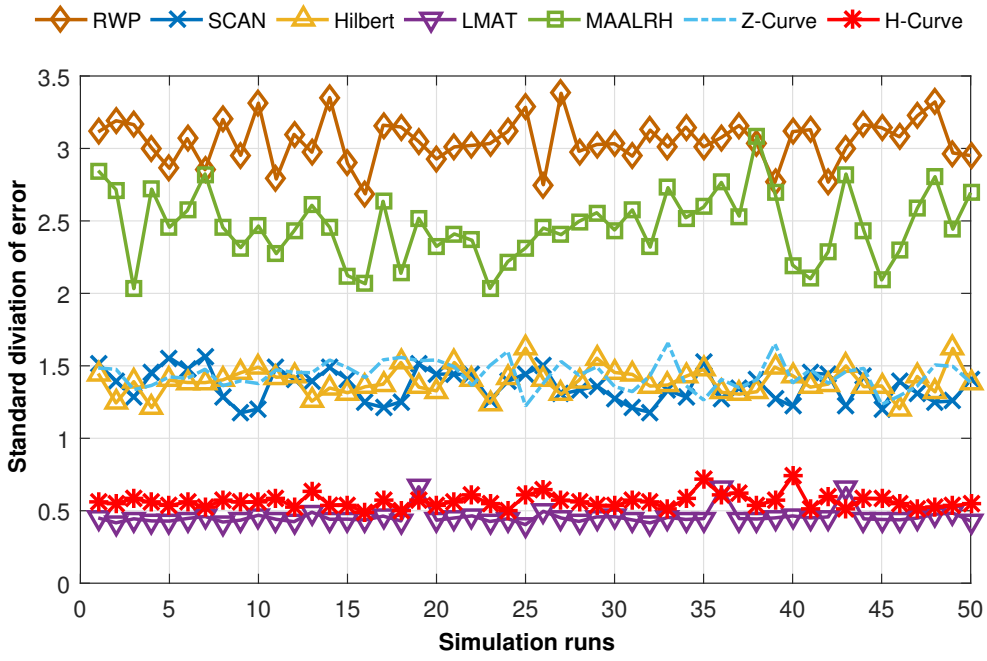

(b)

Figure 3.4: Localization errors and standard deviations of all movement strategies in WCWCL, ($R = 1, \sigma = 3$)

In Figure 3.4, we repeated the same test but with the WCWCL localization algorithm. In general, the path models were improved when this localization algorithm is used. Fewer localization errors occurred, which means more accurate locations were estimated. Our proposed model is in competition with the LMAT model, with a small advancement for LMAT, that is the average localization error for all 50 runs in LMAT is 0.917 m, while in our proposed model is 1.009 m. However, a positive point is the stability of the estimated locations in both models with different deployments of nodes. The other static models perform well when WCWCL is used. However, an important finding to notice here is the improvement of MAALRH when WCWCL is used. RWP gives the poorest results even though it performs better in WCWCL than the one in WCL. For the standard deviations, as shown in Figure 3.4b, LMAT and our model offered very small deviations, around 0.5 m from the average in most cases. The other three static models, SCAN, Hilbert, and Z-Curves, presented better results than those from when WCL is used. MAALRH and RWP tended to show higher standard deviations than the others because of their design since they leave some nodes unreachable.

For the average localization error, we used the parameters shown in Table. 3.1 with two changeable values, the resolution (R) and the standard deviation of noise (σ).

In the first experiment, we ran a simulation of 250 UNs with different resolution values ranging from 0.5 to 2 and σ = 3. Figures 3.5a and 3.6a show the average localization error for the path models when WCL and WCWCL are respectively used, while Figures 3.5b and 3.6b present the standard deviation of errors to the corresponding resolution and errors. With both localization algorithms, H-Curves and LMAT present the best results with small differences. The other static models share similar results with the exception of MAALRH, which performs less well than the others for the reasons that

were discussed above. RWP demonstrates the higher localization error rate, which means that is offers the least accurate locations. There are two main points to notice here. First, increasing the resolution value does not necessarily lead to increased accuracy as shown in the figures. Second, the random movement enables the RWP to perform better than the others when the resolution is 0.5, which means a decreased communication range. Figure 3.5b shows the standard deviation of the localization error when different resolution values of 0.5, 1, 1.5, and 2 were used with WCL and σ = 3. When R = 0.5, all models tended to offer low results in terms of standard deviation; thus, they were closer to the average. When the R value increased, the standard deviation of error increased in general except in one case, with LMAT when R = 1.5. However, the increase differs from one model to another. In all experiments, LMAT and H-Curve showed better results than the others. In WCWCL cases, as shown in Figure 3.6b, the models showed similar results when R = 0.5. Moreover, when R = 0.5, the WCL and WCWCL results were similar. But when R increased, both LMAT and H-Curve showed very small values of standard deviation of error that are very close to the average localization error. Indeed, when R = 1.5, our proposed model reached the best value with less than 0.7 m variation on average.

To prove the statistical significance, the CI of the localization error is also used. A 95% of CI is chosen to test that significant. Figure 3.7 shows again the localization error while the error bars depicted in the figure this time illustrate the 95% confidence interval. The results show that in most cases, the proposed model provides a narrower CI, which implies that the improved performance is statistically significant. This is applicable on both localization techniques of WCL and WCWCL.

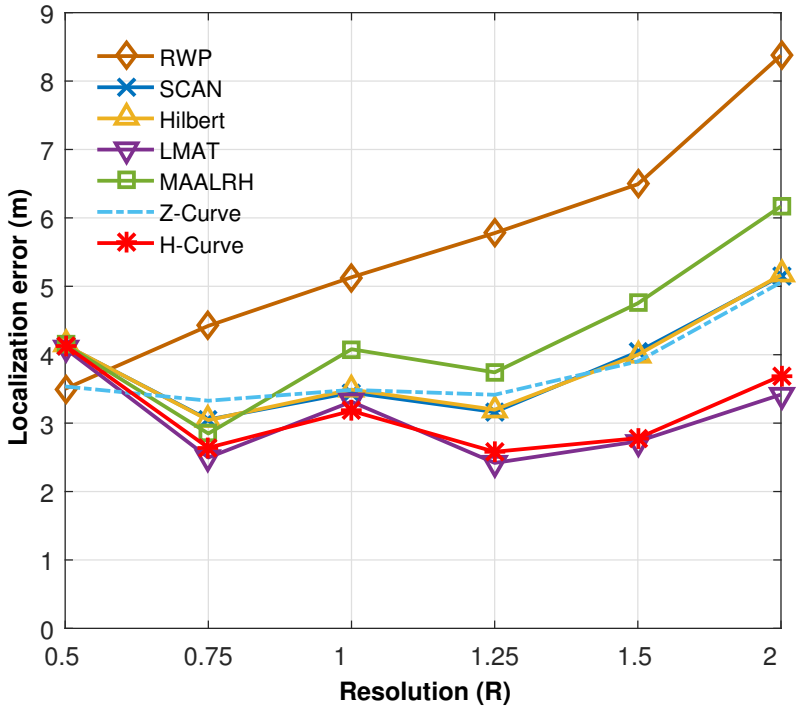

(a)

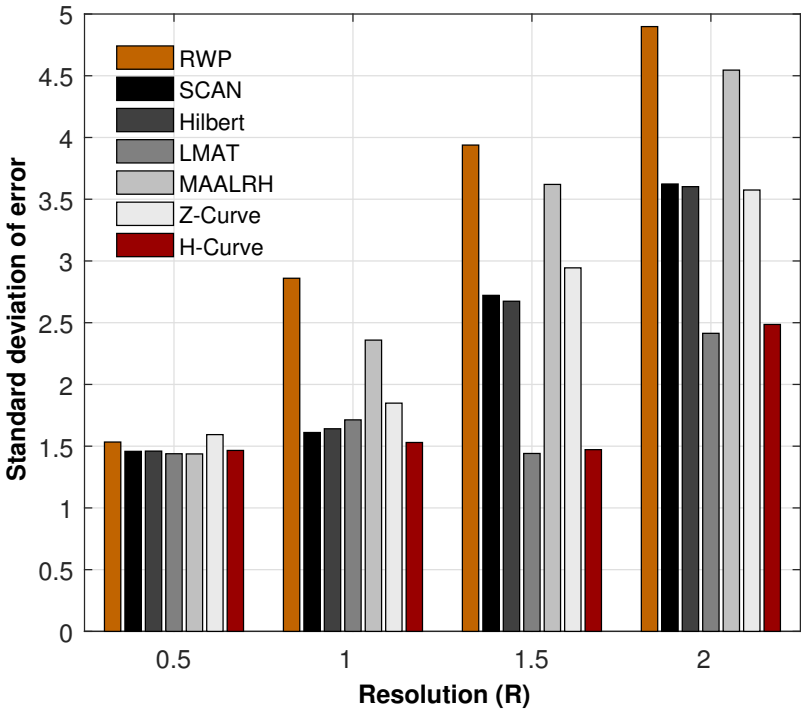

(b)

Figure 3.5: Average localization errors and standard deviation of errors with the corresponding Resolutions in WCL

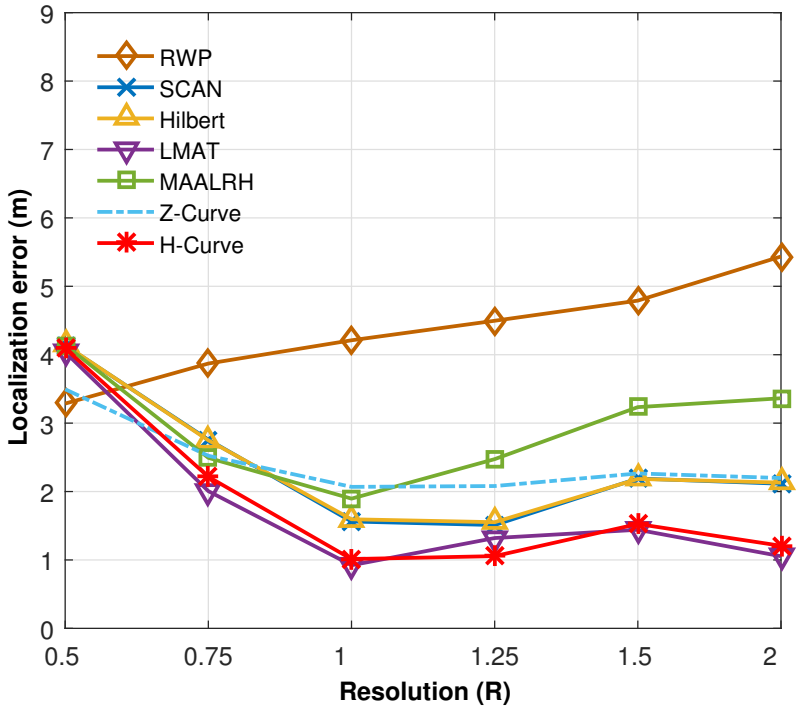

(a)

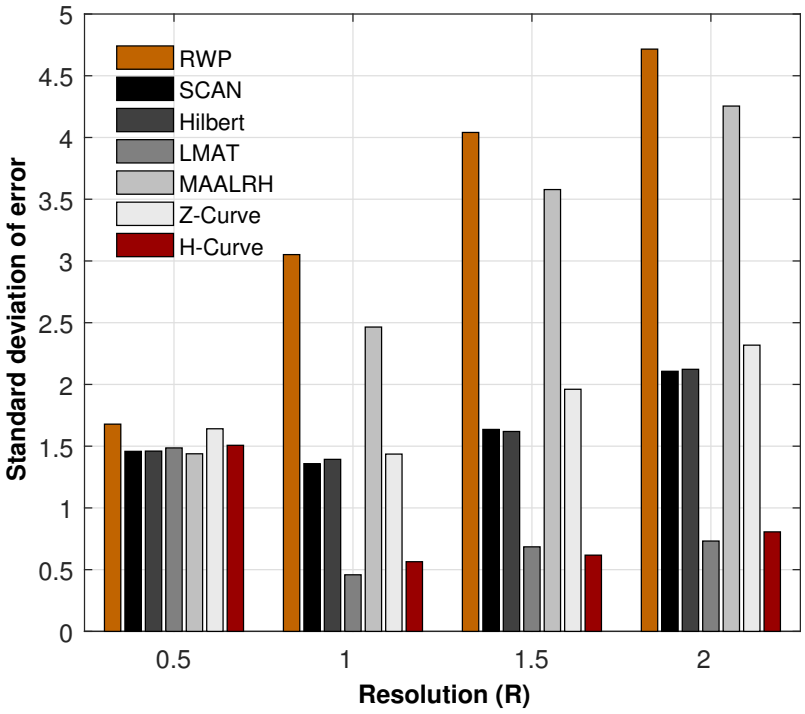

(b)

Figure 3.6: Average localization errors and standard deviation of errors with the corresponding Resolutions in WCWCL

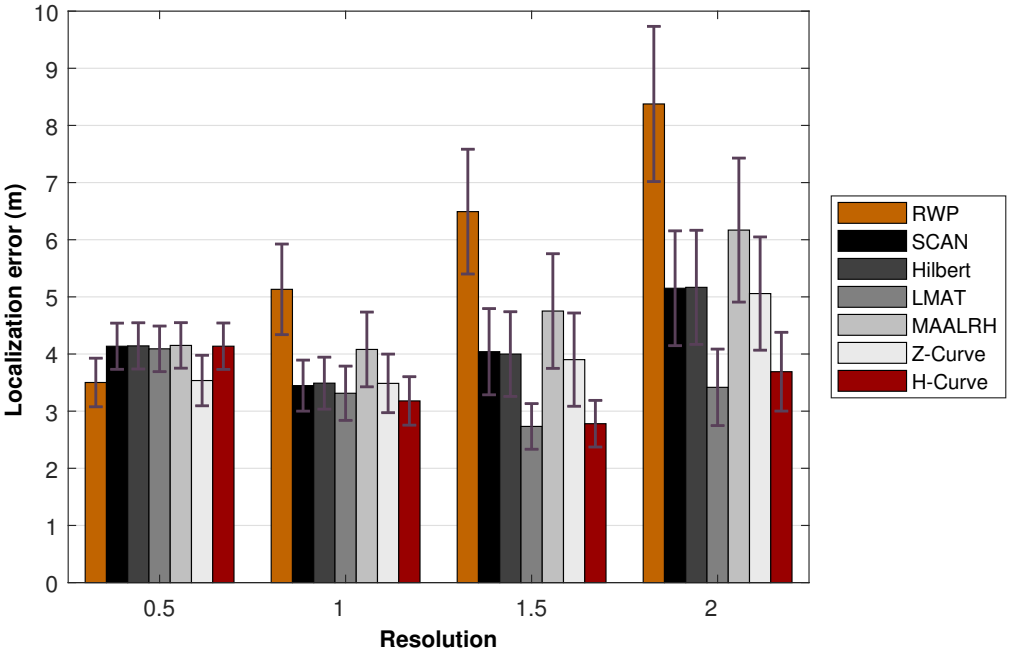

(a)

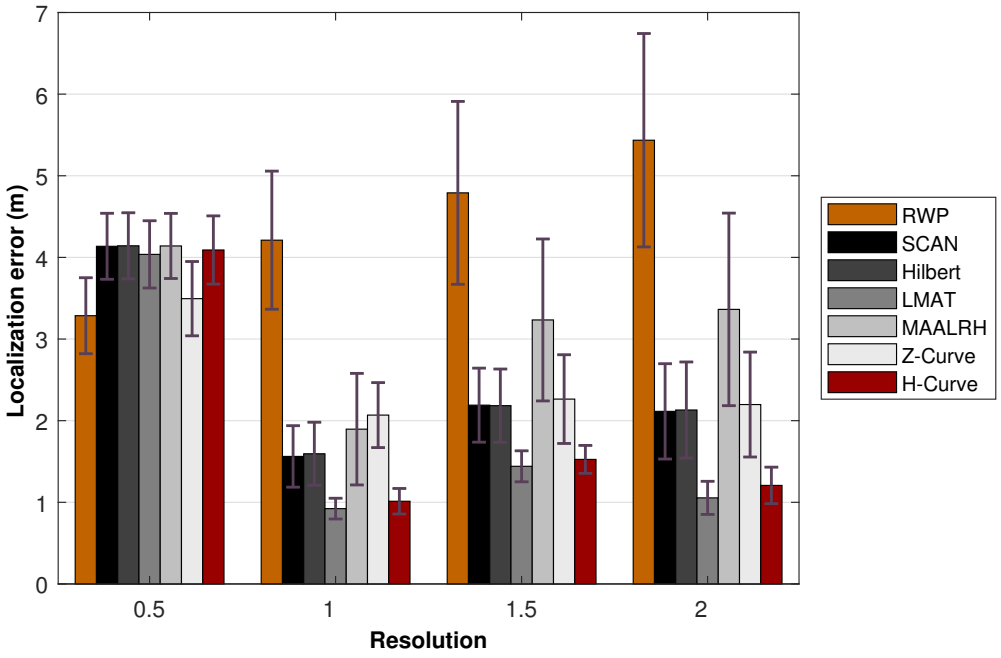

(b)

Figure 3.7: Average localization errors and the 95% confidence interval with the corresponding Resolutions in (a) WCL, and (b) WCWCL

For the second experiment, in Figure 3.8 we repeat the same parameters with a fixed resolution value (R) of 1 and a different standard deviation of noise (σ). Figure 3.8a shows the average localization error rate for the mobility models with a different standard deviation of noise (σ) when the WCL algorithm is applied, and Figure 3.8b shows the same as when WCWCL is applied. In the first algorithm, our proposed model, the H-Curve, outperformed the other models with the lowest localization error rate, which resulted in the most accurate estimates with less than 3.5 m in all runs regardless of the change of the standard deviation of noise (σ) as shown in Figure 3.8a. LMAT offered similar results and was also unaffected by the change in standard deviation of noise (σ). The other static models, including SCAN, Hilbert and Z-Curves, offered similar localization error values of around 3.5 m. MAALRH again demonstrated less accurate estimates than the other static models, while RWP offered the least accurate estimates. In WCWCL in Figure 3.8b, H-Curve and LMAT showed a small localization error of about 1 m only, with a small advantage of LMAT. The positive point here is that using WCWCL helps MAALRH to improve its estimation accuracy in comparison to the WCL algorithm. With the change of standard deviation of noise (σ), the Z-Curve offers reduced localization accuracy when WCWCL is used as compared with WCL.

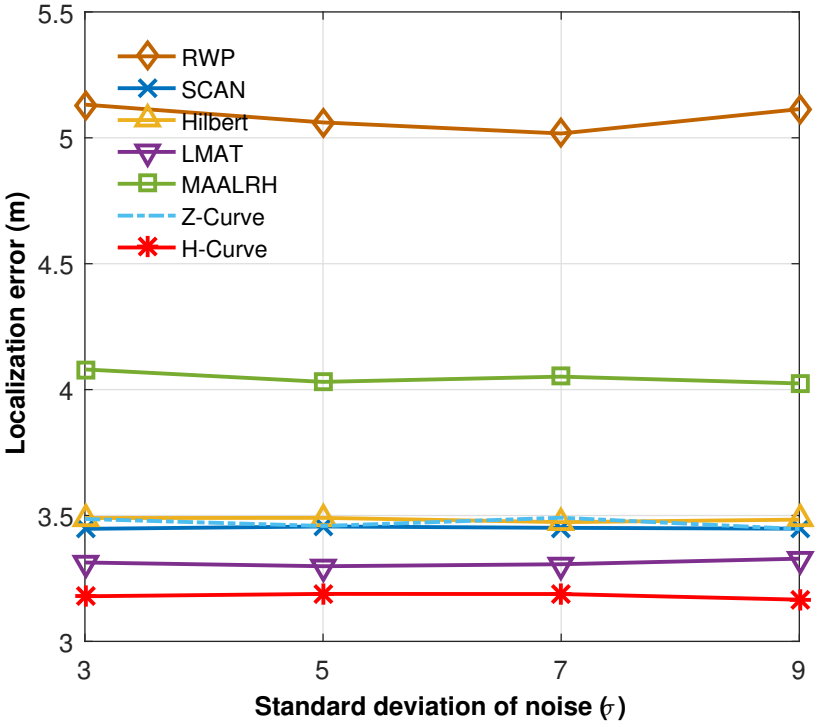

(a)

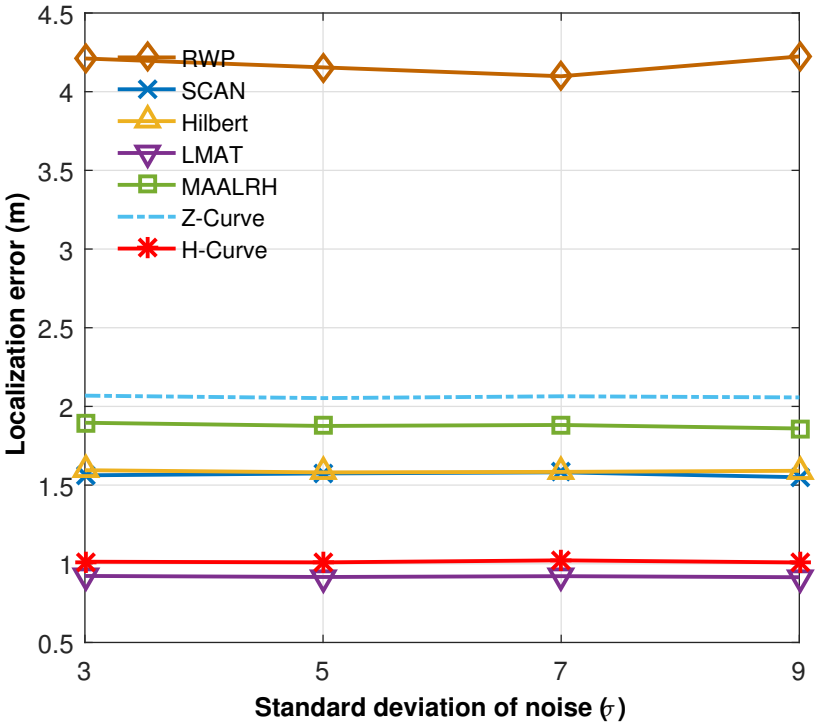

(b)

Figure 3.8: Average localization error of all movement strategies vs the standard deviation of noise (σ) in (a) WCL, and (b) WCWCL

3.5.2 Precision

The localization precision metric is defined as the ratio of how many specific accuracy values are reached [3]. We considered four localization error values that were $< 1.5\ m$, $< 3\ m$, $< 4.5\ m$ and $< 6\ m$. With each localization error value, we calculated the ratio of how many values were achieved. Figure 3.9 shows the result of the precision when R is 1 and σ is 3.

As in Figure 3.9a, none of the models achieved a localization error of $< 1.5\ m$ when the WCL algorithm was used. However, a small improvement in the H-Curve and LMAT models was found when $< 3\ m$ was considered. All of the static models achieved the highest precision ratio when a localization ratio of 4.5 m was used, except MAALRH, which still showed a precision ratio close to 1. RWP was not able to reach the full ratio except in the case where the localization error rate was around 6 m. In WCWCL, as in Figure 3.9b, the highest precision ratio was reached for both H-Curve and LMAT when the localization error was 1.5 m or less. Compared to the previous localization algorithm, both SCAN and Hilbert achieved better results with some values $< 1.5\ m$. However, a large improvement occurred when considering 3 m of localization error, where all static models reached the highest precision ratio. Using WCWCL helped RWP to improve its precision when $< 4.5\ m$ and $< 6\ m$ are considered.

3.5.3 Localization Ratio

In this scenario, we used 250 UNs and different resolutions with a fixed value of σ of 3. Since the localization ratio is almost the same in both WCL and WCWCL, only one of them is shown. Figure 3.10 presents the localization ratio for the implemented path models.

When WCL and WCWCL were used with $R = 0.5$, none of the mobility models successfully localized all of the UNs. However, Z-Curves and our proposed model reached a high localization ratio with about 80% and more. The point here is that, while Z-Curves perform less well than the other static models, except MAALRH,

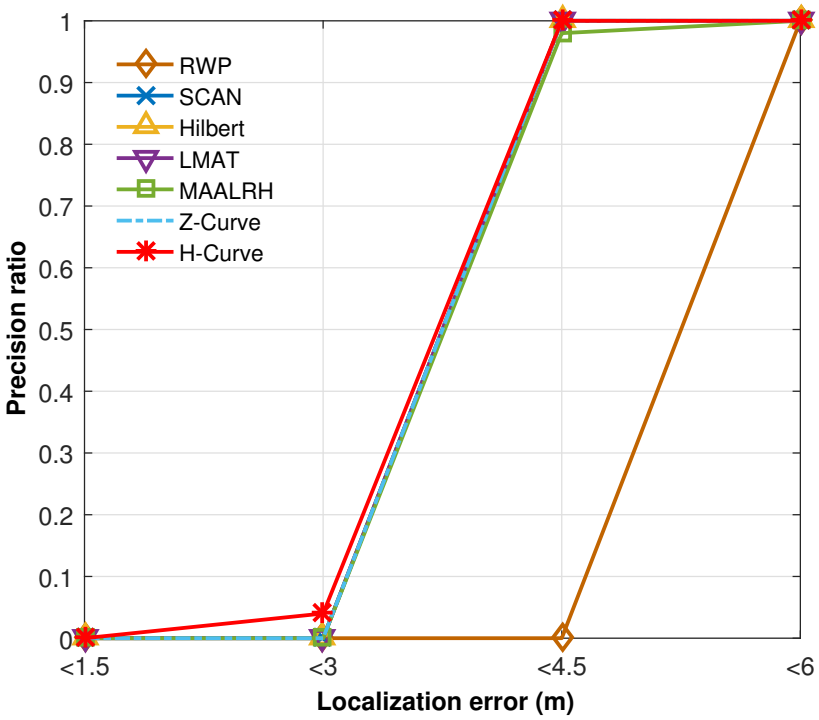

(a)

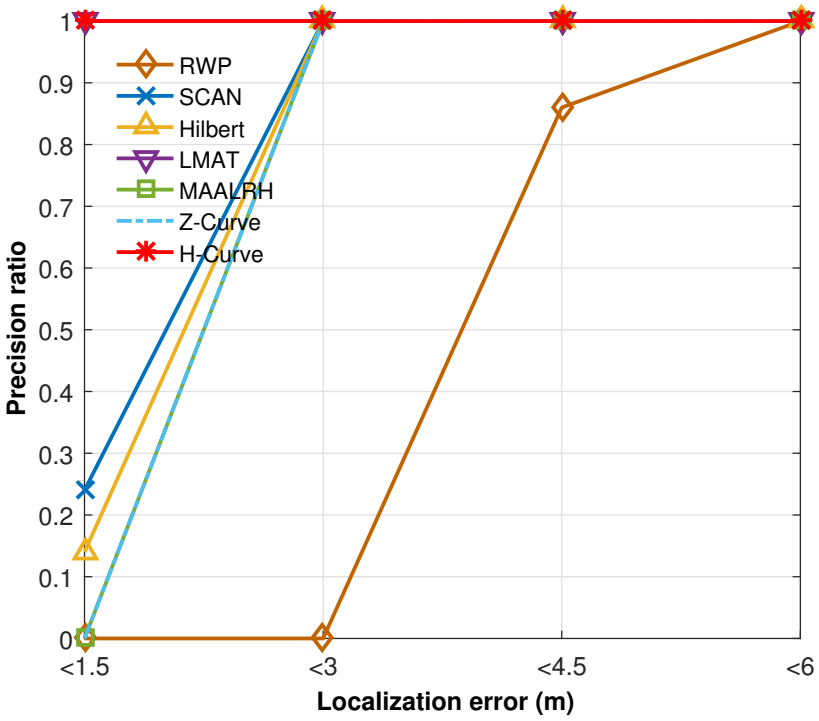

(b)

Figure 3.9: Precision ratio of all movement strategies with the corresponding localization error in (a) WCL, and (b) WCWCL

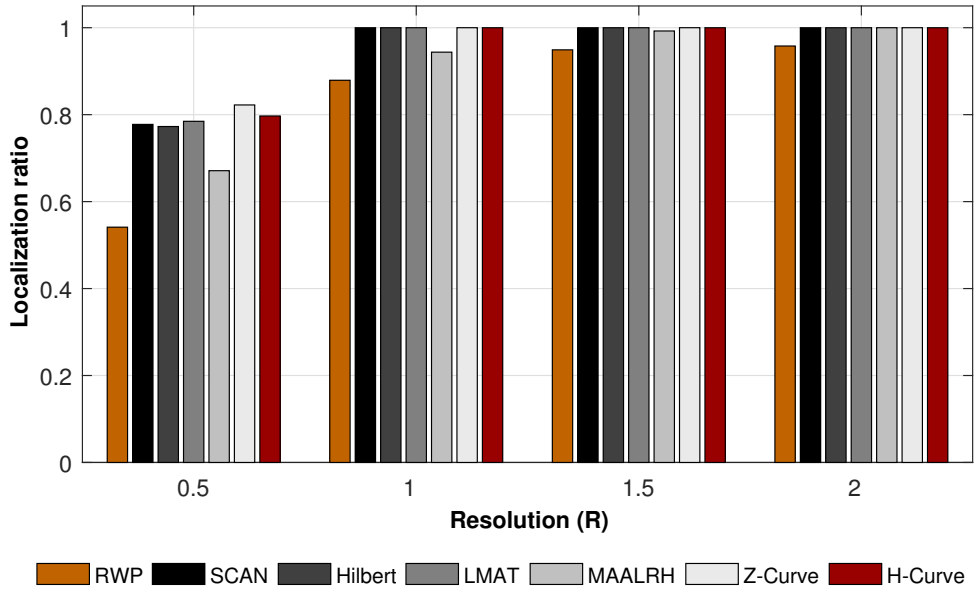

Figure 3.10: Localization ratio of all movement strategies in WCL and WCWCL

in some experiments shown above, it does well here with the highest localization ratio when $R = 0.5$. Increasing the resolution increases the localization ratio. When $R = 1$, all models provided fully localized nodes except MAALRH, which was unable to localize the UNs in the corners of the area, and RWP because its movement is unpredictable. Thus, RWP will never be able to assist all UNs to estimate their locations even if the resolution is doubled to 2. Unlike RWP, MAALRH is able to localize almost all nodes when resolution is 1.5.

3.5.4 Path Length

Although path length does not affect the localization error rate or the number of localized nodes directly, it helps to determine the time needed for the localization process to be completed and may affect other critical metrics such as energy consumption. We calculated the path length according to their design and based on two variables, the network size, S, and the distance between each two points, dm.

In the following equations, we show the path length calculation for each static mobility model. Eq. 3.2 shows the path length calculation for SCAN while Eq. 3.3 shows the path length of Hilbert. Eq. 3.4, Eq. 3.5, and Eq. 3.6, show the path length for LMAT, MAALRH and Z-Curves, respectively. In Eq. 3.7, our H-Curve's path length is shown.

$$L_{SCAN} = \frac{S^2}{dm} - dm \tag{3.2}$$

$$L_{Hilbert} = \frac{S^2}{dm} \tag{3.3}$$

$$L_{LMAT} = \frac{S^2}{dm} + \frac{S}{5} \times dm \tag{3.4}$$

$$L_{MAALRH} = \frac{3}{4} \times \frac{S^2}{dm} + \frac{3}{2}S + 4dm \tag{3.5}$$

$$L_Z = \left[\left(\frac{5}{8} \times 4^3\right) - 1 \right] dm + \left[\left(\frac{5}{8} \times 4^3\right) \right] \times \sqrt{2}dm \tag{3.6}$$

$$L_H = \frac{S^2}{dm} + 18dm \tag{3.7}$$

We set the RWP's number of anchors to be equivalent to our model's in order to get comparable results. Figure 3.11 shows the path length in m for all mobility models.

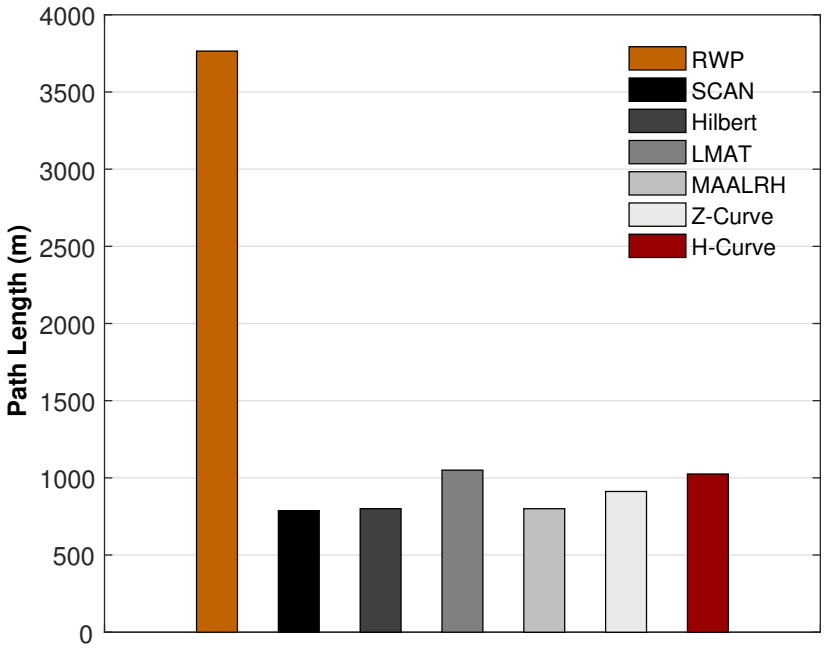

Figure 3.11: The path length for the different mobility models

As shown, RWP travels a long distance around the network with no particular direction with more than 3700 m. The other static models travel shorter distances in contrast to RWP, with 787.5 m for SCAN, and 800 m for both Hilbert and MAALRH. Z-Curves takes somewhat longer with about 912 m of traveling. LMAT and H-Curves take longer trips than the other static models. However, H-Curves gives better results than LMAT with only 1025 m of traveling distance as compared to 1050 m in LMAT.

3.5.5 Energy Consumption

For the energy consumption model in this work, we used a similar model to the one used in [78]. We used the specifications of the low-power wireless mote CC1100 [77]. Because the energy consumption difference in both WCL and WCWCL is insignificant, only the consumption in WCL is shown.

A. Energy consumption by UNs

To calculate the energy consumption for the regular nodes, we need first to calculate the energy consumed per receiving one bit value, E_{rec}, as

$$E_{rec} = P_{rec} \times \frac{P_{size}}{datarate} \tag{3.8}$$

Where P_{rec} and P_{size} are the value of the received power and the packet size, respectively.

By multiplying this energy into the average number of received messages, M_{rec}, we can get the energy consumption for the deployed nodes as

$$E_{nodes} = M_{rec} \times E_{rec} \tag{3.9}$$

According to CC1100 specifications, the value of the received power P_{rec} is 15.5 mA, and the data rate is half of the baud equivalent to 125 $kbps$. We assume a packet size (P_{size}) of 160 $bits$, which is smaller than that assumed in [11].

Figure 3.12a shows the average energy consumption per node for each mobile model. Since the calculation here depends on the total energy spent in localized nodes only, RWP seems to consume less energy than the others. MAALRH comes next in total energy consumption in localized nodes with less than 10 μJ when $R = 0.5$ is used and less than 14 when R is 1. However, both RWP and MAALRH consumption increase when R increases. The energy consumption for the other static models, including H-Curves, was approximately 14.5 μJ, except for a small variation when $R = 0.5$. Overall, the energy consumption of the UNs is not significant. However, taking into account a larger number of nodes will raise the energy consumption gradually.

B. Energy Consumption by MAs

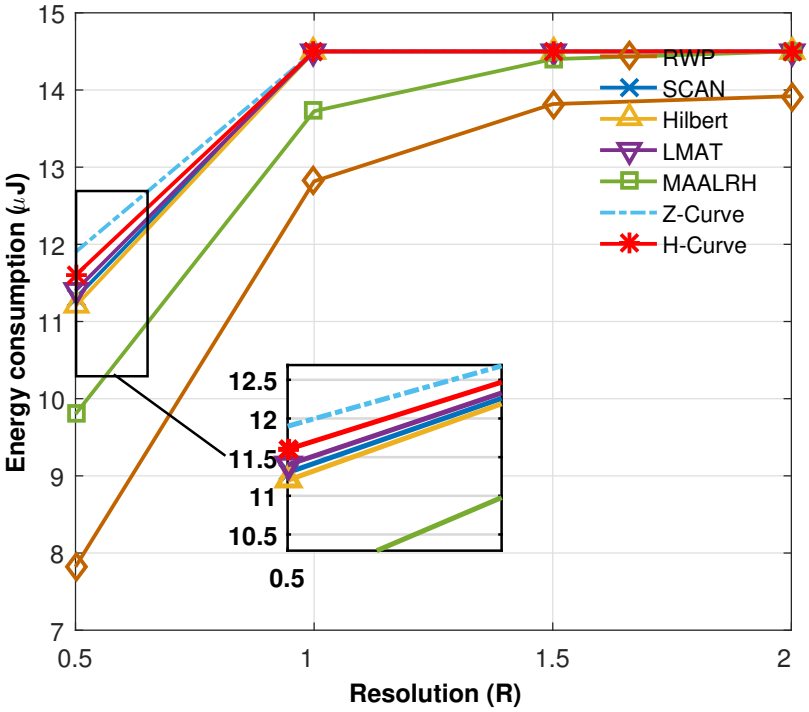

(a)

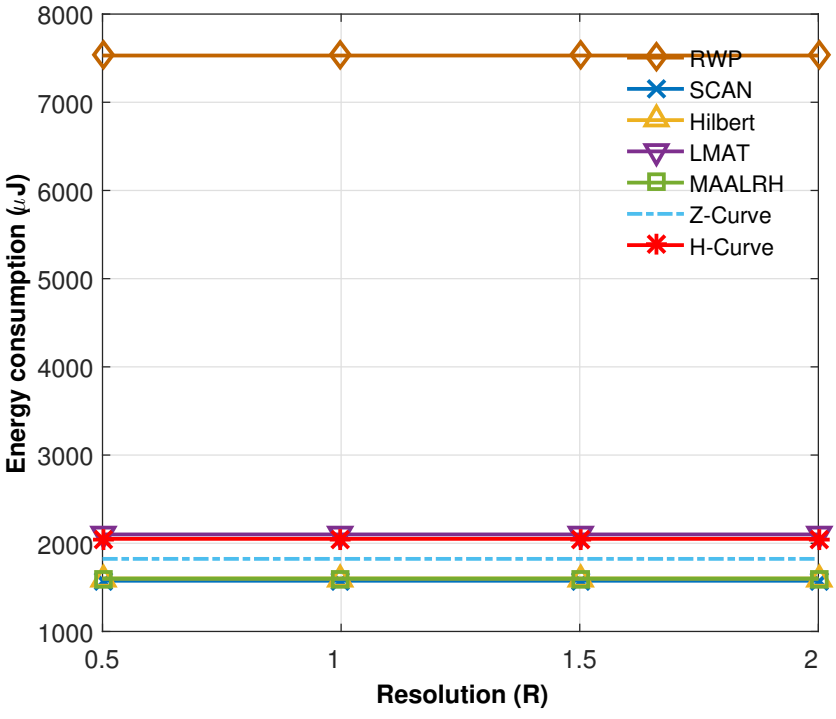

(b)

Figure 3.12: Energy consumption for all movement strategies in: (a) energy consumption in all localized nodes, (b) energy consumption by the anchor in each model

For the MA, the energy consumption can be derived from two parts, the energy spent in the connection process with the deployed nodes, E_{send}, and the energy needed for movement around the area, $E_{movement}$. Hence, the total energy consumption of the MA is

$$E_{anchor} = E_{send} + E_{movement} \tag{3.10}$$

The energy required for messages to be exchanged between the MA and the UNs is calculated as

$$E_{send} = M_{trans} \times E_{trans} \tag{3.11}$$

Where M_{trans} and E_{trans} are the number of transmitted messages and the energy consumption for transmitting each message, respectively. This value, E_{trans}, is calculated using the value of transmitting power, P_{trans}, which is 16.5 mA in CC100, multiplied by the packet size over the data rate.

$$E_{trans} = P_{trans} \times \frac{P_{size}}{datarate} \tag{3.12}$$

The second part, the energy needed for movement around the area, is calculated as

$$E_{movement} = L_{path} \times E_{pm} \tag{3.13}$$

Where L_{path} is the path length for each mobility model, and E_{pm} is the energy consumption for moving one unit of distance (m here). We assume that the energy consumption for traveling per 1 m is 2 J [78,79].

Figure 3.12b presents the total energy consumption by the anchor in each model. Because most energy is spent in traveling, the energy spent in communication goes unnoticed. The longer the traveling distance, the greater

the energy consumed. RWP spends a large amount of energy in comparison to the others with more than 7500 μJ consumed. This is because RWP travels about 3765 m in its journey around the network. The static models seem to be divided into three levels based initially on their path length and, thus, their energy consumption. SCAN, Hilbert, and MAALRH are similar to each other with less than 1600 μJ consumed, while Z-Curves uses more energy at approximately 1822 μJ consumed. Our model, H-Curves, and LMAT both consume approximately 2000 μJ for their anchor node movement. To create a larger picture regarding the energy consumption, we chose to calculate the average energy consumption of localized nodes. The average energy consumption for each mobility model is estimated as

$$E = \frac{E_{nodes} + E_{anchor}}{RN} \tag{3.14}$$

Where RN is the number of localized nodes.

C. Average Energy Consumption by Localized Nodes

Figure 3.13 shows the average energy consumption by localized nodes in each model. For the total amount of energy spent by both sensors and MAs, RWP is the highest energy consumer even though this energy consumption decreases by increasing R. For the other static models, the distinction between them is very small and insignificant. Consequently, and taking into account the other metrics of our model, it is not affected by energy consumption. Figure 3.14 shows the energy consumption of the UNs to the localization ratio in each model when R = 1 and σ = 3.

3.6 The Trade-Off between the Localization and the Designed Mobile Path

Impact of path models on localization in WSNs has been discussed in a number of studies including [55, 65, 78]. They show that the performance of a localization

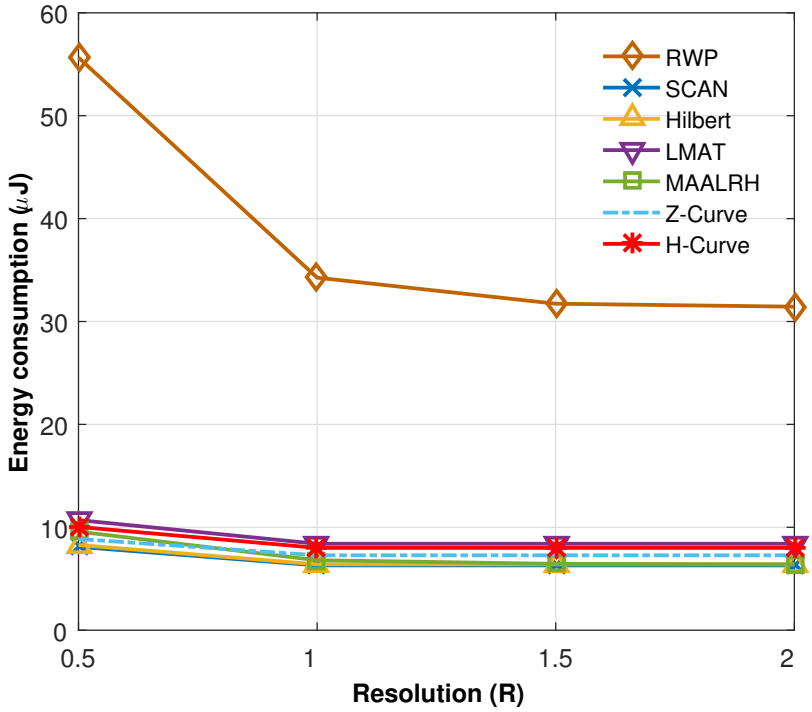

Figure 3.13: the average energy consumption per the number of localized nodes

model will be affected by the designed mobility path including the accuracy of the localization and the localization ratio. However, in this study and based on the obtained results, we observe that there is also an impact of the applied localization model on the performance when a path planning model is used. This means that the results will vary when different localization techniques are used even though the same mobility model is used. Let us take another look, for example, to Figures 3.3a and 3.4a. In Figure 3.3a, H-Curves model gives better results than the other models with localization errors ranging between 3 to 3.5 m when WCL is used. However, when WCWCL is used, the localization errors will decrease to values around 1 m as shown in Figure 3.4a. WCWCL provides almost stable results in all the 50 runs. Another point here is that in some cases the localization technique used may give an advantage to one path model over another. For example, in Figure 3.8a, Z-Curves mobility model offers better results when WCL is used in comparison to MAALRH, however, MAALRH performs better when WCWCL is

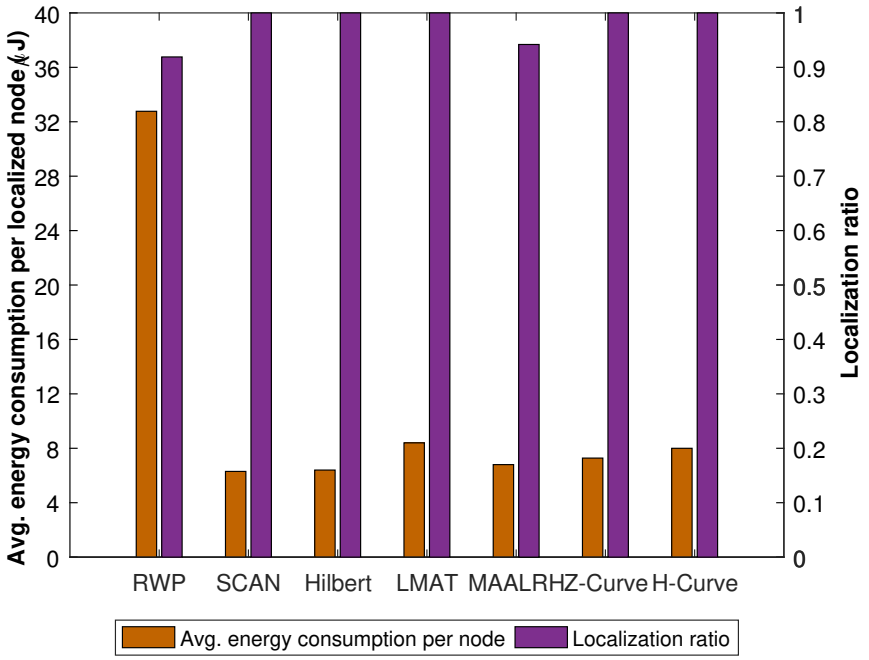

Figure 3.14: Energy consumption of the UNs to the localization ratio in each model ($R = 1, \sigma = 3$)

used as presented in Figure 3.8b. The same is true of of the precision ratio, and localization ratio as well. There is no impact on the mobile path length since the mobile path is not changed and remains static. To sum up, the trade-off between the localization and the designed mobile path should be considered to determine which technique is more suitable for the designed path.

3.7 Conclusion

In this chapter, we introduced a new path planning model, called H-Curves, for mobility-assisted localization in WSNs. Our model guarantees that all UNs can estimate their location with high accuracy and precision, and provides good coverage and low energy consumption. The model is static, which means the MA will not change its path during its movement. The proposed model guarantees that a large portion of UNs are able to estimate their locations based on the information

provided by the MA. This guarantee comes with high accuracy that is led by a small localization estimation error. Compared with other random and static models, our model shows superior result in metrics such as precision, which refers to the ratio of how many times a specific accuracy value is achieved. As compared to other models, H-Curves offers high precision ratio regardless of the localization error in both WCL and WCWCL localization techniques. Coverage is used to ensure the number of localized nodes. Again, regardless of the resolution values, R, H-Curves shows competitive results. Finally, we studied energy consumption in this work. We assume that energy consumption occurs on both sides, in the nodes and the MA. Our model shows energy consumption similar to other models while attaining a better ratio of localized nodes. Indeed, our model consumes less energy than LMAT.

Chapter 4

Three-Dimensional Path Planning Model for Mobile Anchor-Assisted Localization in Wireless Sensor Networks

4.1 Preface

In this chapter, we propose a new path planning model for mobile anchor-assisted localization in WSNs where node deployment occurs in 3D areas. Our proposed static model shows higher localization estimation accuracy, and thus lower localization error in comparison to other similar models.

In many real-world applications, sensors are distributed on planar surfaces where three-dimensional (3D) planes are observed [34,35]. Examples of these surfaces as stated in Section 2.2.1, involve indoor uses, such as floors, walls, tables and doors, and outdoor purposes such as mountains, valleys, hills, and forests [34,35]. Similar to [80], some of the potential applications of our proposed model can be shown as other sensor network tasks. For example, our model can be used to draw a map of the nodes' location to help in 3D geographic routing or to enhance network connectivity by providing nodes with their neighbours' locations.

Section 4.2 presents the network model and assumptions, while section 4.3 shows our proposed model. Section 4.4 shows in detail the performance metrics while Section 4.5 evaluation and the results. Finally, section 4.6 includes future work and the conclusion.

4.2 Network Model and Assumptions

The network area is represented as a three-dimensional field with a side length, S in m. A uniformly distributed set of UNs, N, are spread around the network.

Initially, sensor nodes are not location aware. The UNs are assumed to remain static and do not change their location after the first distribution. Each network contains a fixed number of anchors, M. All anchors can determine their location within the network area. Each MA is able to move freely, in straight lines, in any direction in the network following its path model. For simplicity, we assume that the network area does not contain obstacles that could restrict anchor mobility. The UNs and anchors can connect to each other only if they are located within the same transmission range, R_{Tx}. The UNs cannot share anchor locations with each other. The MAs stop frequently within a fixed distance between each two points, defined as dm. The MAs are not energy constrained.

4.3 Three-Dimensional Path Planning Models for Mobile Anchor-Assisted Localization

This work is intended to design a 3D path planning model for mobility-assisted localization in WSNs. The concept of this work is derived from the 2D path planning for mobile anchor-assisted localization in [9]. Our model consists of several layers L equals to

$$L = \frac{S}{d_m} \tag{4.1}$$

where S is the side length of the network and d_m is the distance between each two points (or layers). To overcome the problem of collinearity, we propose our model to let the MA follow an H-shape with a winding path each time. In 2D scenarios, at least three different points are needed to estimate a node's location; however, in 3D scenarios, at least four points are needed for the estimation. Figure 4.1 shows the proposed model in one layer as in Figure 4.1a and full layers as in Figure 4.1b. For a better representation, we extend the distance between layers to be $2d_m$ in Figure 4.1.

The proposed model works in three simple stages: the mobility movement stage, the localization information exchange stage, and the localization estimation

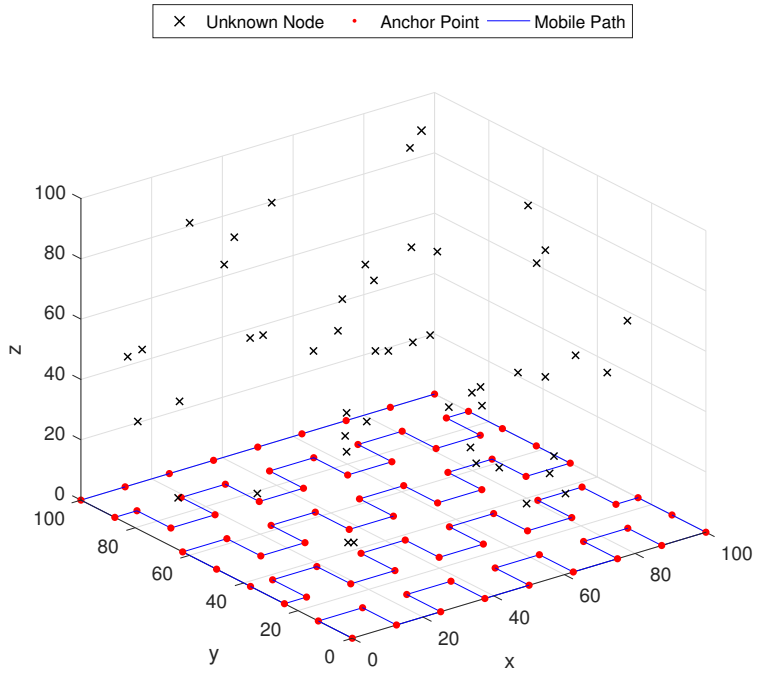

(a)

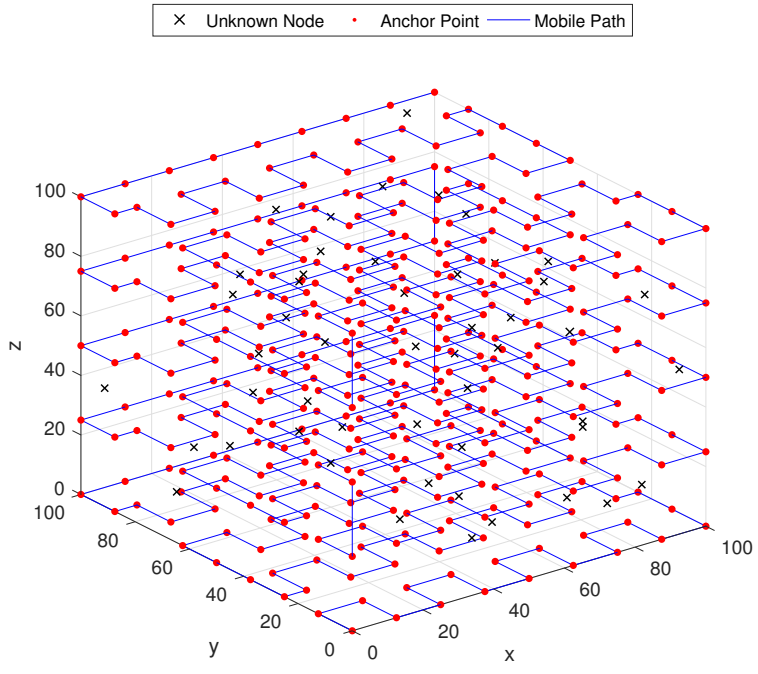

(b)

Figure 4.1: The proposed mobile path model in (a) one layer, and (b) full layers

stage.

4.3.1 Mobility movement

In this stage, the MA leaves the starting point at a corner of the network and moves in one direction, *say* $y - coordinate$. In each step, the MA will make one movement with a travelling distance d_m. The value of d_m remains fixed all the time. After this step, the MA will make another turn toward another direction, *say* $x - coordinate$. The same procedure will be repeated until reaching the border of the network, which means a row of points is completed. It is then time for another row, and so the MA will take a step to form another row, toward the $y - coordinate$ in this example. The MA will go back in the reverse direction of $x - coordinate$, however, it will take $0.5 \times d_m$ only; this is important to prevent the points from being collinear. The same movement will be repeated until reaching the last corner of the deployment area. Here, the MA will move to form another layer by increasing the third coordinate, $z - coordinate$, by d_m. The movement will be taken in the reverse direction until reaching the starting point of the x and $y - coordinates$ with the current $z - coordinate$. The same procedure will be done until reaching a set of layers that is equal to L.

4.3.2 Information Exchange

In 2D scenarios, when three different points are known, the UN can estimate its own location [9]. However, in 3D environments, the UN can estimate its location when four different points are reached. Thus, in each movement, the UN in the communication range of the MA exchanges the location information, stores it, and waits for the next localization information.

4.3.3 Localization estimation

As mentioned above, once four different localization messages are received by a UN, it can start estimating its own location in accordance to the localization technique used.

The procedure is summarized in the following Algorithm 1.

Algorithm 1 MA movement and UNode localization

```
1:  procedure NODE LOCALIZATION
2:      Nodes deployment
3:      MA movement
4:      UNode receives localization message
5:      if ReceivedMessages < 4 then
6:          UNode keeps waiting
7:          go back to 3
8:      Localization estimation
9:      if MAmovement ≠ lastpoint then
10:         go back to 4
11:     Movement ends
12:     Localization done
```

4.4 Performance Setting

To evaluate the performance of our proposed model, we implemented it along with three other models: 3D-RWP, layered-SCAN, and 3D-Hilbert. For fair comparison, two localization techniques were used: the weighted centroid localization (WCL) algorithm [49] and the Weight-Compensated Weighted Centroid Localization (WCWCL) algorithm [45].

For simulation, we used the Matlab environment with 50 run times. A set of 250 UNs, N, is assumed to be deployed in a 3D area with a side length, S, of 100 $m \times 100$ $m \times 100$ m. A single MA, M, is used to traverse the network and exchanges its location with other nodes. Different resolution values, R, are used. The resolution value, R, represents the relation between the communication range, R_{Tx} and the distance between every two points, the d_m of each path. It can be

Table 4.1: Simulation values and parameters in 3D H-Curves

Parameters	Symbol	Value
Network Side Length (m)	S	100
Number of MAs	M	1
Number of UN	N	250
Resolutions	R	0.5, 0.75, 1, 1.25, 1.5, 2
Path Loss Exponent	β	3.5
Power Loss at d_0 (dB)	PL(d_0)	-60
Reference Point (m)	d_0	1
Standard Deviation of Noise	σ	3
Simulation Run		50

derived as

$$R = \frac{R_{Tx}}{d_m} \tag{4.2}$$

We used a realistic wireless channel by applying the specifications of a wireless node equipped with a Chipcon CC1100 radio module [77]. The rest of the parameters are shown in Table 4.1. The simulation tool and parameters were chosen to be consistent with other similar works.

4.5 Evaluation Results

We evaluate the path planning model's performance in two metrics: the average localization error, and the standard deviation errors. All results are based on the average of the simulation run, 50 times.

A. Average Localization Error

In the three dimensional scenarios, the node localization error is estimated as

$$error_{(i)} = \sqrt{(x_i - u_i)^2 + (y_i - v_i)^2 + (z_i - w_i)^2} \tag{4.3}$$

Where (x_i, y_i, z_i) are the real coordinates of the node i, and (u_i, v_i, w_i) are the

estimated coordinates of the same node i.

The average localization error, $error_{avg}$, will be the same as before and is calculated as:

$$error_{avg} = \left(\sum_{i=1}^{N} error_{(i)} \right) / RN \tag{4.4}$$

Figure 4.2a shows the average localization errors and the corresponding resolutions in all models when WCL is used. All path models offer close localization errors between 4 and 5 m when R = 0.5; however, this distinction between the different models increases when the resolution increases. Our proposed model offers lower localization error when R = 0.75 to 2. Our model guarantees that all nodes can receive the localization information and can solve the collinearity problem. The nature of movement in RWP increases the localization error in 3D-RWP since there is no guarantee that all nodes can receive the localization information. Layered-SCAN and 3D-Hilbert perform similarly when WCL is used. When WCWCL is used, as shown in Figure 4.2b, better localization estimation in all path models is achieved except in the case where R = 0.5. Layered-SCAN and 3D-Hilbert perform similarly again, however, the impact of collinearity in Layered-SCAN as in [75], is shown here. 3D-Hilbert was proposed to solve the collinearity problem in localization, but the improvement is relatively small. In all other cases, our proposed model shows superior results over the others, particularly when our model reaches the lowest point of localization error of 1.17 m when R = 1.25. The other models act similarly to the ones in WCL, but with lower errors.

B. Standard Deviation of the Localization Error

The standard deviation of the localization error indicates how close values

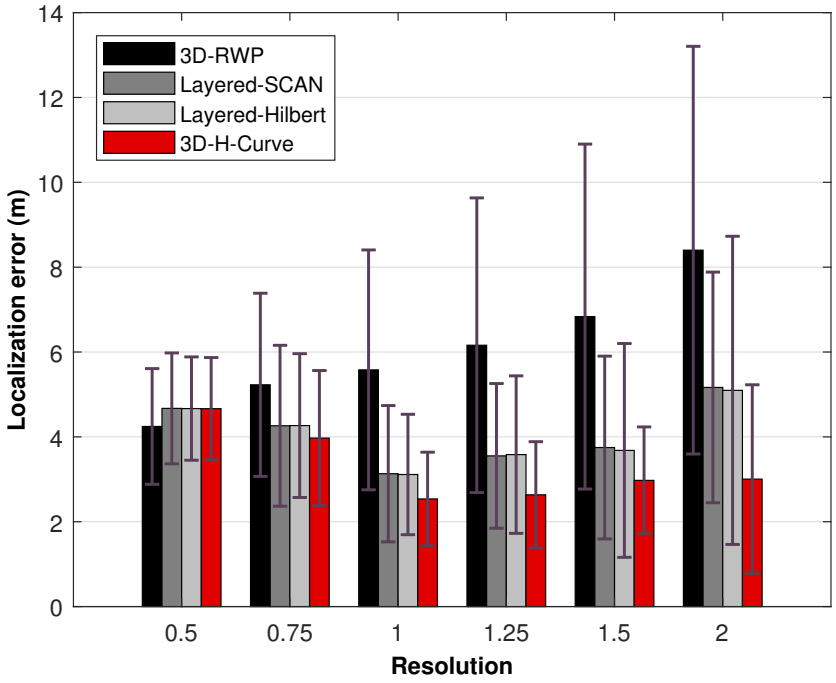

(a)

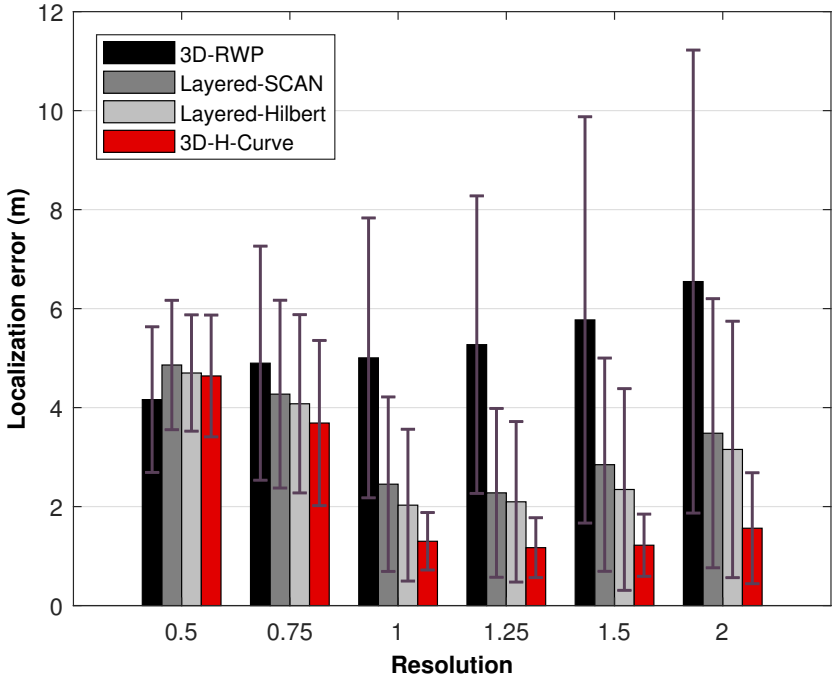

(b)

Figure 4.2: Average localization errors with standard deviation and the corresponding Resolutions in all models in (a) WCL, and (b) WCWCL

are to the average error. The standard deviation of the localization error rate is calculated as

$$error_{std} = \sqrt{\frac{\sum_{i=1}^{N}(error_{(i)} - error_{avg})^2}{RN}} \tag{4.5}$$

Where N is the number of UNs, $error(i)$ is the localization error for node i, and $error_{avg}$ is the average localization error. Figures 4.2a and 4.2b show the average standard deviation errors and the corresponding resolutions in all models in which WCL and WCWCL are used. In both localization techniques, our model provides the lowest standard deviation values, which indicates that they are closer to the average. Indeed, in WCWCL, our proposed model shows an efficient performance with a standard deviation of 0.5 m only.

C. Confidence Interval of the Localization Error

A 95% of CI is chosen to prove the statistical significance. Figure 4.3, in the following page, shows the localization error while the error bars depicted in the figure this time illustrate the 95% confidence interval. The presented results indicate that the 3D-H-Curves model provides a narrower CI in most cases, which means that the improved performance is statistically significant. This is applicable on both localization techniques of WCL and WCWCL.

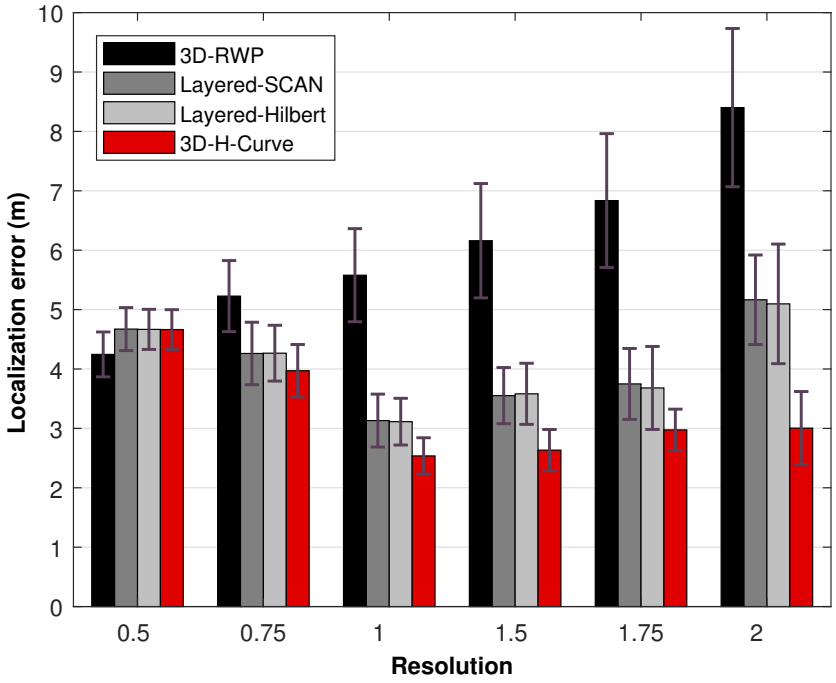

(a)

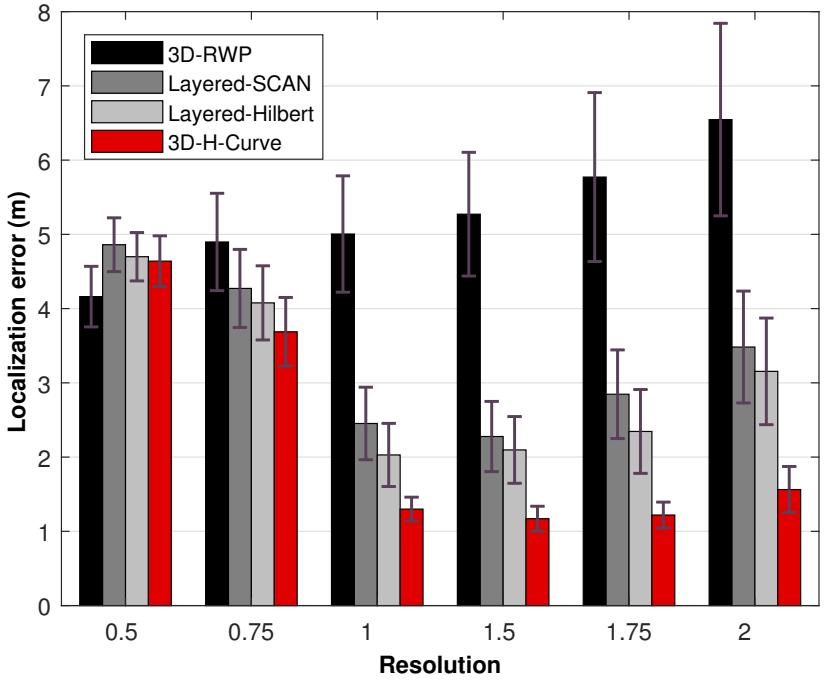

(b)

Figure 4.3: Average localization errors and the 95% confidence interval with the corresponding Resolutions in (a) WCL, and (b) WCWCL

4.6 Future work and Conclusion

In this chapter, we presented our proposed 3D path planning model for mobile anchor-assisted localization in WSNs. Our proposed model shows lower localization error than some existing works, and thus has higher accurate estimation. For future works, we will extend our work to evaluate more of the current 2D models by testing their ability to work in 3D environments. Moreover, more evaluation perspectives will be added, including precision, localization ratio, energy consumption and path length.

Chapter 5

Dynamic Fuzzy-Logic Based Path Planning for Mobility-Assisted Localization in Wireless Sensor Networks

5.1 Preface

In this chapter, we present a novel dynamic Fuzzy-Logic based Path Planning for mobility-assisted Localization in WSNs (FLPPL) that applies various criteria for the movement decision to form the path of the MA. The novelty of this model lies in employing multiple individual inputs in a fuzzy-logic approach for path planning that are important to minimizing the localization error and maximizing the localization ratio. By using a fuzzy-logic, a balanced movement path will be designed in order to achieve the objectives of the process and taking into account the limited movement of the MA. To the best of our knowledge, we are the first to use a fuzzy-logic based model in path planning for localization in WSNs. The proposed model offers superior results in many metrics in comparison to existing models.

Our contribution lies on designing a model for mobility-assisted localization in WSNs that:

1. For the first time, is formed based on multiple inputs. Using fuzzy-logic for processing the various inputs helps to balance the movement decision, which also helps to improve the localization ratio and the accuracy of the localization process.

2. Ensures that a maximum number of the UNs in the network are able to get the localization information when the distance of movement increases, while

considering the limitation of the MA movement. By doing so, a larger quantity of UNs can estimate their own positions in comparison to other models.

3. Offers a competitive localization error. Implementing both the RSSI (Received Signal Strength Indicator) and the distance metrics in a fuzzy logic approach helps to improve the accuracy of the localization.

4. Uses the precision metric for a better evaluation. Precision represents how many specific localization error values are achieved as in [9]. The proposed model offers very high precision in comparison to the other existing models.

This chapter is organized as follows. In Section 5.2, a brief review on Fuzzy-logic (FL) and some of the existing FL's studies in WSNs. Section 5.3 shows the assumption for the system model. Section 5.4 presents our proposed model starting with an analysis of the constraints and the objectives, then shows our proposed FL system in details, and finally describe the localization process. In Section 5.5, we explain the simulation and performance settings, and discuss the evaluation results in Section 5.6. Section 5.7, discusses the potential extension of the current model and the future work as well as the limitations of the proposed work. Then, the conclusion part in Section 5.8 is provided outlining the future works as well.

5.2 Fuzzy Logic in WSNs

Since its introduction by Zadeh in the 1960s, Fuzzy Logic (FL) has gained much attention due to its ease of implementation and simplicity [81]. The applications of FL have grown significantly. FL has been the main tool in many protocols and models in WSNs. For example, FL was used to enhance the networks lifetime as in [82–84]. Another usage of FL in WSNs was introduced by Mhemed et al., in [85], to propose a novel scheme, the Fuzzy Logic Cluster Formation Protocol (FLCFP), that uses Fuzzy Logic Inference System (FIS) in the cluster formation process. The work succeeded in choosing a balanced cluster head (CH) in each cluster and provides a competitive lifetime in comparison to other cluster formation models such

as LEACH. Other similar works using FL are presented in [86–89]. A novel model of implementing FL to dynamically control the traffic lights using WSNs is proposed in [90]. It employs multiple fuzzy-logic controllers for a real-time traffic monitoring using WSNs. Moreover, FL was used in several data routing protocols in WSNs including those in [91–94]. However, to our knowledge, no study of using FL in path planning for mobility-assisted localization in WSNs has been proposed. Therefore, we introduce our FLPPL model.

Simply, the concept behind it is to smooth the classical Boolean logic of True (1 or yes) and False (0 or No) to a partial value located between these values coming in a term of the degree of membership [85]. Such degree is determined based on multiple inputs, a decision function and one or more output functions. The set of inputs will be tested and evaluated together according to the applied set of rules. Rules works as a medium for the logical relationship between the inputs and the outputs. Thus, the results of the rules are combined and defuzzified in order to produce the degree of the final output [81]. Figure 5.1 depicts the generic structure of the Fuzzy-logic system as illustrated in [81].

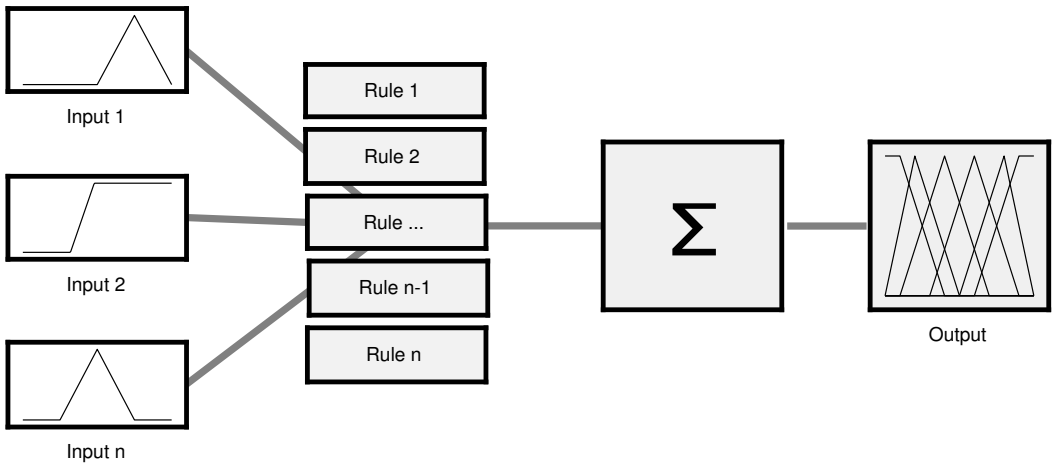

Figure 5.1: Fuzzy-logic system structure

5.3 System Model and Assumptions

The following features are assumed to form the system model:

1. A two-dimensional square network. The area size of the network is denoted as S in m^2.

2. A collection of UNs, are distributed randomly around the network. The number of UNs is denoted as N.

3. Initially, all UNs are not location-aware.

4. The deployed nodes are stationary, thus, no change to their location after deployment.

5. Each sensor node has a stable communication range of R_{Tx} in m.

6. The MA can determine its own position at any point of the network area. It is able to travel freely around the entire network in straight directions. The number of MAs is denoted as M.

7. For simplicity, no obstacles in the deployment area are considered.

8. The movement distance of the MA is limited by the value of the maximum distance to travel, d_{max}, where the MA's movement cannot exceed that value.

9. The MA stops frequently to provide nodes with information containing its current position and continue moving. Each stopping point is called a localization point.

10. Each MA and UN can contact each other only if their locations are within the communication range R_{Tx}.

11. Once a UN receives any three different locations information, it will be able to estimate its own location using the applied localization algorithm.

12. Each node that succeeds in estimating its location, will be converted from a UN to a reference node, RN. Each RN can share its location with the other nodes, helping them to estimate their own locations.

5.4 Proposed Model

5.4.1 Constraints and Objectives Analysis

The main objective of the designed model is minimizing the localization error while maximizing the localization ratio. Similar to most path planning models, a number of constraints are considered in planning the MA movement as follows. First, every visited localization point is unique; this means the MA cannot visit a localization point more than once. Second, in order to avoid the collinearity of localization points, the optimization requires that every three consecutive localization points are not collinear. In addition, and as in [55, 73], another constraint is considered in designing this model that the movement distance is limited, which therefore means MA cannot exceed the maximum traveling distance. These constraints may be broken in only one case where the MA is trapped in a corner or a border of the network. Two objective functions are to be optimized, the minimum average localization error and the maximum localization ratio. They are respectively represented in the following formulas

$$Minimize \;\; Error_{avg} \tag{5.1}$$

$$Maximize \;\; RN \tag{5.2}$$

5.4.2 Fuzzy-Logic Based Movement Decision

The first step in path planning starts with dividing the area of interest into a set of symmetric virtual hexagons. The MA is supposed to travel from the center of one

hexagon to one corner of the same hexagon and the reverse procedure is applied in the next movement. Hexagonal-based movement has been proposed in a number of recent works including [69, 73, 95]. Similar to [73], the hexagons are formed based on the transmission range of R_{Tx}, where the side length of each hexagon is equal to $R_{Tx}/\sqrt{3}\ m$. Figure 5.2 shows an example of the virtual hexagons forms in our system.

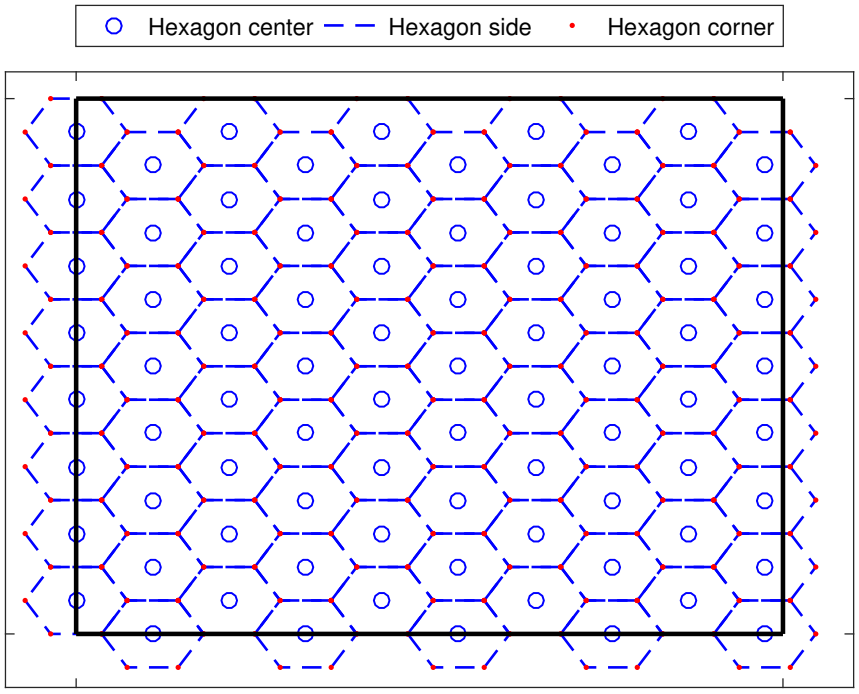

Figure 5.2: The hexagonal network system model of FLPPL (Fuzzy-Logic based Path Planning for mobility-assisted Localization

The movement of MA from one point (either the center or a corner) to another point will be determined in a real-time approach using an FL system. In such system, three inputs will be used namely the Received Signal Strength Indicator (RSSI) level, the number of neighbours, and the distance to each neighbour. These inputs will be measured from the MA's current location. The Mamdani method was used as the main tool to represent the fuzzy system. Mamdani is considered to be intuitive, widespread accepted and well suited to human input [81]. Table

5.1 shows the three input functions along with their membership functions.

Table 5.1: Input functions in FLPPL

Input	**Membership Function**		
RSSI Level	Weak	Medium	Strong
Number of Neighbours	Low	Medium	High
Distance to Each Neighbour	Near	Medium	Far

RSSI input measures the strength of the signal of all UNs located within the range of the current location of MA. A scale of -100 dBm to 0 dBm is used in this model, where the closer the value to 0, the stronger the signal is [96]. The RSSI membership function used in this model is close to the one in [97]. All UNs within the range of the MA will exchange their neighbour table information with the MA. This table includes the node id, the number of neighbours, the neighbour ids, the RSSI strength and the localization status, whether localized (1) or not (0). An example of this table is shown in the following Table 5.2.

Table 5.2: Node's Neighbours Table in FLLPL

N_ID	**Type**	**Nbrs_#**	**Nbrs_IDs**	**Nbrs_Types**	**Nbrs_RSSI**
20	0	3	$48, 147, 226$	$0, 0, 0$	$-89.92, -57.91, -82.44$

In the second input, and from its current location, the MA contacts each UN located within its range. Each UN exchanges its neighbours list and the MA evaluates them based on the number of neighbours. A higher chance will be given to the UN with higher number of neighbours. This is meant to reach the maximum number of UNs by considering the ability of each nodes to share its information to as much neighbours as possible. In the third input, although the locations of both the MA and the UN are required to calculate the distance between each of them, it is still possible to estimate using the RSSI. The closer the distance is, the higher chance is given. Considering the module in [45] and assuming $d_0 = 1$, the distance extracted from the RSSI values is estimated as

$$d = 10^{(-RSSI+P_L(d_0)+N_\alpha)/(10\times\beta)} \tag{5.3}$$

where $P_L(d_0)$ is the power loss at the reference point (d_0) in dB, N_α is the zero-mean Gaussian random variable with a standard deviation α and β is a constant path loss exponent.

Two membership functions were chosen to present our parameters, Triangular and Trapezoidal. They are simple, direct and easy to apply in many applications [81, 98]. Simply, triangular membership function is a collection of three points forming a triangle. It is represented using the following equation

$$\mu_{A1}(x) = \begin{cases} 0 & x \leq 0 \\ \dfrac{x - a1}{b1 - a1} & a1 \leq x \leq b1 \\ \dfrac{c1 - x}{c1 - b1} & b1 \leq x \leq c1 \\ 0 & c1 \leq x \end{cases} \tag{5.4}$$

Trapezoidal membership function is like the Triangular function with a flat top. It is formed as

$$\mu_{A2}(x) = \begin{cases} 0 & x \leq a2 \\ \dfrac{x - a2}{b2 - a2} & a2 \leq x \leq b2 \\ 1 & b2 \leq x \leq c2 \\ \dfrac{d2 - x}{d2 - c2} & c2 \leq x \leq d2 \\ 0 & d2 \leq x \end{cases} \tag{5.5}$$

As in [85, 86], we used the triangular function for the middle variables while the trapezoidal member function was used for the boundary variables. The values used in both the Triangular and the Trapezoidal membership functions are shown in the following Table 5.3.

Table 5.3: The values of membership functions in FLPPL

RSSI	Neighbours	Distance
Weak: [−102 −100 −90 −70]	Low: [−0.5 0 6 8]	Near: [−0.25 0 3.125 6.25]
Medium: [−90 −70 −30]	Medium: [6 8 12]	Medium: [3.125 6.25 9.375]
Strong: [−70 0 2]	High: [8 12 25 25.5]	Far: [6.25 9.375 12.5 12.75]

Figure 5.3 illustrates the inputs functions and degrees of relationship of FLPPL, Figure 5.3a the RSSI level input, Figure 5.3b the number of neighbours input and Figure 5.3c the distance to each neighbour input.

The correlations between each two input functions and the output can be represented as a three-dimensional curve. The following surface plots in Figure 5.4, depict the correlations between the fuzzy inputs in our FLPPL approach, starting with the Distance to RSSI as in Figure 5.4a, Distance to Neighbours in Figure 5.4b and Neighbours to RSSI in Figure 5.4c.

The system output function in our model is identified as the chance (probability). The chance represents the probability of the MA's next point from the current location. The MA will move to the closest point in distance to the higher chance node. For example, consider the three nodes (N_ids = 1, 2 and 3) shown in Figure 5.5. The MA's current location is in the center of the hexagon, which by default means that the next movement will be to a corner of the hexagon. Now, the MA will contact each node, exchange their information and analyze it. Using the fuzzy-logic model, the MA will estimate each node's chance considering the three membership function inputs. While still taking into account the rules of constraints described in Section 5.4.1, the MA will move to the closest point (in green) to the highest chance node (N_id = 2 in the example).

Nine output degrees are defined in this system similar to those used in [85]. They range from (very weak) as the lowest degree to (very strong) as the highest one. Table 5.4 shows the output function along with the nine membership functions.

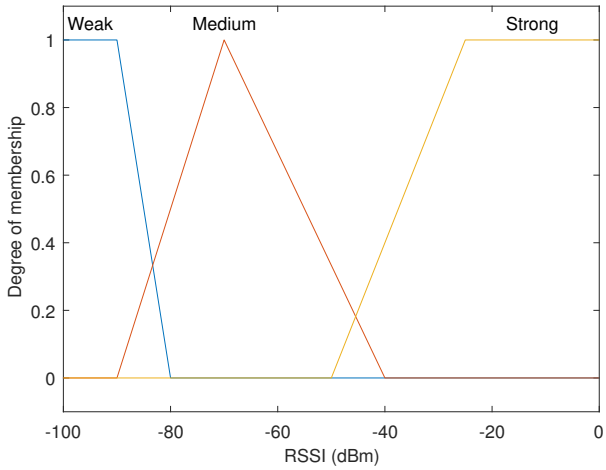

(a)

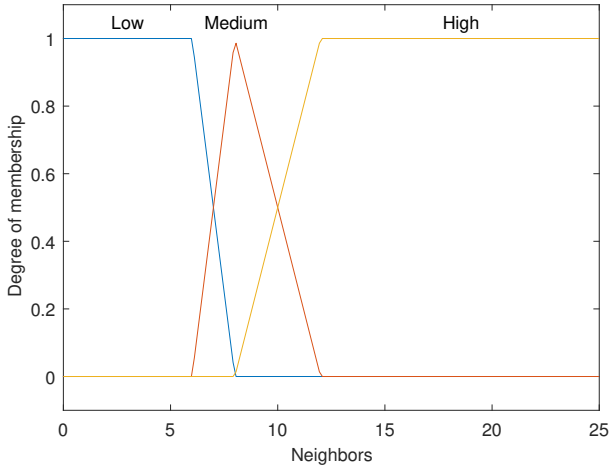

(b)

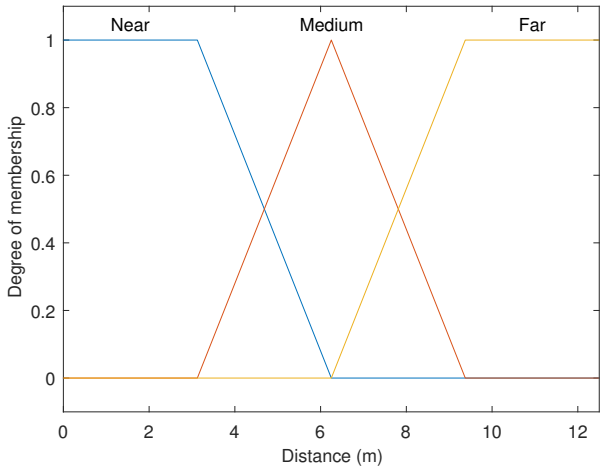

(c)

Figure 5.3: Inputs functions and degrees of relationship of FLPPL, (**a**) the RSSI level input, (**b**) the number of neighbours input and (**c**) the distance to each neighbour input.

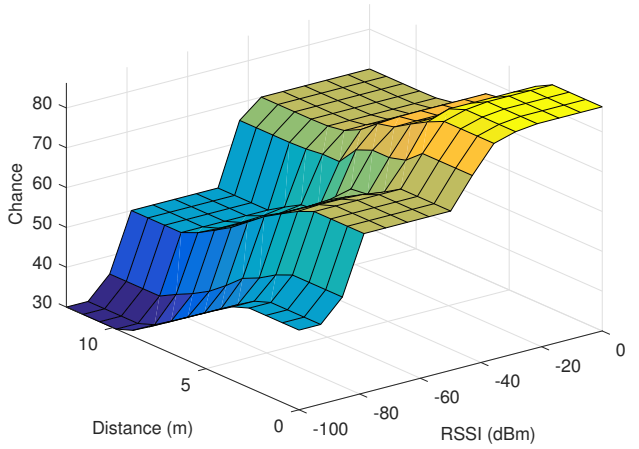

(a)

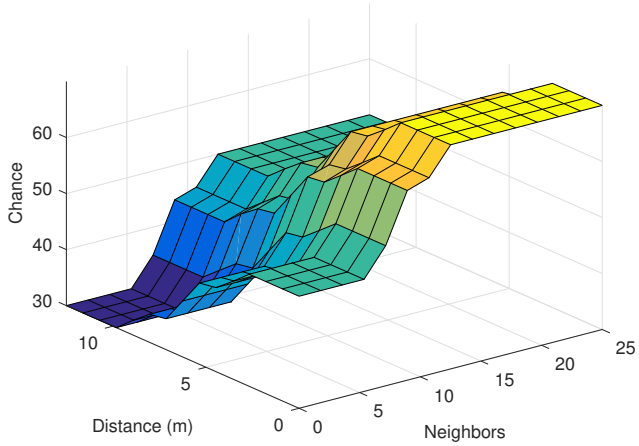

(b)

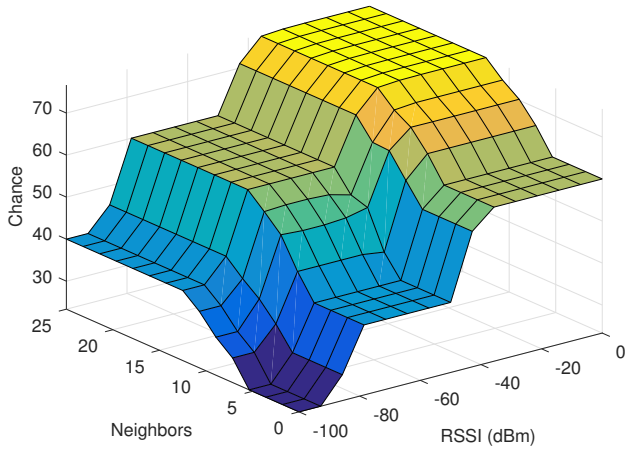

(c)

Figure 5.4: Relationship among fuzzy inputs of FLPPL, (**a**) distance vs. RSSI, (**b**) Distance vs. Number of Neighbours, (**c**) Number of Neighbours vs. RSSI. The darker the color is, the lower the chance is.

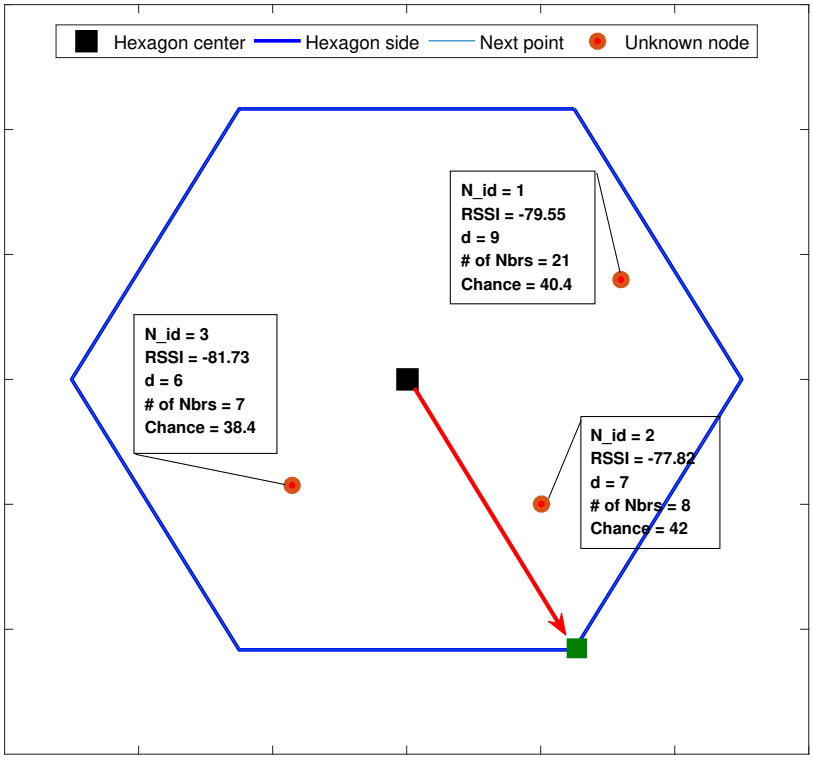

Figure 5.5: Example of selecting the next movement of the MA

Table 5.4: Output functions in FLPPL

Output	**Membership Functions**
Chance	Very Weak
	Weak
	Little Weak
	Little Medium
	Medium
	High Medium
	Little Strong
	Strong
	Very Strong

Any fuzzy-logic system depends on the IF-Then rule statements that are used to formulate the conversion from the input functions to the output one. A simple

fuzzy IF-Then rule is stated as

$$if\ x\ is\ A,\ then\ y\ is\ B \tag{5.6}$$

where A and B are the linguistic values defined by the fuzzy sets on the ranges x and y [81]. The following Table 5.5 defines the fuzzy if-then rules.

Table 5.5: The Fuzzy rules of if-then in FLPPL

RSSI	**Neighbours**	**Distance**	**Chance**
Weak	Low	Far	Very Weak
Weak	Low	Medium	Weak
Weak	Low	Near	Little Weak
Weak	Medium	Far	Weak
Weak	Medium	Medium	Little Weak
Weak	Medium	Near	Little Medium
Weak	High	Far	Little Weak
Weak	High	Medium	Little Medium
Weak	High	Near	Medium
Medium	Low	Far	Little Weak
Medium	Low	Medium	Little Medium
Medium	Low	Near	Medium
Medium	Medium	Far	Little Medium
Medium	Medium	Medium	Medium
Medium	Medium	Near	High Medium
Medium	High	Far	Medium
Medium	High	Medium	High Medium
Medium	High	Near	Little Strong
Strong	Low	Far	Medium
Strong	Low	Medium	High Medium
Strong	Low	Near	Little Strong
Strong	Medium	Far	High Medium
Strong	Medium	Medium	Little Strong
Strong	Medium	Near	Strong
Strong	High	Far	Little Strong
Strong	High	Medium	Strong
Strong	High	Near	Very Strong

Figure 5.6 plots the degree of Membership, in the range of 0 to 1, versus the chance values of FLPPL.

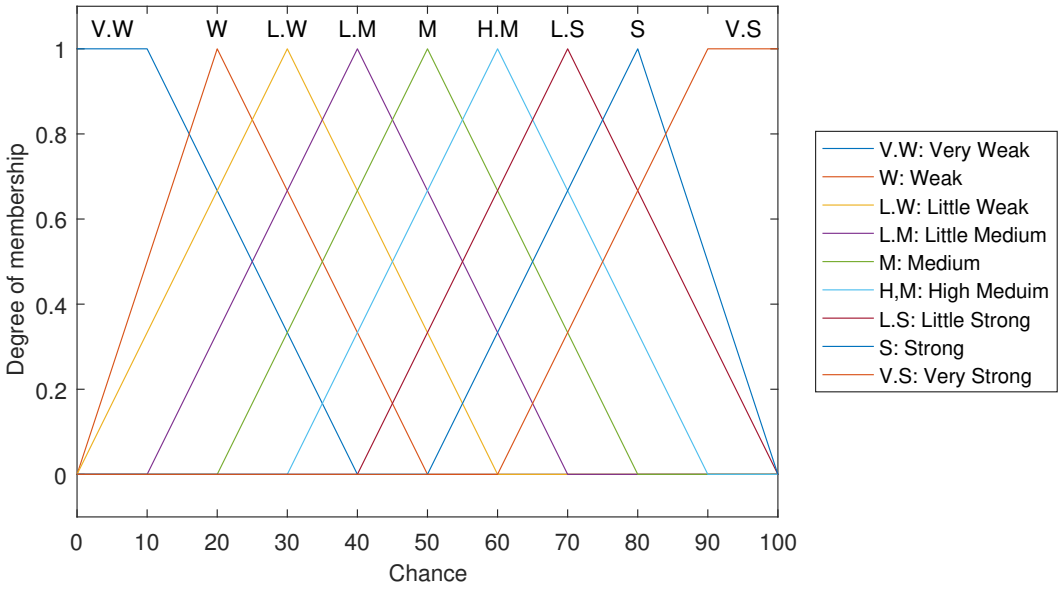

Figure 5.6: Output membership function of FLPPL

Therefore, the complete system model of FLPPL consists of three inputs with three membership functions and nine degrees of chance as shown in Figure 5.7.

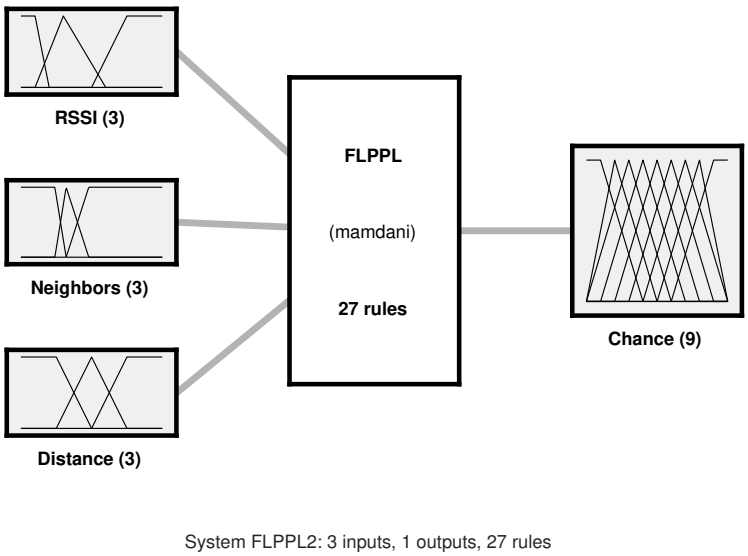

Figure 5.7: The system scheme of FLPPL

5.4.3 Mobility Movement and Localization Process

The mobility movement and localization process are conducted simultaneously in two sides, the UN's side and the MA's side as follows.

A. Procedure in UN's Side

(a) The UNs will be deployed randomly.

(b) Each node will communicate with its neighbours' node that are located within its communication range, collecting their information and adding them to its neighbours table was shown above in Table 5.2.

(c) When the MA arrives at each node, the node will exchange its table with the MA.

(d) When three different locations are received by each UN, it will be able to calculate its own location.

B. Procedure on MA Side

(a) The MA will start its journey from a starting point, the starting point can be set in advanced or random.

(b) The MA has a maximum distance value.

(c) The first three movements will be random in any direction.

(d) After each movement, the MA will stop and communicate with all nodes in its communications range, providing them with its current position.

(e) It will update its routing table, which has the following information:

i. Node IDs

ii. Node's status

iii. Number of neighbours

iv. Neighbours IDs

v. Neighbours' status

vi. RSSI value

(f) The MA will evaluate all nodes and elect one based on the previous chance table.

(g) The next point of the hexagonal will be the shortest point in distance to the elected node.

(h) The MA will travel to that point and provide its current position information.

(i) TheMA keeps moving till reaching the maximum distance, d_{max}.

The flowchart in Figure 5.8 presents the localization procedure done on the UN's side, while the flowchart in Figure 5.9 presents the localization procedure done in the MA's side.

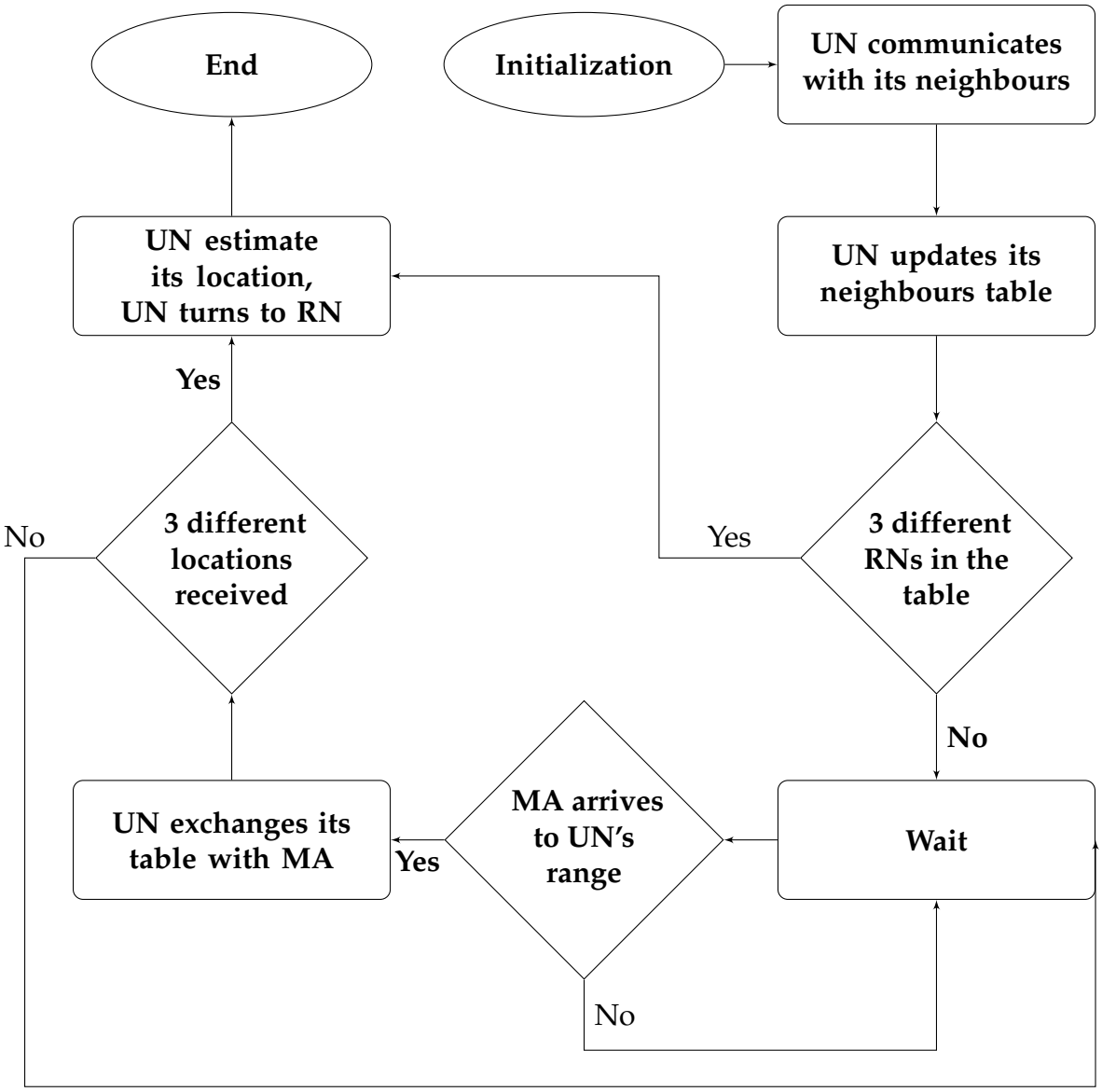

Figure 5.8: The node localization process in the UN.

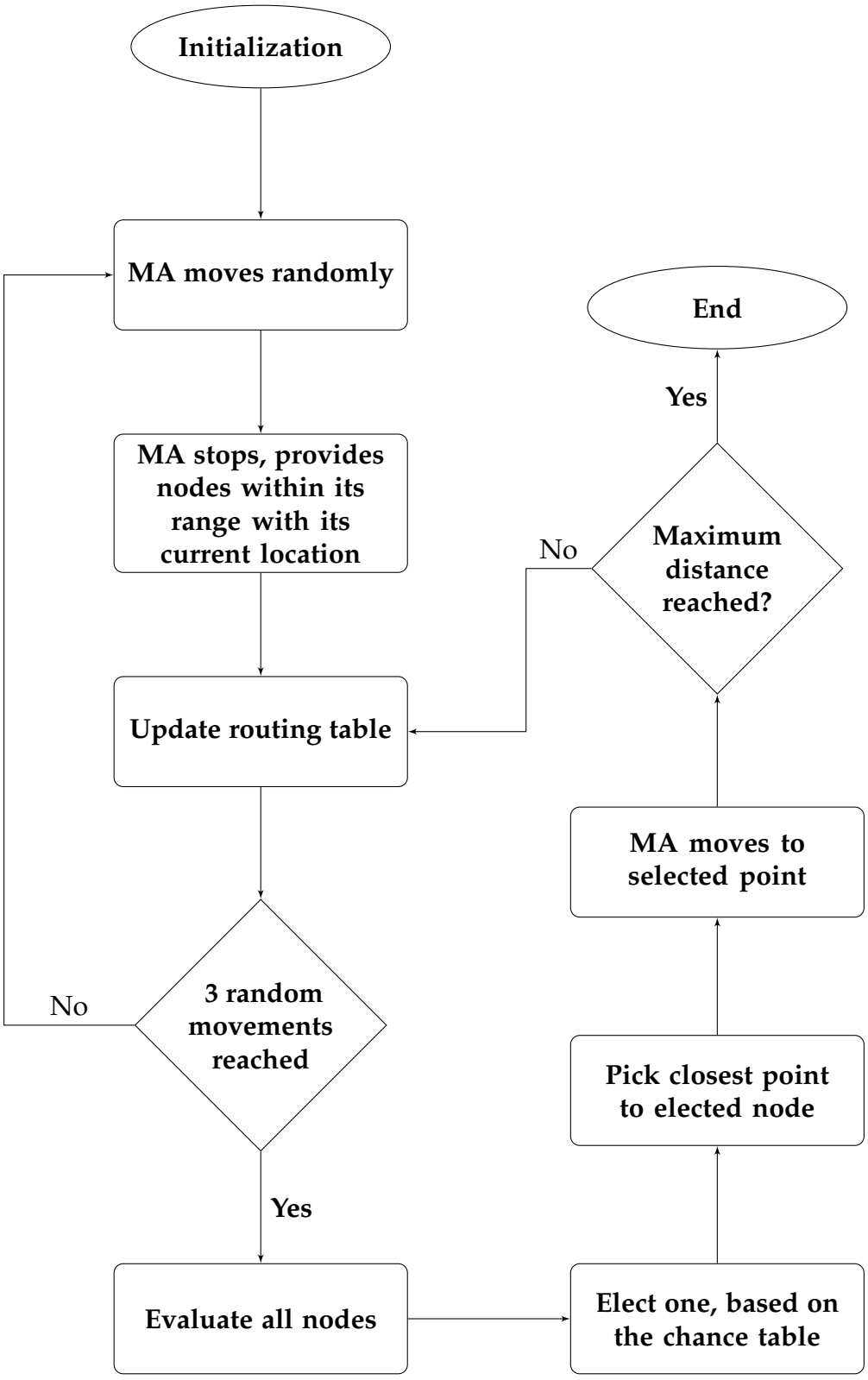

Figure 5.9: The movement and node localization process in the MA.

5.5 Performance Settings

Three static path planning algorithms and one dynamic model were implemented to evaluate the performance of FLPPL. SCAN, LMAT and Z-Curves are the static models while the NLA_MB model was used as a dynamic algorithm.

The two localization algorithms, Weighted Centroid Localization (WCL) [49] and Weight-Compensated Weighted Centroid Localization (WCWCL) [45], were implemented to analyze the effectiveness of the mobility models implemented. Figure 5.10 shows an enlarged example of the FLPPL mobility movement and the estimation of location of the nodes deployment in the WCL algorithm.

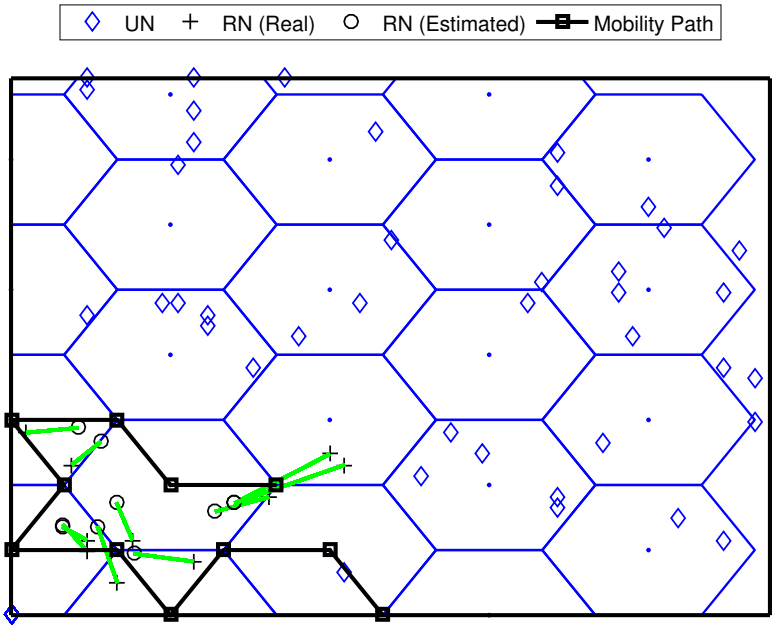

Figure 5.10: An example of the FLPPL mobility movement and the estimation of location of the nodes deployment in WCL

We evaluated the performance of the proposed FLPPL model using MATLAB environment and compared it with the other implemented models of SCAN, LMAT, Z_Curve and NLA_MB in terms of localization accuracy, localization precision and localization ratio and coverage respectively. The simulation tool and implemented

parameters were chosen in accordance with some other similar works, we used them here for consistency. A square network area is assumed with a size, S, of 100 $m \times 100$ m. A randomly distributed set of 250 nodes, N, is used with only one MA, M. The maximum movement, d_{max} indicates the maximum distance that the MA can take in travelling around the network. Different maximum movements were used to evaluate the models. A random starting point approach was used in each run for each model. A realistic wireless model was used by implementing the characteristics of a wireless node that is equipped with a Chipcon CC1100 radio module [77]. Such specification were already used in similar works including [9, 45].

The rest of the parameters are shown in the following Table 5.6.

Table 5.6: Simulation values and parameters in FLPPL

Parameters	**Symbol**	**Value**
Network size (m)	S	100×100
Number of MAs	M	1
Number of UNs	N	250
Maximum movement distance (m)	d_{max}	35, 70, 105, 140, 175
Path loss exponent	β	3.5
Power loss (dB) at d_0	$PL(d0)$	-60
Reference point (m)	$d0$	1
Standard deviation of noise	σ	3, 5, 7, 9
Simulation run		50

5.6 Evaluation and Results

To assess the efficiency of the proposed model, we studied the models considering the following aspects, discussed below: accuracy, precision, and localization ratio.

5.6.1 Localization Accuracy

In this work, we study the accuracy from two perspectives, the average localization error and the standard deviation of the localization error in each model.

A. Average Localization Error

To study the behaviour of the proposed model and compare it to the others, we first executed a test of 50 simulation runs with 250 UNs, a maximum movement distance, d_{max}, of 140 m, and a standard deviation of noise, σ, of 3. Figure 5.11 shows the performance of the different models based on localization error when both WCL and WCWCL were used.

Figure 5.11a shows that FLPPL offers lower error rate, thus, higher localization accuracy in most of the presented results when WCL was used. A range of localization errors between 0.3 m and 2.58 m were achieved. The dynamic path planning of NLA_MB also presented a better performance in comparison to the other static models of SCAN, LMAT and Z-curves. While LMAT was proposed for a better performance as a static model [9,11], when the MA movement is constrained, there is no significant difference to the other static models. This may help to prove that the dynamic path planning models are more suitable in such cases where the MA movement is limited and there is a need to take the network topology and nodes deployment into account in the movement decision making. All path planning models offer low standard deviation of error results ranging between 0.42 m and 0.55 m, which means that most of the results are very close to the average.

The same assumptions were used again with WCWCL scheme, as shown in Figure 5.11b. Higher localization estimation was achieved by decreasing the localization error using WCWCL. FLPPL again provided higher performance of accuracy by offering lower localization error, which therefore means more accurate estimation. Once more, NLA_MB shows higher estimation of node locations with minimal locations error compared to the implemented static models. On average, WCWCL attained better results than WCL due to the nearby anchors having more impact on the estimation and calculation of the locations. For example, FLPPL yielded an average of 0.601 m with a range of errors between 0.08 m and 2.17 m in comparison to the higher results of the

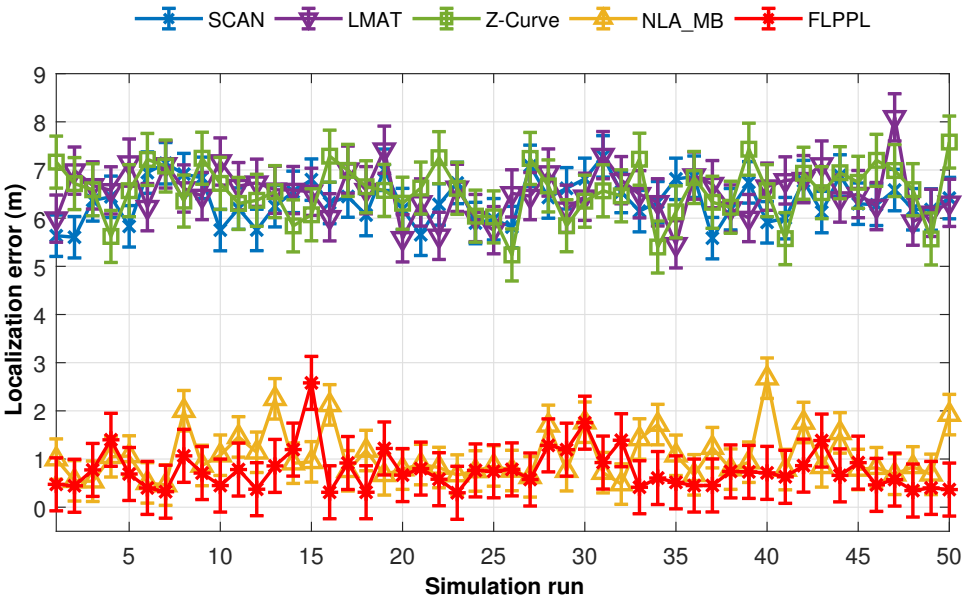

(a)

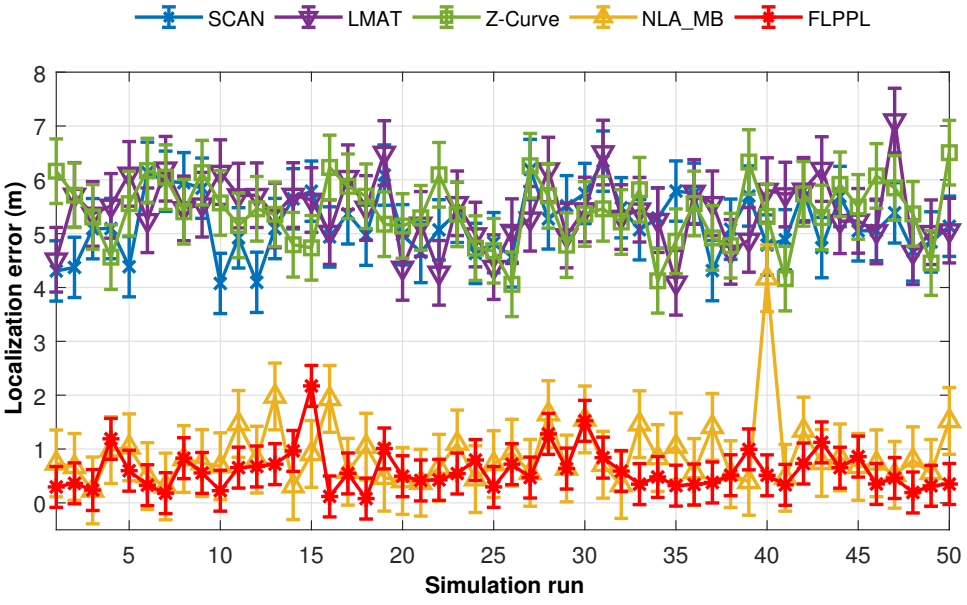

(b)

Figure 5.11: Localization errors of all mobility models in (**a**) WCL, and (**b**) WCWCL, ($d_{max} = 140m, \sigma = 3$)

same assumptions in WCL.

Moving on to the average localization error for all path models when different maximum movement distance, d_{max}, are used, Figure 5.12 shows the performances when WCL and WCWCL are implemented. We conducted two experiments using the parameters shown in Table 5.6 with two changeable values, the maximum movement distance, d_{max}, and the standard deviation of noise, σ.

In the first trial, we ran a test of 250 UNs with different movement distances ranging between 35 m and 210 m and $\sigma = 3$.

Figure 5.12a presents the average localization error for the proposed model along with the others when WCL is used, while Figure 5.12b shows the average localization error when WCWCL is used. FLPPL and NLA_MB offered the best results with slight distinctions in both WCL and WCWCL. FLPPL shows superior results with all movement allowances. In general, WCWCL provides better results with all path models including the statics. However, the difference between the dynamic models of FLPPL and NLA_MB, and the rest of SCAN, LMAT and Z-Curve is very significant. For example, the localization error of the models when only 35 m of distance is allowed are 7.41, 8.06, 8.15, 1.90 and 1.78 m for SCAN, LMAT, Z-Curve, NLA_MB and FLPPL respectively when WCL is used. These results improved to 6.59, 6.94, 7.11, 1.52 and 1.56 m when WCWCL is used.

Moreover, to verify the statistical significance, the CI of the localization error is also used. A 95% of CI is chosen to test that significant. Figure 5.13 shows the localization error while the error bars depicted in the figure this time illustrate the 95% confidence interval. The results explain that in most cases, FLPPL model provides a narrower CI, which means that the improved performance is statistically significant. This is applicable to both localization techniques of WCL and WCWCL.

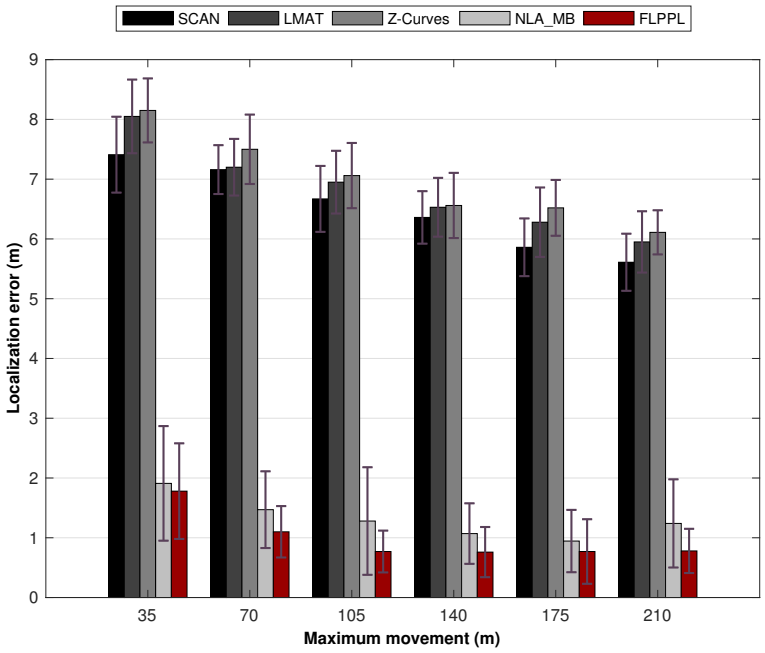

(a)

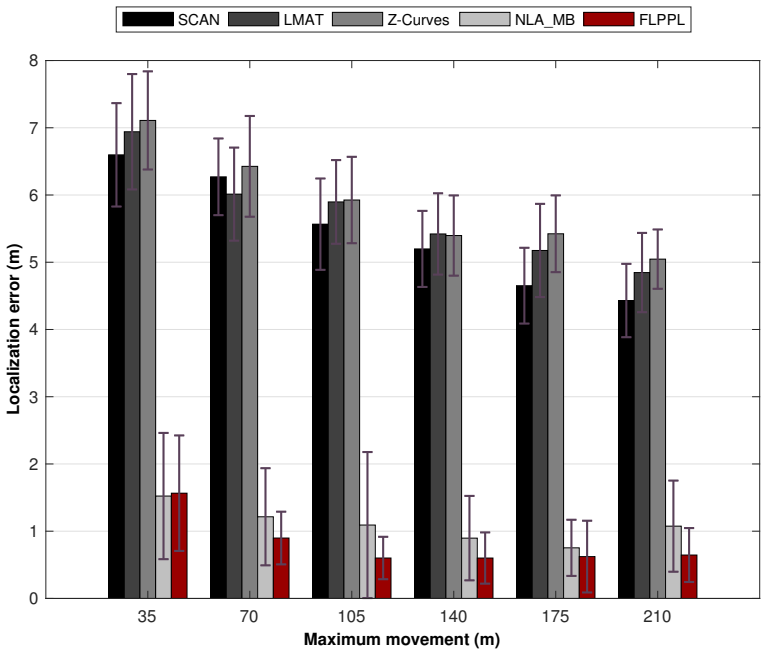

(b)

Figure 5.12: Average localization errors with standard deviation of errors versus maximum movement in (**a**) WCL, and (**b**) WCWCL

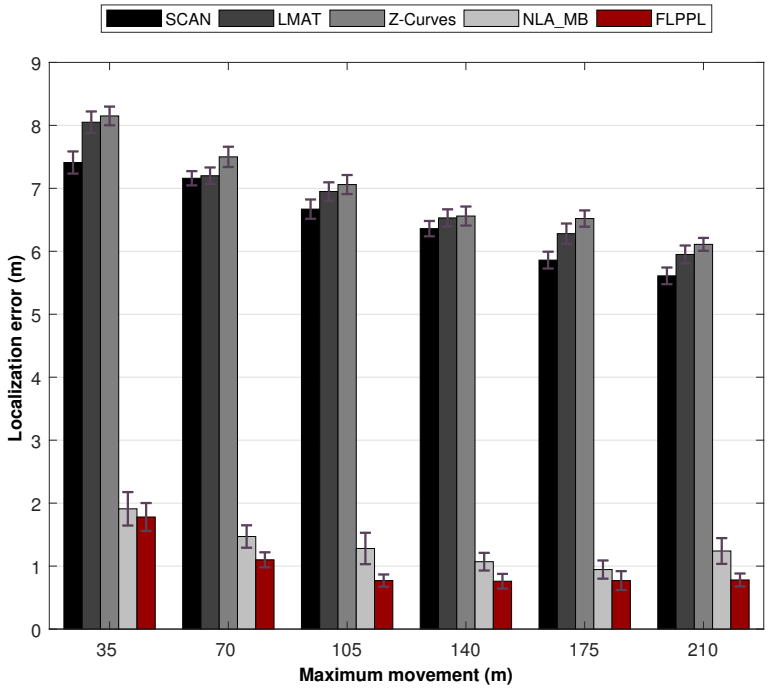

(a)

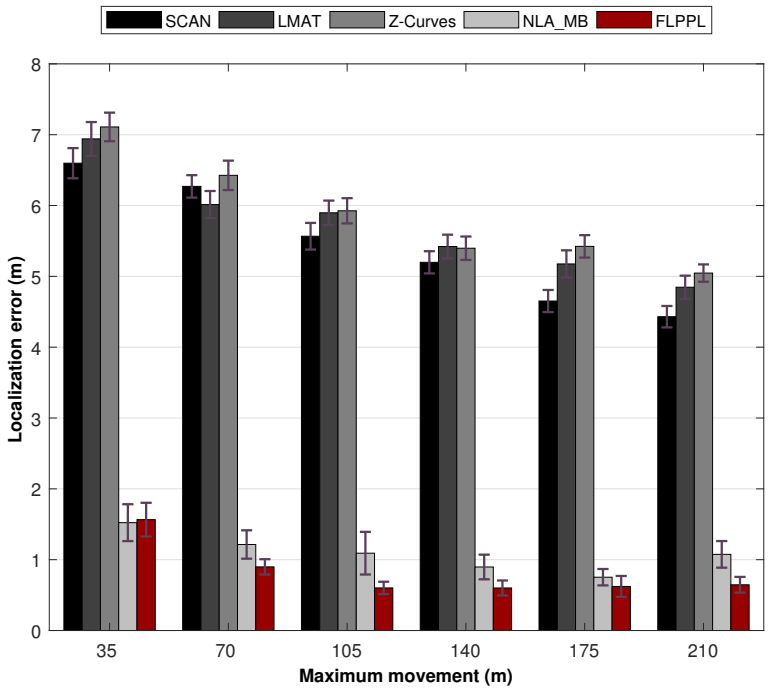

(b)

Figure 5.13: Average localization errors and the 95% confidence interval with the corresponding maximum movement in (a) WCL, and (b) WCWCL

Two interesting points here to mention. First, while increasing the movement distance showed better localization in most trials, it is not always true. Increasing the maximum movement distance does not always mean that the accuracy will increase as shown in the figures. Second, the static models behave differently based on the implemented localization algorithm. For example, Z-Curve shows better performance than SCAN and LMAT when WCWCL is used with 105 m.

In the second experiment, shown in Figure 5.14, we conducted the same parameters with a fixed maximum distance, d_{max}, of 70 m and a different standard deviation of noise, σ.

Figure 5.14a and 5.14b show the average localization error for the chosen models with a different deviation of noise, σ, when WCL and WCWCL algorithms respectively are used. In all runs and regardless of the value of the standard deviation of noise, σ, our proposed model, FLPPL, offered the most accurate estimations, with a localization error of less than 1.5 m in both WCL and WCWCL. Indeed, FLPPL was able to achieve even lower results than 1 m when the values of 5 and 7 were used as standard deviation of noise, σ in WCWCL. NLA_MB showed closed results and the impact of changing the standard deviation of noise, σ, was insignificant. Static models offered better results when σ increases to 5. Once more, static models with WCWCL outperformed those with WCL.

To sum up this point, taking into account the strength of the node's RSSI signals, locations and distance of both the MA localization points and the localized neighbour nodes helped to achieve high accuracy values in FLPPL using both WCL and WCWCL. Moreover, in FLPPL, the localized nodes are given the opportunity to provide their neighbours with their own localization information; therefore, the UN can determine its own location based on the most accurate information received. NLA_MB also consider the usage of

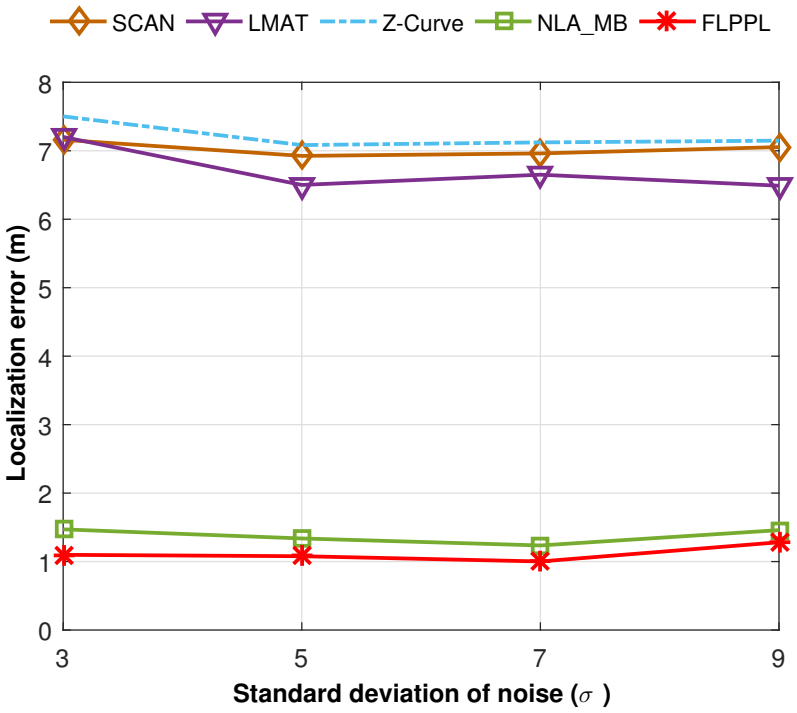

(a)

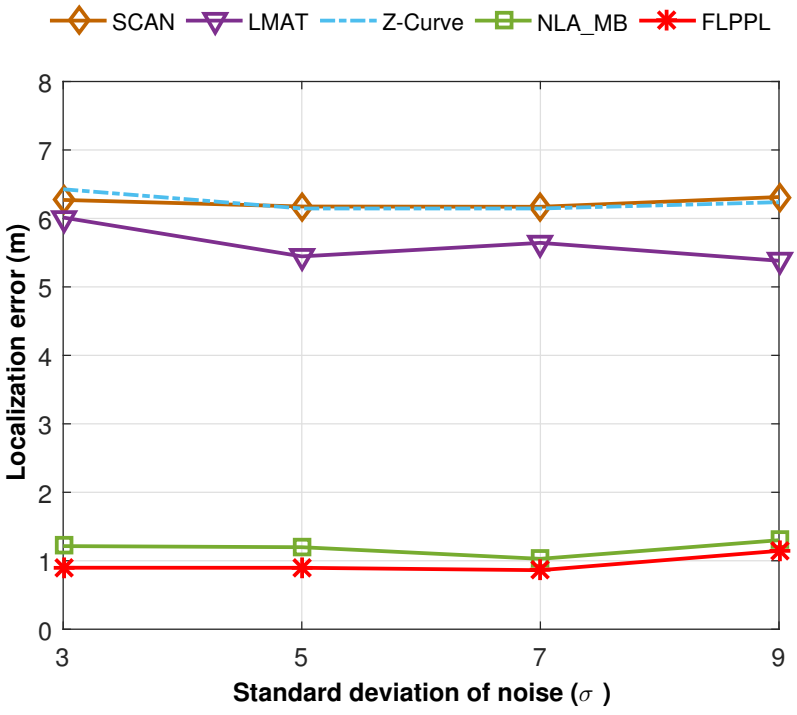

(b)

Figure 5.14: Average localization error versus the standard deviation of noise (σ) of the mobility models in (**a**) WCL, and (**b**) WCWCL

the nearby localized nodes to supply their own neighbour with their locations, which helps to increase such ratio.

5.6.2 Precision

We also used the precision metric. Five localization error values are considered as follow, <1.5 m, <3 m, <4.5 m, <6 m and <7.5 m. The ratio of how many values were attained is calculated with each of the previous localization error values in the 50 simulation runs. Figure 5.15 shows the precision evaluation results when d_{max} = 70 and σ = 3.

In Figure 5.15a and when WCL is used, the number of the localized nodes with localization error within 1.5 m is very high with over 0.8 precision in FLPPL. Again, the reason behind it is the consideration of employing both the RSSI values and the distance metrics in the decision movement which therefore leads to a better localization. In fact, all localization error values were kept in control under 3 m in FLPPL. NLA_MB also provided a high precision when compared to the other static models with more than 0.6 within less than 1.5 m and more than 0.9 precision within less than 3 m of errors. The static models of SCAN, LMAT and Z-Curve acted very weakly only few values reached within 6 m of the real locations. This precision increased slightly with 0.46 in Z-Curve, 0.7 in SCAN and 0.74 in LMAT when a localization error of 7.5 m is considered which means the rest of the localized nodes in each model were achieved in more than 7.5 m or error rate.

When WCWCL is applied, the precision was improved as shown in Figure 5.15b. This is because WCWCL modified the weight calculation and gave more effect of the distance and nearby anchors. FLPPL obtained about 0.9 of precision where localization error was kept less than 1.5 m. All FLPPL localization errors were under 3 m of error. Even in NLA_MB, the precision increased from 0.66 when WCL was used to 0.7 in WCWCL when less than 1.5 m was considered. The impact of WCWCL is clear on the static models precision as well. The precision values improved gradually from 4.5 m to less than 7.5 m.

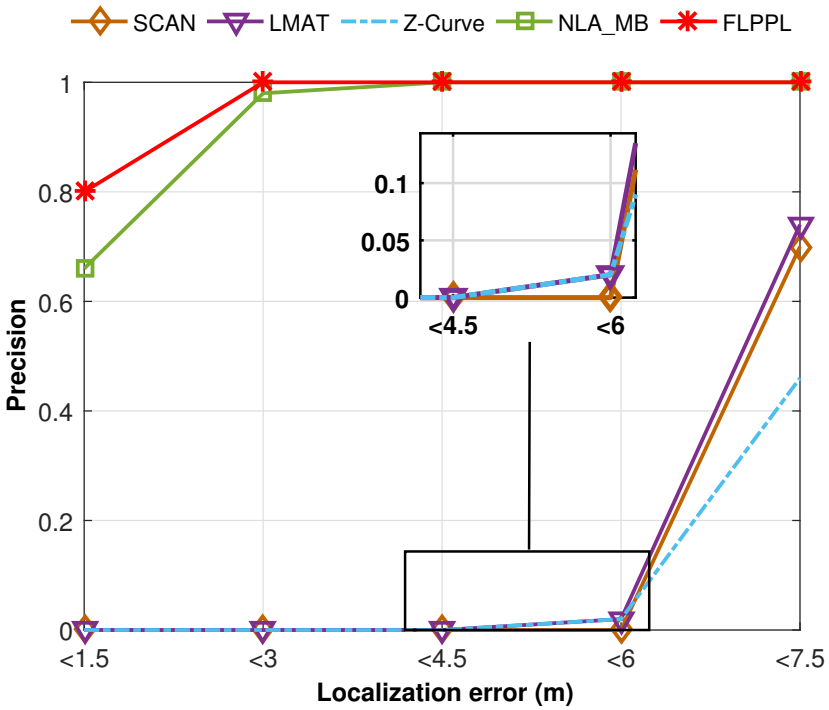

(a)

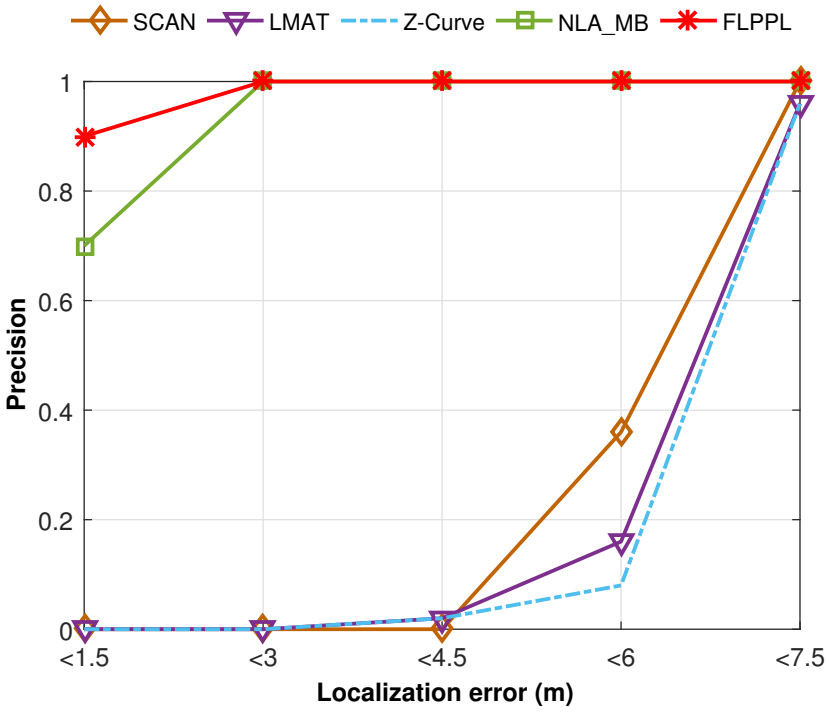

(b)

Figure 5.15: Precision of all mobility models versus the localization error in (**a**) WCL, and (**b**) WCWCL, ($d_{max} = 70, \sigma = 3$)

5.6.3 Localization Ratio

A set of 250 UNs is used with different movement distances, d_{max} with the default value of standard deviation of noise, σ = 3. Since the localization ratio is almost the same in both WCL and WCWCL, we only show one of them here. Figure 5.16 presents the localization ratio for the implemented path models.

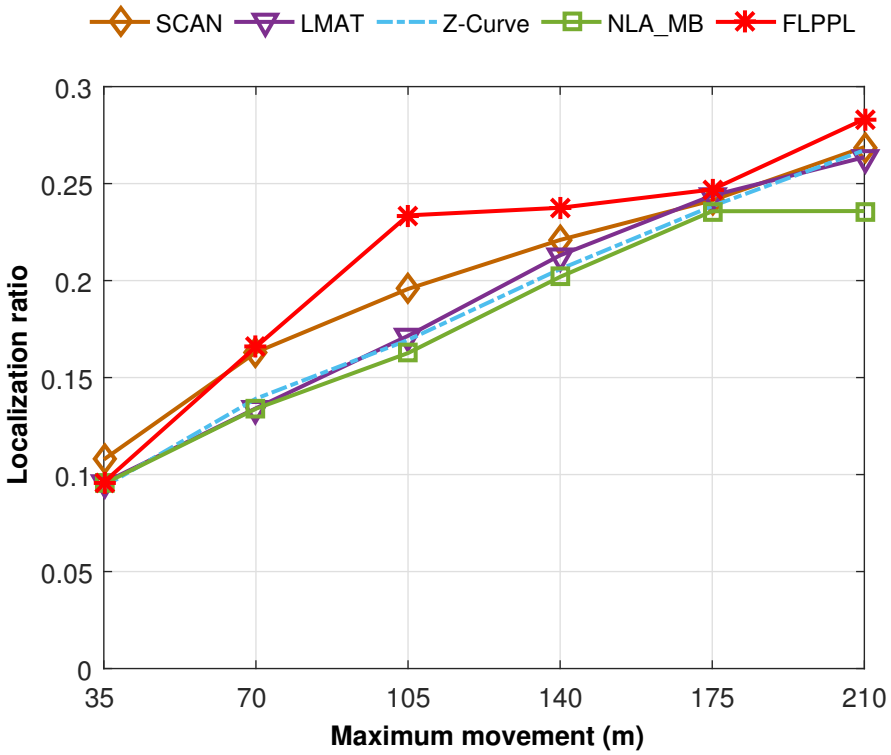

Figure 5.16: Localization ratio all mobility models in both WCL and WCWCL

When d_{max} = 35, all paths, including FLPPL and NLA_MB, provided insufficient ratio of localization. The very short movement allowance had its negative impact on the number of localized nodes. With increasing the maximum distance, the localization ratio improves. FLPPL is the only model that takes the number of neighbours of each node in its movement decision. Hence, it showed a better performance starting with d_{max} = 70 till d_{max} = 210. Another reason is that nodes in FLPPL are able to share their own location, which helps to spread the localization information. This feature is applied in NLA_MB as well. However, while

NLA_MB provides a competitive localization error, the other static models offered higher localization ratio in most cases. The distance between each two points in the static models is farther than those in NLA_MB which means more nodes will receive the localization information than those in NLA_MB.

5.7 Discussion

In this section, we highlight the limitations and the points that are not considered in this work.

5.7.1 Limitations

The proposed model was designed for a densely deployed network, assuming that the area includes a sufficient amount of sensor nodes. In case there is an insignificant number of sensor nodes, the inputs of the fuzzy system might be affected (especially the number of neighbours), thus, affects the optimization of the path planning. On the other hand, most of the model operations exist in the MA's side. Assuming that the MA is not energy-constrained and is able to complete the assigned movement distance, we did not consider the computation load or energy consumption in this model. In a special scenario where the MA has a trivial source of energy, it might be unable to even complete its limited distance. Although our proposed model shows a significant improvement of localization ratio in comparison to other models, it is very difficult to guarantee that all UNs will be able to receive the localization information. Two reasons behind that, the limited movement distance of the MA and the nature of the dynamic models of forming the mobility movement based on the information received from the deployment area.

5.8 Conclusions

In this chapter, we introduced a dynamic mobility path model for node localization in WSNs. The proposed path model is formed based on a number of inputs in

a fuzzy-logic approach which helps to design a superior path when the movement of the MA is limited. Two types of mobility, represented by four different models, are implemented in this work to test and examine our proposed model. The results show that our model, FLPPL, increases the network's localization efficiency in terms of localization coverage, localization accuracy, and localization precision. We were able to draw conclusions based on the three metrics studied:

1. **Localization accuracy:** Represented by the localization error, the final results show leading outcome for our proposed model along with the dynamic model of NLA_MB as shown in Figures 5.12, 5.14.

2. **Localization precision:** The FLPPL dynamic model presents superior precision results with the highest ratios in both WCL and WCWCL as indicated in Figure 5.15.

3. **Coverage:** In general, the static models perform better than the others in terms of network coverage. However, this not necessarily true when MA movement is constrained and limited. FLPPL consider three inputs in its movement decision, the RSSI signal, the distance between nodes and anchors and the number of neighbours of nodes which increases the number of localized nodes effectively. These results hold in both experiments when using different distances of movement as shown in Figure 5.16.

To conclude, we have shown that employing multiple inputs for forming a movement path has positive impacts in several regards.

Chapter 6

Swarm Intelligence Optimization Techniques for Obstacle-Avoidance Mobility-Assisted Localization in Wireless Sensor Networks

6.1 Preface

This chapter introduces two novel dynamic meta-heuristic optimization techniques for mobility-assisted localization in WSNs. The suggested path planning models are based on two new optimization algorithms, namely the Grey Wolf Optimizer (GWO) [19] and the Whale Optimization Algorithm (WOA) [20]. The proposed models are respectively called Grey Wolf optimizer based obstacle-avoidance Path Planning (GWPP) and Whale Optimization algorithm based obstacle-avoidance Path Planning (WOPP). The novelty of our proposed models lies in employing an optimization algorithms to direct the path formation of the MA, which helps to maximize the localization ratio and minimize the localization error. By using the optimization algorithms, the MA movement is formed in real-time; it also avoids the obstacles, takes into account the maximum distance constraint, and simultaneously achieves the objectives of the entire localization process. To the best of our knowledge, we are the first to use swarm based optimization techniques assuming such scenarios in path planning for localization in WSNs. The proposed models provide outstanding results in several metrics in comparison to some existing works. The rationale of adopting swarm-based algorithms in general, and GWO and WOA in particular, lies on their ease to implement and computational efficiency in many optimization problems.

We work on designing an obstacle-avoidance path for mobility-assisted localization in WSNs. We summarize our contribution in the following points:

1. For the first time, the MA path is dynamically formed based on meta-heuristic optimization models. Using either GWO or WOA in the movement decision helps to increase the number of localized nodes and more importantly minimize the localization error.

2. While considering all of the area's and nodes' constraints, the proposed models ensure that a larger number of UNs can receive the MA's localization information compared to other models. This number increases when the maximum distance increases. In comparison to other existing models, our proposed models offer better localization ratios.

3. The objective function comes first. In every movement step, the MA will make its decision for next movement based on the fitness of the objective function. Therefore, both models show a competitive accuracy.

4. Regardless of the number of obstacles, locations, or dimensions, the optimized MA movement can sense and find them. Thus, the MA can consequently act by ignoring the direction of the obstacles and consider the alternative directions while also taking other constrains into account.

5. Unlike the other models, in which the MA has to go around the obstacles and keep moving in the same movement pattern, the MA in our proposed models is free to change its own direction based on the applied optimization model. This freedom is important for avoiding to have the MA being trapped in a small region.

The rest of this chapter is organized as follows: Section 6.2 provides an overview of swarm intelligence based works in WSNs, and the two optimization models used in this work, GWO and WOA. Section 6.3 states the system model assumptions. We introduce our proposed models starting with the constraints and the objective analysis, then present the GWPP and WOPP approaches in details, and ending with describing the localization process all in Section 6.4. In Section 6.5 and

6.6 respectively, we show the simulation and performance setting, and discuss the evaluation results. Section 6.7 offers a discussion on both proposed models based on the shown results, and we conclude our work by Section 6.8 and ending by stating the future works.

6.2 Swarm Intelligence in WSNs

In recent years, Meta-heuristics have gained an attention and have been applied in many fields. The term Meta-heuristic denotes an area of general algorithms and frameworks that are designed to deal with complex optimization problems [99]. Simplicity of concept, ease of implementation, and its applicability to be used in different problems are few reasons behind its successful spread [20]. Their inspiration, typically, is based on mimicking a natural phenomenon [20, 99]. Generally speaking, the Meta-heuristics can be categorized into three main classification, evolution-based, physics-based, and swarm-based methods [19]. Genetic Algorithms (GA) [100] is the most popular example of the first category, the evolution-based algorithms. In physics-based category, we can mention the Simulated Annealing (SA) [101] as a popular example, while in the swarm-based methods, there is a list of existing models that includes Particle Swarm Optimization (PSO) [102], Ant Colony Optimization (ACO) [103], Artificial Bee Colony (ABC) algorithm [104], and many other existing algorithms. Since our techniques focuses on swarm-based optimization, we limit our discussion only to such methods. Swarm-based, or Swarm Intelligence (SI), optimization is a relatively new field that showed a novel direction in optimization research [105]. Simply, swarm-based algorithms are optimization models that try to solve the researched problem by imitating the social behavior of creatures, especially animals [19]. In WSNs, swarm-based optimization models have been used for many purposes including routing [106, 107], energy efficiency [108–110], reliability [111] and other applications. For instance, in [108], the authors introduce a hybrid swarm intelligence energy efficient algorithm that works to enhance the clustering and routing processes using both ABC

and ACO algorithms. In [109], a new energy efficient cluster head selection algorithm based on the PSO, called PSO-ECHS, is proposed. It consists of two phases, a cluster head selection phase that is based on PSO, and a cluster formation phase, which depends on the residual energy of nodes. In node localization in WSNs, several works have been done considering the SI algorithms. In [112], another SI based model is proposed for node localization this time. The work introduces two different localization models that use PSO and ABC together. The localization algorithms are evaluated in both single-stage and multi-stage localization. The evaluation results show that the PSO-based localization algorithm performs better than the one that uses ABC. However, no comparison to other existing localization works was performed. A multi-objective PSO localization algorithm, MOPSOLA, is presented in [113] to enhance the localization in WSNs. The investigated objective functions consist of the space distance constraint and the geometric topology constraint. The proposed model shows better results in terms of localization error compared to other similar models. Another direction of localization is considered in [114], where the UNs are assumed to be moving and distributed in underwater WSNs. The proposed localization model is based on mobility prediction and PSO. The results show that the nodes locations can be estimated along with their velocity and movement can be predicted. However, to best of our knowledge, no study of using SI in controlling the MA movement and path planning for obstacle-exist networks in localization assistance in WSNs has been proposed. Therefore, we propose our GWPP and WOPP models. More details about the proposed models will be shown in Section 6.4, but an overview about GWO and WOA will be first presented in the following sections 6.2.1 and 6.2.2 respectively.

6.2.1 Grey Wolf Optimization

Proposed by Mirjalili et *al.* in [19], Grey Wolf Optimizer (GWO) is a new metaheuristic algorithm that mimics the natural leadership hierarchy system of the grey wolves. Grey wolves live in small groups of members. They have a special social

dominant hierarchy that divides the group into four hierarchical parts starting of the top leaders called alphas (α), then betas (β), delta (δ), and the lowest ranking of the hierarchy is omega (ω). Each of these kinds leads the subgroup that is located in its lower ranking. For example, Delta wolves are followers of alphas and betas but they can lead the omegas. Figure 6.1 depicts the social pyramid of the Grey Wolf in nature.

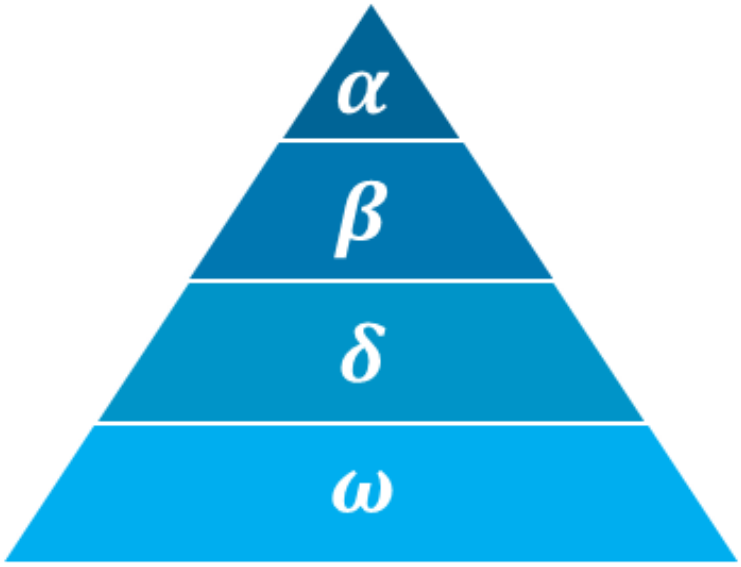

Figure 6.1: Hierarchy of grey wolf (adopted from [19])

For the mathematical modelling, alpha (α), beta (β), and delta (δ) represent the best three candidate solutions within the search space respectively. The optimization process is guided by these candidates. All other candidate solutions are considered as omegas (ω). Each candidate solution is represented as a vector in

$$\vec{X} = x_1, x_2, ..., x_n \tag{6.1}$$

Where x_i is the current position of the grey wolf, and n is the dimension of the search space [115]. Mathematically, the hunting process represents the optimization, while searching for the prey represents the available solutions. The grey wolf hunting behavior consists of three main phases starting with encircling the prey, hunting, and attacking the prey. The first phase, prey encircling, is mathematically

modelled as

$$\vec{D} = |\vec{C}.\vec{X}_P(t) - \vec{X}(t)| \tag{6.2}$$

$$\vec{X}(t+1) = \vec{X}_P(t) - \vec{A}.\vec{D} \tag{6.3}$$

Where t indicates the current iteration, $\vec{A}$ and $\vec{C}$ are two coefficient vectors, $\vec{X}_P$ is the position vector of the prey, and $\vec{X}$ indicates the position vector of a grey wolf.

The two coefficient vectors of $\vec{A}$ and $\vec{C}$ can be calculated as

$$\vec{A} = 2\,\vec{a}.\vec{r}_1 - \vec{a} \tag{6.4}$$

$$\vec{C} = 2\,\vec{r}_2 \tag{6.5}$$

Where components of $\vec{a}$ are linearly decreased from 2 to 0 over the iterations course, and $\vec{r}_1$, $\vec{r}_2$ are vectors chosen randomly in the range of [0, 1]. Initially, the grey wolves are able to locate potentially the prey positions in order to hunt them. This localization is guided by the first best solutions, namely (α), beta (β), and delta (δ). Thus, these three best candidate solutions so far will be saved and updated over the iteration times in order to support other wolves (ω) finding their own positions. This process of hunting is represented using the following formulas

$$\vec{D}_\alpha = |\vec{C}_1.\vec{X}_\alpha - \vec{X}| \tag{6.6}$$

$$\vec{D}_\beta = |\vec{C}_2.\vec{X}_\beta - \vec{X}| \tag{6.7}$$

$$\vec{D}_\delta = |\vec{C}_3.\vec{X}_\delta - \vec{X}| \tag{6.8}$$

Where $\vec{D}_\alpha$, $\vec{D}_\beta$, and $\vec{D}_\delta$ are the updated distance vectors between the position of

each leader wolf and the other wolves. $\vec{C}_i$ is the required coefficient vector that is calculated using the formula in equation 6.5, and $\vec{X}$ is the position of other wolves. Each $\vec{X}_i$ represents an estimated position calculated based on the distance vector between the omega wolf and each leader wolf of $\vec{D}_\alpha$, $\vec{D}_\beta$, and $\vec{D}_\delta$ respectively. They are calculated as

$$\vec{X}_1 = \vec{X}_\alpha - \vec{A}_1.(\vec{D}_\alpha) \tag{6.9}$$

$$\vec{X}_2 = \vec{X}_\beta - \vec{A}_2.(\vec{D}_\beta) \tag{6.10}$$

$$\vec{X}_3 = \vec{X}_\delta - \vec{A}_3.(\vec{D}_\delta) \tag{6.11}$$

The updated new position vectors are given as $\vec{X}_i$ where $\vec{X}_1$ is the new position based on alpha position $\vec{X}_\alpha$ and the distance vector $\vec{D}_\alpha$, $\vec{X}_2$ is the new position based on alpha position $\vec{X}_\beta$ and the distance vector $\vec{D}_\beta$, and $\vec{X}_3$ is the new position based on alpha position $\vec{X}_\delta$ and the distance vector $\vec{D}_\delta$. The coefficient vectors of $\vec{A}_i$ are calculated as in equation 6.4. Therefore, using the average sum of all previous positions, the new position vector is calculated as

$$\vec{X}(t+1) = \frac{\vec{X}_1 + \vec{X}_2 + \vec{X}_3}{3} \tag{6.12}$$

The third phase, the prey attacking, comes after the hunting phase. In this phase, the value of $\vec{a}$ is decreased, which therefore decreases the value of $\vec{A}$. The value of $\vec{A}$ is limited by the range $(-2a, 2a)$. In order to find a better solution, $\vec{A}$ value has to be more than 1.

Since its first appearance, GWO has caught growing attention. It has been used in tremendous engineering and optimization problems. In WSNs, GWO is used varying from routing [116], energy efficiency and clustering [117], and localization [115].

6.2.2 Whale Optimization Algorithm

Whale Optimization Algorithm (WOA) is another new swarm intelligence optimization model that was recently proposed [20]. As indicated by its name, WOA simulates the social behavior of humpback whales. Whales have the ability to think, learn, communicate and have a higher level of smartness in comparison to many other creatures. An interesting social behavior of whales is their special strategy of hunting, so-called bubble-net feeding. This strategy consists of two main maneuvers, upward-spirals and double-loops. The proposed WOA is based only on the former one. In this maneuver, whales dive deeply in the water and start creating bubble around the prey in a spiral shape, and swim up toward the surface of the water. The spiral shape movement is similar to number '9'. The mathematical model of WOA consists of three phases, prey encircling, spiral bubble-net feeding maneuver, and search for prey. In the first phase, the prey encircling, the whales are assumed to recognize the location of the prey and encircle them. Initially, the WOA considers the target prey as the current best candidate solution, since the position of the optimal solution is not known a prior. This search candidate will be updated in case a better candidate solution is achieved. Similar to GWO, this behavior is formulated as

$$\vec{D} = |\vec{C}.\vec{X}^*(t) - \vec{X}(t)| \tag{6.13}$$

$$\vec{X}(t+1) = \vec{X}^*(t) - \vec{A}.\vec{D} \tag{6.14}$$

Where $\vec{C}$ and $\vec{A}$ are coefficient vectors, $\vec{X}^*$ is the so far obtained best solution of position vector, and $\vec{X}$ is the position vector. The value of $\vec{X}^*$ is updated continually with each iteration. The two coefficient vectors of $\vec{C}$ and $\vec{A}$ are calculated as

$$\vec{C} = 2\,\vec{r} \tag{6.15}$$

$$\vec{A} = 2\vec{a}.\vec{r} - \vec{a} \tag{6.16}$$

Where, similar to GWO, $\vec{r}$ is a random vector in the range of [0, 1], and $\vec{a}$ is a linearly decreased value from 2 to 0 over iterations course. Adjusting the values of $\vec{C}$ and $\vec{A}$ leads to give different places around the best candidate achieved. In the second phase, the bubble-net attacking method is represented mathematically as the exploitation phase. This behavior of bubbling is done following two approaches, the shrinking encircling mechanism and the spiral updating position. The former approach is achieved by decreasing the value of $\vec{a}$, which therefore decreases the value of $\vec{A}$. In the latter approach, the distance between the whale current location and the prey location is calculated. A spiral equation is formulated to mimic the whales' movement between the two locations as follows

$$\vec{X}(t+1) = \vec{D'}.e^{bl}.\cos(2\pi l) + \vec{X^*}(t) \tag{6.17}$$

$$\vec{D'} = |\vec{X^*}(t) - \vec{X}(t)| \tag{6.18}$$

Where $\vec{D'}$ indicates the best solution so far (the distance of the ith whale to the prey), b is a constant value that defines the logarithmic spiral, l is a random number in the range [-1, 1]. The whales swim simultaneously within a shrinking circle in a spiral-shaped path. Similarly, the WOA has a 50% of choosing the shrinking encircling mechanism or the spiral model and updates the new position based on that. This is mathematically modelled as

$$\vec{X}(t+1) = \begin{cases} \vec{X^*}(t) - \vec{A}.\vec{D}, & \text{if p} < 0.5 \\ \vec{D'}.e^{b1}.\cos(2\pi l) + \vec{X^*}(t), & \text{if p} \geq 0.5 \end{cases} \tag{6.19}$$

Where p is a random value in [0, 1]. The last phase, search for prey, is simulated as the exploration phase in WOA. Unlike the previous phase, the whales search for prey randomly according to the position of each other. For this reason, the value

of $\vec{A}$ is chosen randomly. However, it has to be greater than 1. This is intended to let the whale exploration to perform a global search. This is formulated as

$$\vec{D} = |\vec{C}.\vec{X}_{rand} - \vec{X}| \tag{6.20}$$

$$\vec{X}(t+1) = \vec{X}_{rand} - \vec{A}.\vec{D} \tag{6.21}$$

Where $\vec{X}_{rand}$ is a random value representing a random position vector (a random whale) selected from the current population.

Generally, the WOA is initiated with a set of random solutions. With every iteration, the search agents update their location based on either the best solution obtained so far or a random search agent.

Although, it was published recently, the WOA is used in many engineering application including WSNs. The work introduced in [118] proposes a lifetime maximization of WSNs using WOA.

6.3 System Model and Assumptions

The following assumptions are used to form the system model:

1. A two-dimensional plane network following a square shape. S one side of the square area of the network in m.

2. The network area is assumed to have a set of obstacles. The number of obstacles is denoted as O. The dimensions of each obstacle is given as O_{size} in m. For simplicity, the obstacles are assumed to be rectangles.

3. A set of UNs are distributed following an arbitrary form. The number of these nodes is introduced as N.

4. At first, all UNs inside the network have no prior knowledge about their current locations.

5. All deployed nodes are static, which means no node is able to change its own location once the distribution process is done.

6. Each node has a fixed communication range R_{Tx} in m.

7. An MA is able to move freely in the network in straight directions except in locations where obstacles exist. It is also assumed to have the ability to locate itself in any point in the network. The number of MAs is denoted as M.

8. The MA is able to detect any obstacle in its direction using any detection method. Examples of those detection methods include infrared (IR) sensors or passive infrared (PIR) sensors [119]. Unlike the active IR, the PIR depends on the received IR that is emitted by the objects.

9. The MA movement is constrained by the value of maximum distance (d_{max}), where the MA movement cannot go beyond this value.

10. While the MA is moving, it frequently stops to provide nodes within its communication range with its current position. Each of these positions called a localization point.

11. The MA and UNs cannot communicate with each other except if their locations are within the communication range of each other.

12. Once any three different location information of MA are received by a UN, it estimates its own location by the used localization model.

13. Once the UN succeeds in estimating its location, it turns into a reference node (RN). The RN can share its own location information with other UNs located within its range, which will help in estimating their locations.

6.4 Proposed Models

In this section, we discuss the constraints and objectives of this model and then introduce the two movement techniques. Then, we describe the localization process from both side, on the MA's side and on the UN's side.

6.4.1 Constraints and Objectives Analysis

As in many path planning models in WSNs, a number of constraints is assumed. In this model, we assume four different constraints as follow:

1. In the network area, every visited localization point must be unique. This means that the MA cannot visit a localization point more than once and cannot return to the same point at any time.

2. To avoid the collinearity problem that affects the localization results, the model forces the MA movement to be not collinear by assuming that every three consecutive localization points are not on the same line.

3. The MA cannot exceed the limited movement distance (d_{max}). Once this distance is reached, the MA stops.

4. The network area includes a set of obstacles distributed randomly around the network. The MA has no prior knowledge about the obstacles' locations and has to detect them during its movement, thus, avoid them.

Although it is a rare situation to have the MA trapped in a small area of network, the MA can any of the first three constraint rules once it happens in order to keep moving. The last constraint cannot be broken since the MA is unable to move over the obstacle.

The main objective function of this model is to minimize the average localization error of the deployed nodes. It is represented as

$$Minimize \;\; Error_{avg} \tag{6.22}$$

6.4.2 Movement Decision

Before starting the MA movement, a few rules regarding the movement pattern will be assigned. The network area will be virtually divided into a set of lines, each line includes a set of guide points. The distance between each two lines is fixed. Also, the distance between any two guide points in the same line will be fixed, denoted as d_p. Similar to [21], this distance is given as $R_{Tx}/\sqrt{3}\,m$. Therefore, to maintain the condition of fixed distance between each two neighbor points in any direction, the distance between each two lines are given as $d_p/2\,m$. However, the starting point in each consecutive lines will be incompatible. In other words, if the starting point of line a is (x, y), the next line b will be starting a half of d_p as $(0.5x, 2y)$. This is intended to overcome the collinearity problem forming a triangle-shape of virtual points. In addition, since the MA has to consider the movement constraints, a few rules are considered as shown in Figure 6.2.

Initially, as in Figure 6.2a, the MA is surrounded with six different points, any of which can be chosen as a next point to visit based on the optimization model decision. Let us say that the MA has the following points in its range $\{a, b, c, d, e, f\}$. Based on the optimization decision, the MA selected the point f as next point to move to. Now, a new set of points will be formed. The last point that MA has just left will be a new point in the new form, called c in Figure 6.2b. However, this point will be excluded from the potential visiting point since it has already been visited. Thus, the MA will never visit it again. Two more points in Figure 6.2b will be ignored as well, namely $\{e, f\}$. These points will be excluded for different reasons. The point e is located in an obstacle direction, which MA has to avoid, by considering other directions. On the other hand, the point f will not be considered because of the collinearity problem, which imposes that three consecutive points cannot be collinear. Thus, only the other three points, namely $\{a, b, d\}$, will be considered. The decision of moving to one of them will be made based on the applied optimization model. In this example, the MA selects the point a as the next point, and the same procedure concept will be repeated.

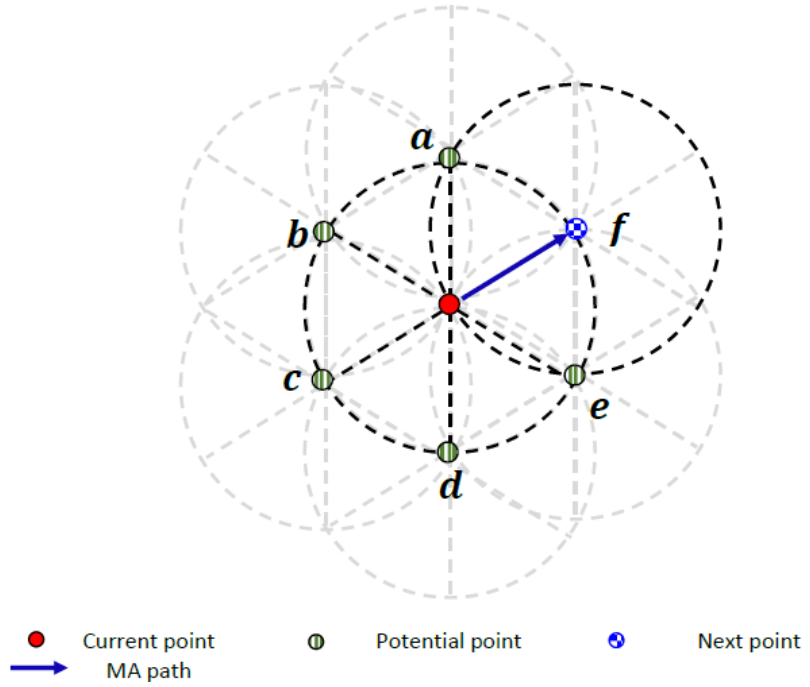

(a)

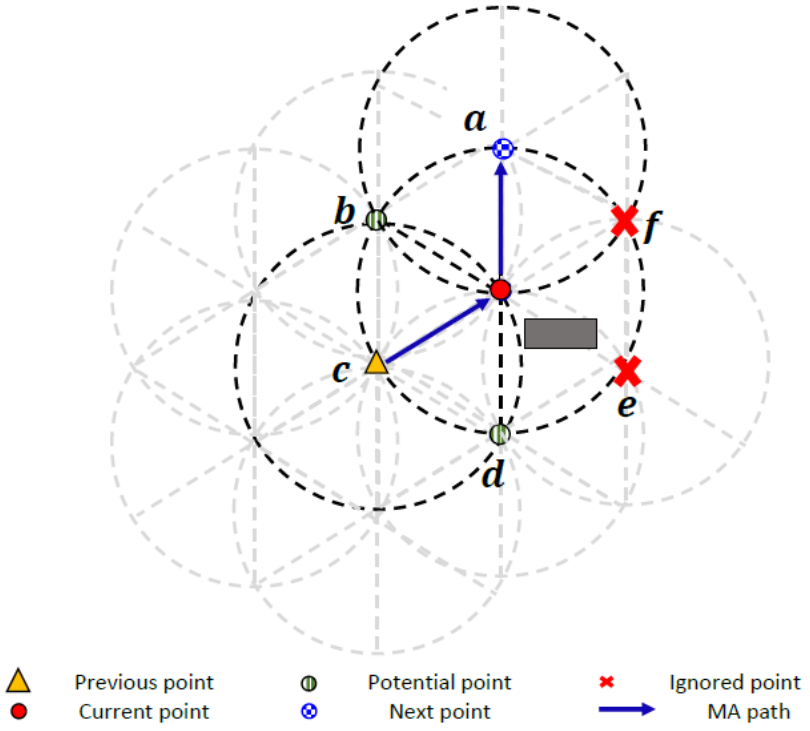

(b)

Figure 6.2: The base of selecting the next movement point in (**a**) first movement, and (**b**) next movements.

A. Grey Wolf Optimizer based Obstacle-Avoidance Path Planning (GWPP)

Once the MA receives the information of the network area and forms its movement virtual points, it starts its journey by making three random movements. This is meant to let the MA to get more information about its starting area [21,73]. With every movement, the MA will be providing its current location to the nearby UNs. Once three random movements are done, it is time for the optimized movement. In the next movement steps, the MA will select the path to satisfy the collinearity condition and avoid the obstacles. Based on such considerations, the MA will use the GWO to define a candidate direction point by calculating the fitness value of each direction point. The fitness function used here is the objective function, minimizing the localization error rate. It is represented as

$$error_{total} = \Big(\sum_{i=1}^{N} error_{(i)} \Big) \tag{6.23}$$

Where $error_{(i)}$ is the localization error of node i and can be given as

$$error_{(i)} = \sqrt{(x_i - u_i)^2 + (y_i - v_i)^2} \tag{6.24}$$

Where (x_i, y_i) are the real coordinates of the node i, and (u_i, v_i) are the estimated ones of the same node i. The MA will evaluate all nodes within its range, run the GWO optimization and select the point that satisfies most the fitness function. The modified pseudo code of GWO is given as follows:

Algorithm 2 Pseudo code of the GWO algorithm in GWPP

Initialize the number of movement steps $X_i (i = 1, 2, ..., n)$
Initialize a, A, and C
Calculate the fitness of each candidate point
X_α = the best candidate point
X_β = the second best candidate point
X_δ = the third best candidate point
while $t < T_{max}$
  for each candidate point
Update the position of the current point by the eq. 6.12
  end for
  Update a, A, and C
  Calculate the fitness of all candidate points
  Update X_α, X_β, and X_δ
  $t = t + 1$
end while
return X_α

Where the X_i here indicates the number of MA movement steps (the grey wolf population), given as the maximum distance of MA divided by the distance between each two points as

$$X_i = \frac{d_{max}}{d_p} + 1 \tag{6.25}$$

Each potential candidate represents a point search agent , and X_α is the best candidate point (the best search agent) to move to. t is the current iteration and T_{max} is the maximum number of iterations.

B. Whale Optimization Algorithm based Obstacle-Avoidance Path Planning (WOPP)

Similar to GWO, the movement decision here will be made based on the optimization model of WOA. However, it starts first with three random movements. The modified pseudo code of WOA is given as in algorithm 3, where the whale population X_i here denotes the number of MA movement steps,

each search agent indicates the candidate next points, and X^* is the best candidate point.

Algorithm 3 Pseudo code of the WOA algorithm in WOPP

```
Initialize the number of movement steps X_i(i = 1, 2, ..., n)
Calculate the fitness of each candidate point
X* = the best candidate point
while t < T_max
   for each candidate point
   Update a, A, C, l and p
      if p < 0.5 then
         if |A| < 1 then
            Update the position of the current candidate point by the eq. 6.14
         else
            Select a random candidate point X_rand
            Update the position of the current candidate point by the eq. 6.21
         end if
   else if p ≥ 0.5 then
         Update the position of the current candidate point by the eq. 6.17
      end if
   end for
   Check if any candidate point goes beyond the search space and amend it
   Calculate the fitness of each candidate point
   Update X* if there is a better solution
   t = t + a
end while
return X*
```

WOA includes more details about the movement pattern, as shown in algorithm 3; there might be a chance to select a random point among the available points. However, this randomness should not conflict with other related constraints, specifically the collinearity and obstacle points. This random selection is based on the 50% chance of choosing either shrinking encircling mechanism or the spiral model shown above in equation 6.18, in Section 6.2.2 (WOA model).

6.4.3 Mobility Movement and Localization Process

The movement of the MA and localization procedure are simultaneously preformed in two aspects, the MA side and UN side as follow:

A. Procedure in UN's Side

The following steps are performed in the UNs side:

(a) All UNs are distributed randomly.

(b) Each node will initiate a neighboring table, which includes all neighbor nodes located within the communication range of that UN. The neighboring table will include the node id, the node type, the number of neighbors, the neighbor ids, and neighbor status of localization. The node type here indicates the localization status and can be either a UN or an RN.

(c) Each UN will wait for MA arrival. Upon the MA arrival to each node, the node will exchange its table with the MA.

(d) Once three varied points are received, the UN estimates its own location.

(e) When a UN get its location estimation, it turns into an RN, and updates its table.

(f) Each RN will share its updates table with all neighboring nodes.

The entire process is shown in the following algorithm 4.

Algorithm 4 Pseudo code of the node localization process in the UN

```
do Initialize the localization process
do UN communicates with its neighbors
do UN updates its neighbors table
if three different RNs in the table equals No
   set three different locations received to No
   while three different locations received equals No
      set MA arrives to UN's range to No
      while MA arrives to UN's range equals No
         do wait
         if MA arrives to UN's range equals Yes:
      exit while
      do UN exchanges its table with MA
      if three different locations received equals Yes:
   exit while
do UN estimate its location, UN turns to RN
```

B. Procedure on MA Side

The following steps are performed in the MA side:

(a) MA initiate its movement from a starting point, which can be either randomly chosen or set in advance.

(b) MA will be given the maximum distance of movement.

(c) The first three movements of MA will be chosen randomly, in any direction. However, it must to be only on the guide points.

(d) With each movement, MA stops and contacts all nodes located within communication range to provide its current coordinates.

(e) Every movement after that will be made only based on the applied optimization model

(f) After each movement, MA will update its localization table that is similar to the neighboring table of each UN.

(g) MA will terminate its movement once the maximum movement distance is reached.

More details about the procedure are shown in the following Algorithm 5.

Algorithm 5 Pseudo code of the movement and node localization process in the MA in GWPP or WOPP

```
do Initialize the movement process
set three random movements reached to No
set maximum distance reached to No
while three random movements reached equals No, do
   do MA moves randomly
   do MA stops, provides nodes within its range with its current location
   set three random movements reached to Yes
   while maximum distance reached equals No, do
      do Update routing table
      if three random movements reached equals No
           exit while
      end if
      if three random movements reached equals Yes
         do Evaluate all candidate points within range
         do Identify collinear points
         do Identify previously visited points
         do Run GWO algorithm as outlined in Algorithm 2, or WOA algorithm
as outlined in Algorithm 3
         do MA moves to selected point
         if maximum distance reached equals Yes
            exit while
         end if
      end if
   end while
end while
```

Figure 6.3 shows an example of the MA movement when both (GWPP) and (WOPP) models are applied. The initial setting are intended to be the same, which include the random starting point, the three first movements, the same obstacles locations, and the same nodes distribution. Figure 6.3a presents the MA path planning when GWO is used, while Figure 6.3b shows the movement of MA when WOA is applied. Note how each optimization model works differently and makes its distinctive path although all network settings are the same.

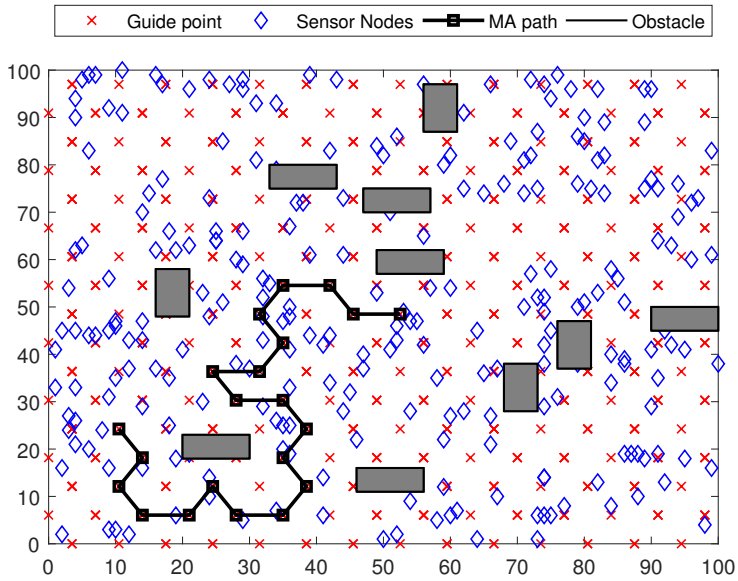

(a)

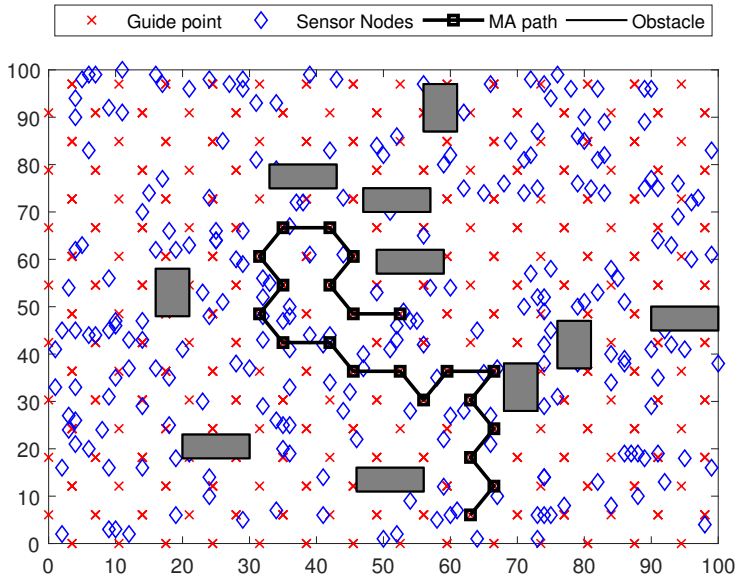

(b)

Figure 6.3: The obstacle-avoidance path planning of the two models in (**a**) GWPP, and (**b**) WOPP.

6.5 Performance Settings

To evaluate the performance of our proposed models, we implemented them along with two obstacle-avoidance models, Z-Curves and Snake-Like. For a better assessment, we used the two localization algorithms that we used before, the WCL [49] and WCWCL [45]. Figure 6.4 shows a magnified example of WCWCL localization model in one of the optimization based movement. A small number of nodes has been used for a better representation.

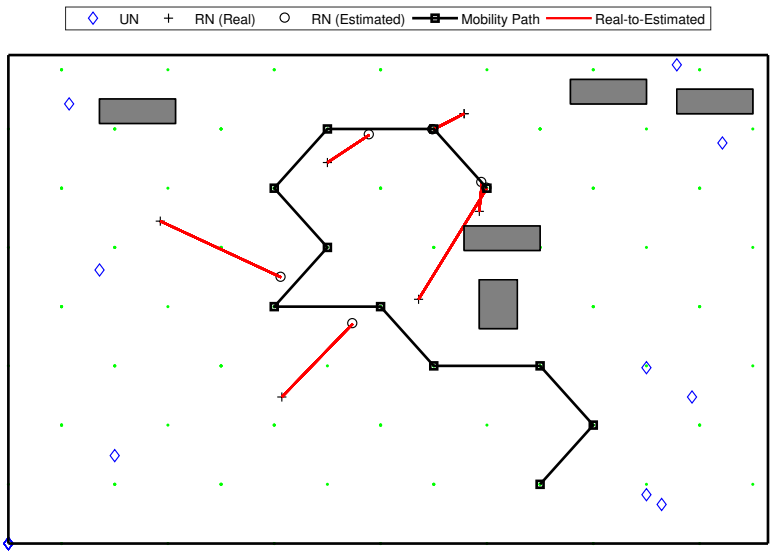

Figure 6.4: An example of the localization estimation when one of the optimization based movement is used in WCWCL

Matlab was used to model the proposed framework and for performance evaluation of GWPP, WOPP and the other two models. The evaluation has been done in terms of five performance metrics: localization accuracy, localization precision, localization ratio and coverage, and the computation time of the two proposed models. The simulation environment and parameters used were selected for consistency with some other similar works. The network area is assumed to be square with a size, S, of 100 $\times$ 100 m. A set of 250 randomly distributed nodes, N, is used with a single MA, M. Various maximum movements, d_{max}, are applied. The

value of d_{max} indicates the maximum distance that MA can take before its ends its journey. In this work, the starting point in all runs is chosen randomly. Chipcon CC1100 radio module [77] specifications are employed as realistic simulation parameters. Such characteristics were already employed in similar proposals including [9, 21, 45]. For simplicity, we round the value of d_p to the nearest integer number. The rest of the parameters are presented in Table 6.1.

Table 6.1: Simulation values and parameters in GWPP and WOPP

Parameters	Symbol	Value
Network size (m)	S	100×100
Number of MA	M	1
Number of UNs	N	250
Maximum movement distance (m)	d_{max}	35, 70, 105, 140, 175
Communication range (m)	R_{Tx}	12.5
Resolution	R	0.5, 0.75, 1, 1.5, 1.75, 2
Path loss exponent	β	3.5
Power loss (dB) at d_0	$PL(d_0)$	-60
Reference point (m)	d_0	1
Standard deviation of noise	σ	3
Number of obstacles	O	10
Obstacles dimensions (m)	O_{size}	5×10
Maximum number of iterations	T_{max}	50-300
Simulation run		50

6.6 Evaluation and Results

To assess the performance of the proposed models, we tested the following metrics, accuracy, precision, and localization ratio from two aspects: the impact of maximum movement distance and the impact of resolution. We also evaluated the computation time for the two algorithms of GWPP and WOPP.

6.6.1 Localization Accuracy

To analyze the behavior of the planned models in comparison to the others when different maximum movement distances (d_{max}) are applied, we first performed a

test of 50 simulation runs with 250 UNs, 12.5 m of R_{Tx} that is equivalent to R = 1, 140 m of d_{max}, and a standard deviation of noise (σ) of 3. The rest of parameters are fixed as shown in Table 6.1. In addition to evaluating the localization error, we also evaluate the standard deviation of the localization error. The results in Figures 6.5 shows the performance of all models according to their localization error when the two localization algorithms of WCL and WCWCL are applied.

When WCL is used, as shown in Figure 6.5a, both of our proposed models offer superior accuracy with the lowest error rate in all of the results shown. In most of the 50 run cases, both models provide a high accuracy with less than 3 m of error. Based on the deployment of nodes and location of obstacles, the results from both models vary over the simulation runs. Both GWPP and WOPP show similar performance during the different simulation runs. Most run results show values less than 1.5 m of standard deviations. On the other hand, Z-Curves and Snake-Like models provide unstable performance. One reason behind this behavior is the inability of the static models to dynamically change their planned path. In case of facing an obstacle in their way, Z-Curves and Snake-Like models will only avoid the obstacle and then continue on the statically planned path, which will affect the performance of the models and may create a collinearity problem. Indeed, the Snake-Like model does not present a solution to deal with the collinearity problem. This is clear in their performance of accuracy where most runs achieve results around 6.5-7.5 m of error rate. In fact, some results are close to 8 m of error rate depending on the network topology. On the other hand, when WCWCL is used as in Figure 6.5b, improved outcomes for all models are achieved. However, this improvement is more noticed in both of GWPP and WOPP as they accomplished high accuracy. The localization accuracy is improved in both Z-Curves and Snake-Like models. We start to notice some results around 5 m of localization error in Z-Curves. In general, both models performs better in WCWCL than in WCL.

A. The Impact of Maximum Movement Distance

Then, the average localization error for all movement models when different

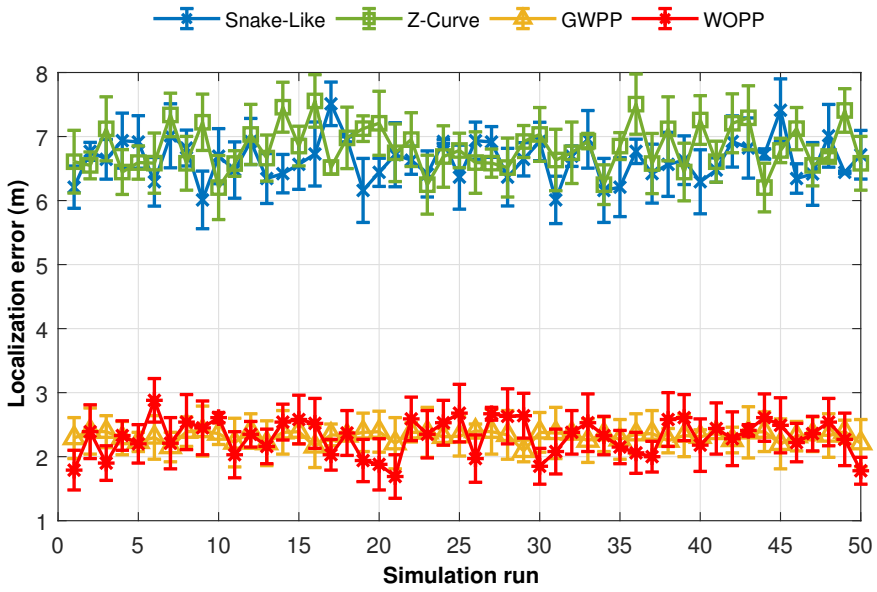

(a)

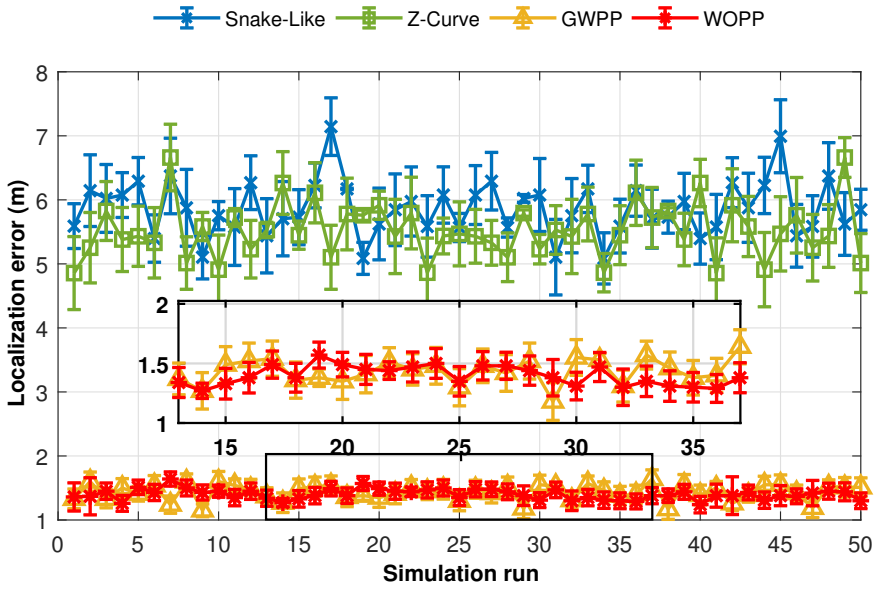

(b)

Figure 6.5: Localization errors of all mobility models in (**a**) WCL, and (**b**) WCWCL, ($d_{max} = 140, R = 1$)

maximum distances (d_{max}) are applied, is calculated. For a better evaluation, we performed different experiments with changeable values of the maximum distance of movement (d_{max}). The values of d_{max} range from 35 m to 175 m. The area consists of 250 UNs, 10 obstacles of 5×10 m each. The resolution value (R) of 1 is assumed. Figure 6.6 presents the performance of the path models when WCL and WCWCL are used.

Figure 6.6a shows the average localization error and the corresponding d_{max} for all models when WCL is used, while Figure 6.6b shows the average localization error when WCWCL is used. Five different d_{max} values of 35 m, 70 m, 105 m, 140 m, 175 m are applied.

With both localization algorithms, our proposed path models of GWPP and WOPP offer higher accuracy. Indeed, it is noticed that when d_{max} increases, the localization error decreases. In general, and with both WCL and WCWCL, WOPP offers better performance than GWPP. However, the difference between their performances is small. The main reason that WOPP provides better results than GWPP is that WOPP calculates the next visiting point based on satisfying a fitness function, whereas the next visiting point in GWPP is based on the mean of the three best candidate points. Also, WOPP makes a random movement when an optimum next visiting point is not found. On the other hand, Z-Curves and Snake-Like provide a lower performance of accuracy in comparison to GWPP and WOPP in both WCL and WCWCL localization. However, all path planning models performs better with WCWCL. The localization error for Z-Curves and Snake-Like using both WCL and WCWCL decreases with increasing maximum movement, d_{max}, as shown in Figue 6.6a. However, their localization error using WCL is more than 6.5 m when d_{max} is 175 m, more than twice that of our proposed models GWPP and WOPP.

In WCWCL, as presented in 6.6b, Z-Curves and Snake-Like become better

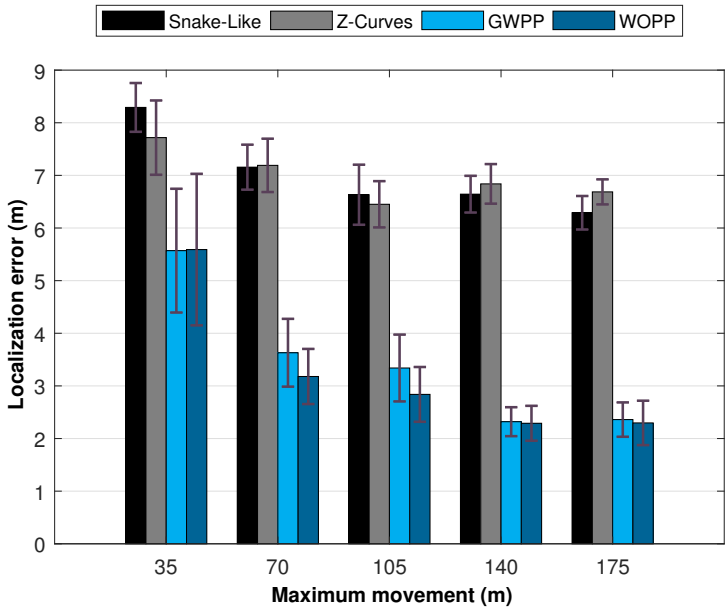

(a)

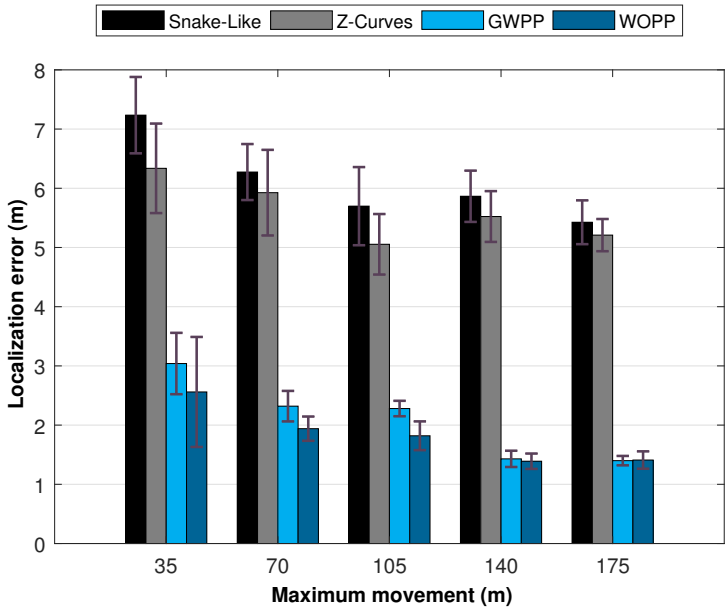

(b)

Figure 6.6: Average localization errors with standard deviation of errors versus maximum movement in (**a**) WCL, and (**b**) WCWCL

and the error rate decreases to close to 5.5 m in some cases. In general, Z-Curves performs better when WCWCL is used. Z-Curves takes into account the collinearity problem in its design while Snake-Like does not. GWPP and WOPP have high accuracy with WCWCL with only approximately 2.32 to 1.4 m of error when d_{max} increases from 35 m to other distances.

The CI of the localization error is also used to prove the statistical significance for all models. A 95% of CI is selected to test that significant. Figure 6.7 shows the average localization errors and the 95% confidence interval with the corresponding maximum movement. The results explain that in most cases, both of our proposed models, GWPP and WOPP, provide narrower CIs, implying that the improved performance is statistically significant.

B. The Impact of Resolution

In addition to evaluating the localization error when different d_{max} values are applied, we also evaluate the impact of resolution R on the localization error. The resolution values R refer to the relationship between the communication range, R_{Tx}, and the distance between every two points in each static path planning model. It has been used in some other similar works including [9, 37, 38]. However, in this work and since the distance between every two points is fixed as described before, the change will be only in the value of R_{Tx}. For example, when R = 0.5, communication range will be $0.5 \times R_{Tx}$ and so on. Figure 6.8 shows the average localization error with different R when d_{max}=140 m. When R = 1, the standard R_{Tx} = 12.5.

In the first test where WCL is used, as in Figure 6.8a, the accuracy of all model is substantially decreased when small resolution values of 0.5 and 0.75 are used. This is applicable to all models. In fact, error values of 13 m and 11 m are shown in Snake-Like and Z-Curves respectively. Even in our models, localization error of 7 m are presented when the same resolution of 0.5 is used. However, in all models, increasing R decreases the error. Very high accuracy is achieved when R of 2 is used, with less than 2 m of error in GWPP and

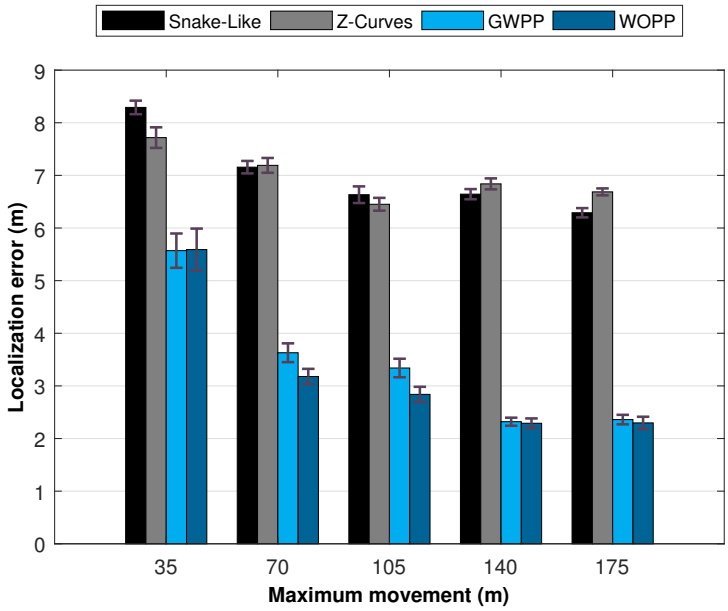

(a)

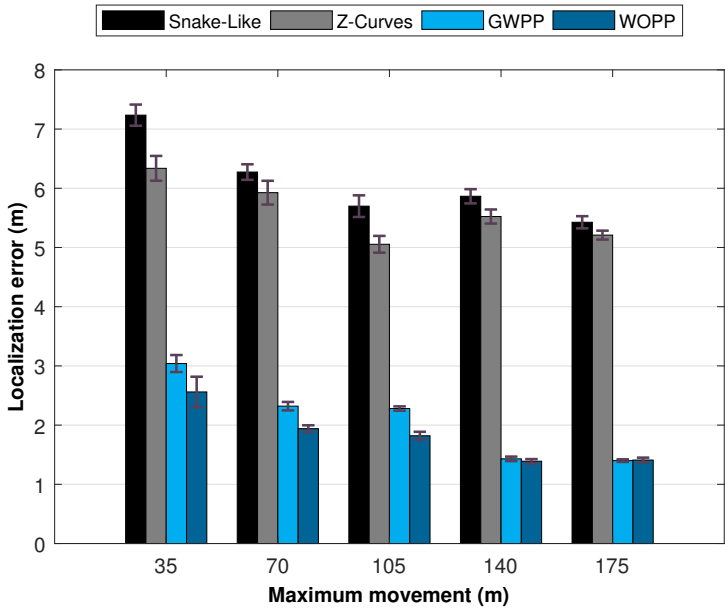

(b)

Figure 6.7: Average localization errors and the 95% confidence interval with the corresponding maximum movement in (a) WCL, and (b) WCWCL

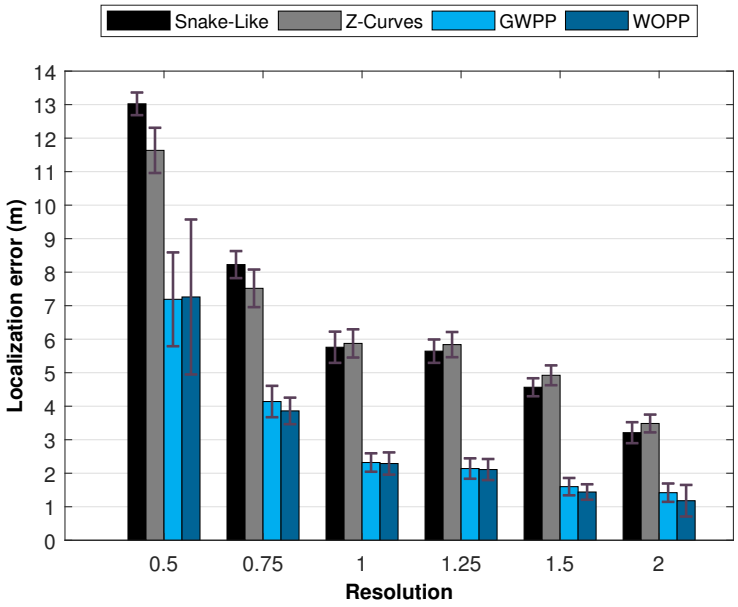

(a)

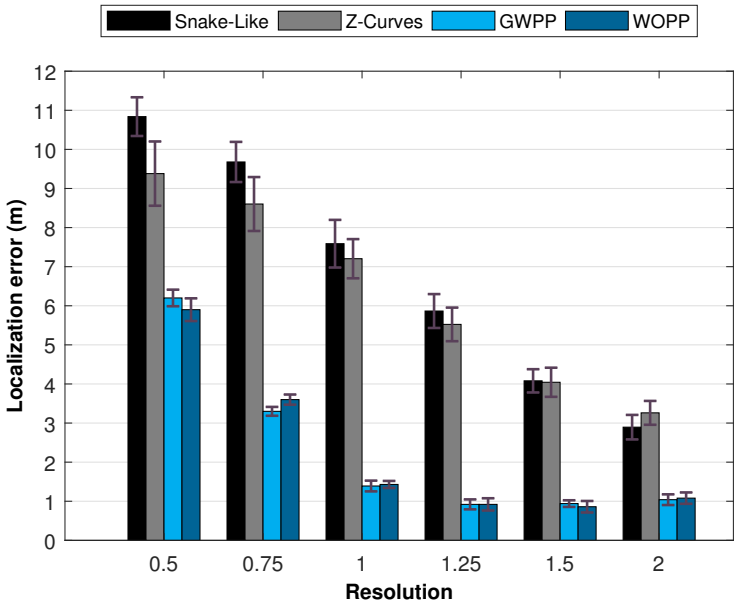

(b)

Figure 6.8: Average localization errors with standard deviation of errors and resolution in (**a**) WCL, and (**b**) WCWCL.

WOPP. The same concept is shown also when WCWCL is used as presented in Figure 6.8b. However, the results in general are better than these in WCL. Indeed, we can attain an acceptable accuracy around 1 m when R is 1.

Again, a 95% of CI is used here. Figure 6.9 shows the average localization errors and the 95% confidence interval with the corresponding resolution of both WCL and WCWCL.Both of our proposed models, GWPP and WOPP, provide narrower CIs, which proves that the improved performance is statistically significant.

6.6.2 Precision

We considered five precision values as follows: less than 1 m, less than 3 m, less than 5 m, less than 7 m, and less than 9 m. Each localization precision is the mean of 50 different simulation runs, when d_{max} = 140 m, and R = 1. Figure 6.10 shows the precision evaluation using WCL and WCWCL.

In Figure 6.10a, none of the four models achieved less than 1 m of localization error. However, GWPP and WOPP show an advanced level of precision where all of their localization error values are located within a range of 3 m. Unlike the dynamic models, the static models of Snake-Like and Z-Curves are unsuccessful to emulate in terms of precision. No result of them is located within 5 m of range. Such results improve progressively with 7 m of localization error. However, all results are in the range of 7 to 9 m of range. In Figure 6.10b, the precision of GWPP and WOPP is still very high. On the other hand, Z-Curves and Snake-Like get some improvements in the ratio of around 90 percentage of them are located in less than 7 m. All Z-Curves and Snake-Like results are within 9 m of localization error.

6.6.3 Localization Ratio

In this work, we evaluate the localization ratio from two perspectives, the impact of maximum movement distance d_{max}, and the impact of resolution value R.

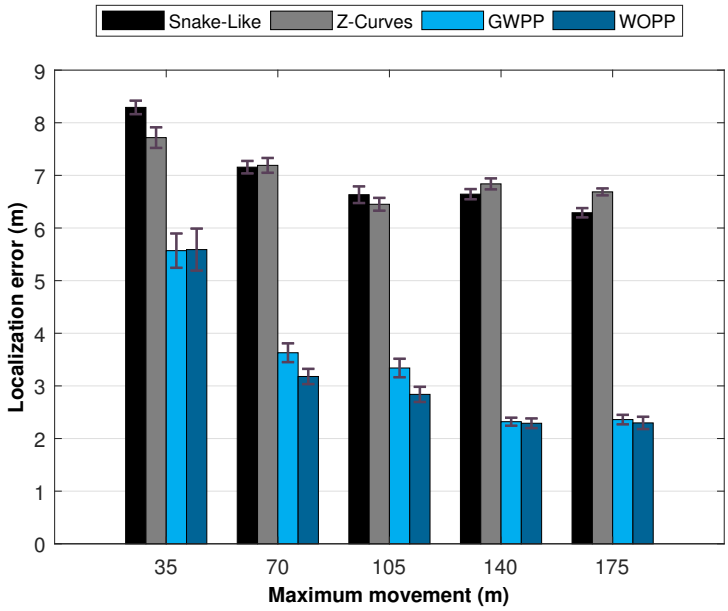

(a)

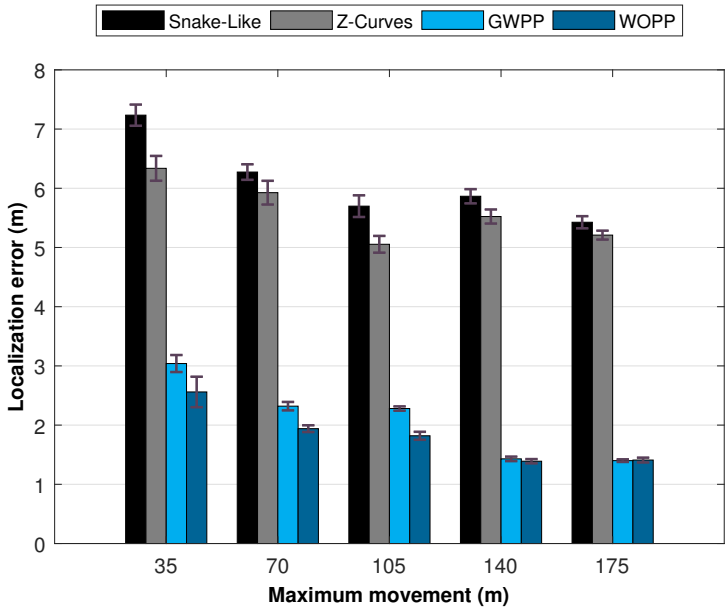

(b)

Figure 6.9: Average localization errors and the 95% confidence interval with the corresponding resolution in (a) WCL, and (b) WCWCL

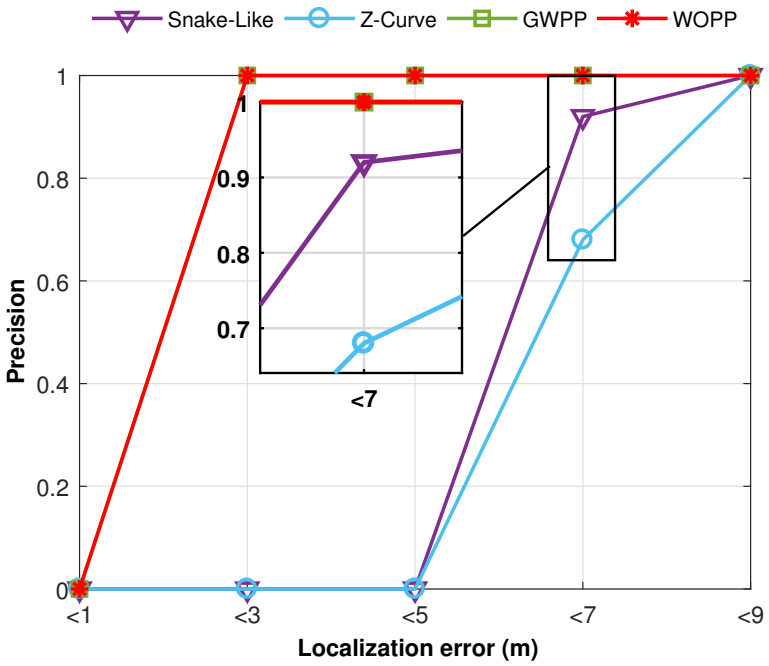

(a)

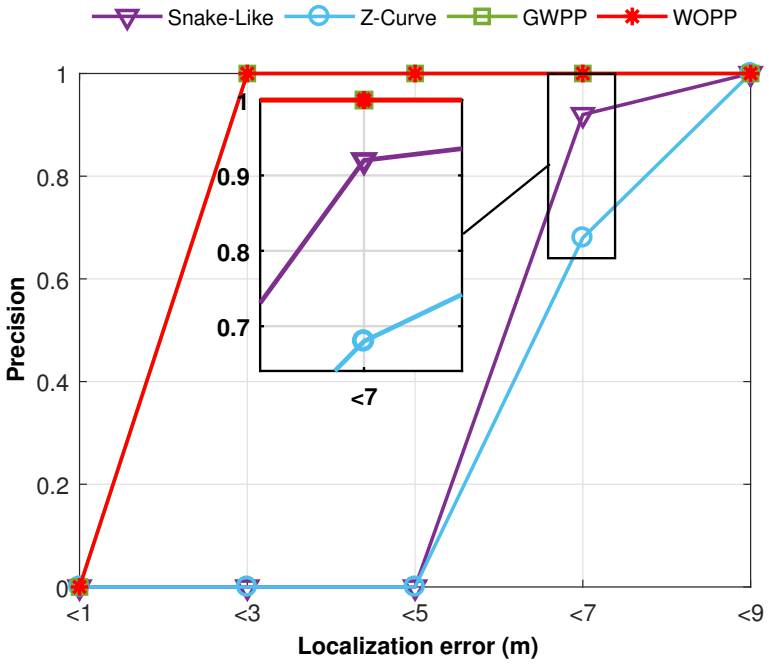

(b)

Figure 6.10: Precision of all mobility models versus the localization error in (**a**) WCL, and (**b**) WCWCL, ($d_{max} = 140, R = 1$)

A. The Impact of Maximum Movement Distance

A collection of 250 sensor nodes is used with various d_{max}, and R of 1. In this metric, only one of the localization algorithms is shown, since their localization ratios are similar. Figure 6.11 show the localization ratio for the four implemented movement models.

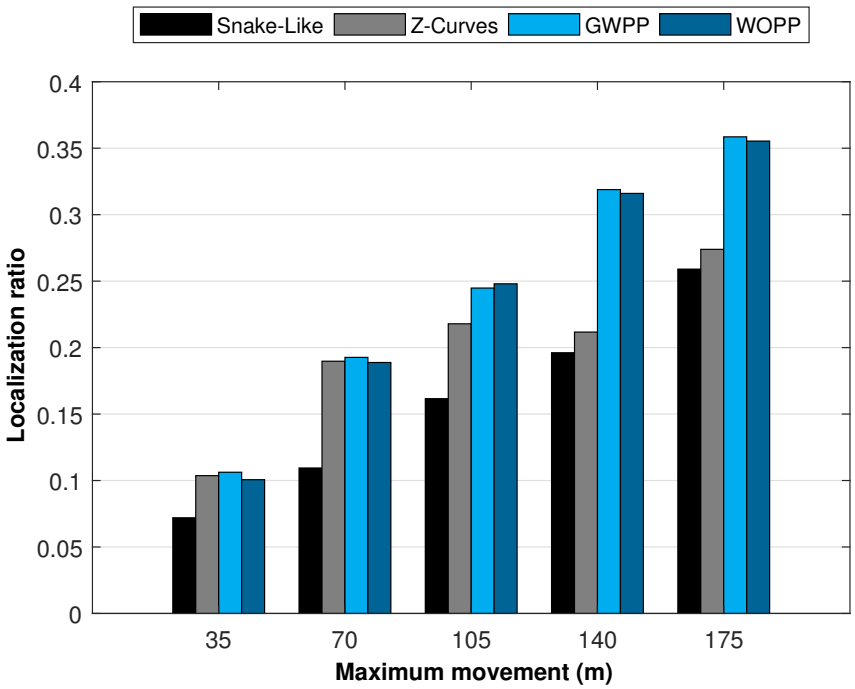

Figure 6.11: Localization ratio versus the maximum movement distance of all mobility models in both WCL and WCWCL

Unlike the static path planning models, dynamic models do not guarantee that all nodes inside the network will be able to receive the localization information. In addition, since there is a limited distance of MA movement, it is difficult to cover the entire area with such assumption. However, both of our dynamic models, GWPP and WOPP, offer higher localization ratio in most cases in comparison to other two models. All four models provide weak localization ratios when d_{max} is short as 35 m. This ratio get improves with the increase of d_{max}. When the d_{max} is 175 m, the proposed models can achieve about 35 percentage of localized nodes. Snake-Like and Z-Curves can acquire

less than 28 percentage in its best case.

B. The Impact of Resolution

In the other experiment, we assessed the localization ratio in terms of different resolution values. We used similar assumptions of those in the former experiment presented in Section 6.6.3**A.**, except with a fixed d_{max} of 140 m, and changeable R. The results are plotted in Figure 6.12.

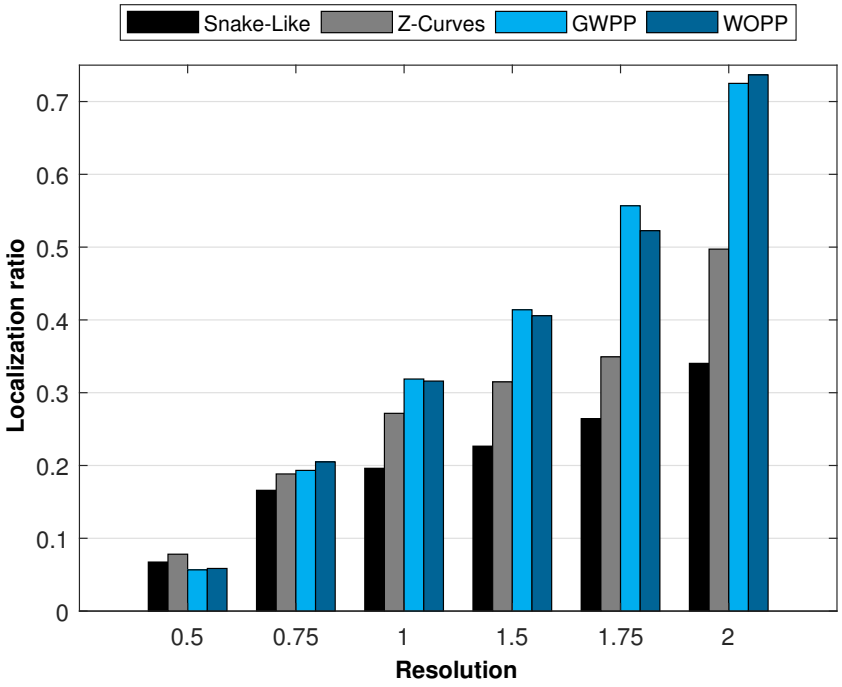

Figure 6.12: Localization ratio versus the resolution of all mobility models in both WCL and WCWCL

When a resolution value R of 0.5 is used, the localization ratio of all models is poor. More nodes are covered when R increases, thus, more UNs will be able to estimate their locations. When R is 1.5, more than 40 percentage of nodes are localized in GWPP and WOPP comparison to less than 35 percentage when R = 1. The ratio increases gradually when R = 1.75. Both GWPP and WOPP can achieve high results of more than 72 percentage of localized nodes when R = 2, while Z-Curves can cover about 50 percentage of its UNs when

the same assumption is applied. Snake-Like still performs poorly with all R values since it is affected by the collinearity problem.

6.6.4 Computation Time

We also extended our performance metrics evaluation to compare the computation time for the proposed models. Computation time here refers to the time spent from the first execution of the code to the end of it. The computation time is measured in seconds (s). A comparison of 50 runs with different maximum iteration times (T_{max}) for both models are conducted. The average of every 50 runs of T_{max} is taken. The following parameters were used for the performance, 250 UNs, d_{max} = 140, R = 1, and the rest are fixed as shown in Table 6.1. The executed computation time is shown in Figure 6.13.

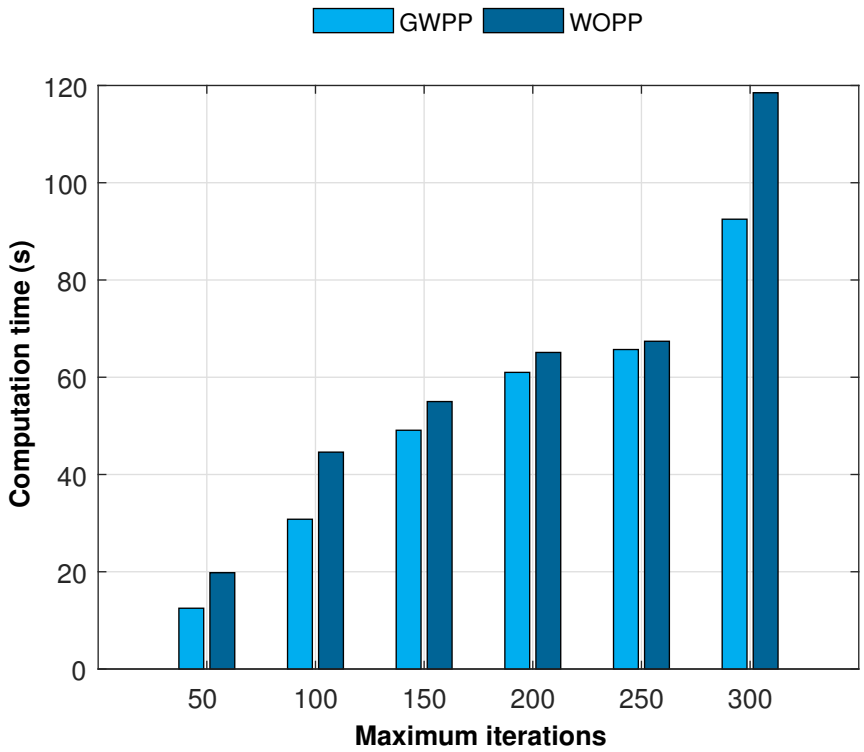

Figure 6.13: Average computation time for both techniques in seconds

The result of computation time shows that GWPP takes less time to run in comparison to WOPP regardless of the value of T_{max}. When T_{max} increases the computation time increases. GWPP spends only 12.5 seconds when a T_{max} of 50 is used, while WOPP takes 19.8 seconds for the same T_{max}. The time spent on execution of both models increases gradually. However, even in its longest period, GWPP and WOPP need 92.5 seconds and 118.5 seconds respectively when T_{max} is 300.

6.7 Discussion

As seen above, the dynamic proposed models and their optimized base help to improve their performance in many metrics. Both models provide better accuracy compared to the other two models. The flexibility of the MA moving based on the network parameters and node locations improves such metric. Unlike the other models, GWPP and WOPP can avoid obstacles, avoid collinearity, avoid visited points, and make their own path in real-time based on information from the network. In addition, all movements will depend on the fitness function. Moreover, GWPP and WOPP have high precision. Our proposed dynamic models GWPP and WOPP provide better localization ratio than the static models Snake-Like and Z-Curves, even in the presence of obstacles and with limited movement distance. Indeed, when high resolution values are considered, both models get competitive accuracy. In general, WOPP has a better performance than GWPP. However, GWPP has a shorter run computational time. Thus, choosing which model to apply can be based on these metrics. If time is an important constraint, GWPP may be preferable. Alternatively, WOPP may be the better candidate if high performance is required.

6.8 Conclusion and Future Works

In this work, we introduced two dynamic obstacle-avoidance path planning models, called GWPP and WOPP, for mobile anchor-assisted localization in WSNs. The

proposed models work on optimizing the path design based on the real-time information from the network. The optimization models help not only to avoid the obstacles located in the MA's way but also to design an outstanding path when the MA has a limited movement. To examine the efficiency of the proposed models, we compare them to other two models that consider obstacle-avoidance methods in their design. The final results demonstrate that our proposed models, GWPP and WOPP, maximize the localization efficiency in the aspects of accuracy, localization precision, and localization ratio (coverage) when they are tested from two aspects, the maximum movement distance and the resolution values. We also compared the proposed models in terms of computation time in order to study them from different aspects. We were able to summarize the outcomes of this paper based on the four metrics analyzed as follow:

1. **Localization accuracy :** indicated as localization error, the results show that our proposed models offer superior outcomes in both experiments as shown in Figures 6.6, 6.8.

2. **Localization precision :** The dynamic models of GWPP and WOPP present the best outcomes of precision in WCL and WCWCL as presented in Figure 6.10.

3. **Localization ratio**: Typically, static path planning models provide better performance than the other kinds of mobility in terms of coverage. However, when the MA has a limited and constrained movement distance, and there are some obstacles in the area, the static models performance is affected. GWPP and WOPP consider the network and node distribution, and take them into account when they design their path. The results show that they still provide competitive performance as shown in Figure 6.11. Higher localization ratio can be obtained when the resolution values increase as shown in Figure 6.12.

4. **Computation time :** To make the final decision of choosing either of GWPP

or WOPP, we also analyzed the computation time. The results show that GWPP has shorter computation time than WOPP as shown in Figure 6.13, which may be beneficial when a faster optimized model required.

To sum up, we have shown that employing an optimization model for forming a movement path leads to an improved outcomes over other works in a number of metrics.

Chapter 7

Conclusion and Future Work

A summary of the thesis contributions and directions for future works are reviewed in this chapter. Section 7.1 summarizes the four main contributions discussed in this thesis, while Section 7.2 suggests some potential future works that may be considered.

7.1 Summary of Contributions

The primary objective of this thesis was to propose and design path planning models for mobility-assisted localization in WSNs. Four different scenarios and assumptions are considered. Therefore, four main contributions in path planning in WSNs are produced as follows:

1. In the first contribution, a new static path planning model for mobile anchor-assisted localization in WSNs is introduced in Chapter 3. In the proposed model, all sensor nodes in the network will be able to receive the localization information from the MA, and thus be able to estimate their own locations. This comes with higher localization accuracy in comparison to some other similar models. Nonetheless, the static path is modified to avoid the collinearity problem, resulting in both lower localization error and a higher localization ratio compared to some random and static path planning models.

2. The second contribution, proposed in Chapter 4, derives its central concept from the former one. However, it is suggested to work in three-dimensional

scenarios. The three-dimensional path planning model for mobile anchor-assisted localization in WSNs offers higher accuracy compared to other three-dimensional path models.

3. In the third contribution, discussed in Chapter 5, a new direction for research in path planning in WSNs is introduced. Fuzzy-Logic-based Path Planning for mobile anchor-assisted Localization (FLPPL) is a novel range-free movement scheme for when the MA's movement is limited. The novelty of this model is to form the movement of the MA in real time based on multiple inputs using a fuzzy-logic model. Compared to other models and considering the limitations of the MA's movements, the FLPPL model provides excellent performance in terms of accuracy, precision and localization ratio.

4. In the fourth contribution, presented in Chapter 6, two types of swarm intelligence are suggested to use to direct the movement of the MA when a number of constraints exist. Based on GWO and WOA, the GWPP and WOPP path planning models offer better performance in comparison to Z-Curves and Snake-Like models in networks in which obstacles exist. In addition, a similar assumption to this in the former chapter of having limited MA movement is examined. The overall evaluation shows that both models of GWPP and WOPP perform well in avoiding obstacles in their path with a higher accuracy, higher precision and higher localization ratio than those obtained in Z-Curves and Snake-Like.

7.2 Future Research Directions

A set of possible extension of the proposed models for our future work is suggested as follows

1. In FLPPL work, we assumed that the area of interest is obstacle-free. Therefore, we did not consider the ability of the FLPPL model to work when obstacles exist nor how the MA can avoid them. As a future work, we aim to

study the effects of the obstacles that exist in the area on localization accuracy, localization ratio, precision and the path length and compare them to those achieved in GWPP and WOPP.

2. We also plan to extend our experiments on FLPPL, GWPP, and WOPP to three-dimensional scenarios and test their ability to work in such environments.

3. Another task is to assess the current models when multiple MAs are used. Using various MAs will decrease the localization time but will bring more complexity in utilizing the movement of the MAs, which might be a potential area of research.

4. Recently, a new research area suggested using Particle Swarm Optimization (PSO) to optimize the membership functions of the Fuzzy Logic Controller (FLC) in WSNs [120], which combines both of our optimization techniques (FL and SI). PSO has shown promising results in many research studies including [121,122]. Such a proposal can be useful to improve the performance of our model.

5. We may consider a multi-objective optimization model that forms the designed path based on the localization error and localization ratio as well.

6. Also, we may assume irregular obstacle shapes and let the MA control its movement based on this assumption.

Bibliography

[1] L. M. Borges, F. J. Velez, and A. S. Lebres, "Survey on the characterization and classification of wireless sensor network applications," *IEEE Communications Surveys Tutorials*, vol. 16, no. 4, pp. 1860–1890, Fourthquarter 2014.

[2] Z. Fei, B. Li, S. Yang, C. Xing, H. Chen, and L. Hanzo, "A survey of multi-objective optimization in wireless sensor networks: Metrics, algorithms, and open problems," *IEEE Communications Surveys Tutorials*, vol. 19, no. 1, pp. 550–586, Firstquarter 2017.

[3] H. Karl and A. Willig, *Protocols and architectures for wireless sensor networks*. Hoboken, NJ: Wiley, May 2005.

[4] S. Halder and A. Ghosal, "A survey on mobile anchor assisted localization techniques in wireless sensor networks," *Wireless Networks*, vol. 22, no. 7, pp. 2317–2336, 2016. [Online]. Available: http://dx.doi.org/10.1007/s11276-015-1101-2

[5] S. Alikhani, M. St-Hilaire, and T. Kunz, "icca-map: A new mobile node localization algorithm," in *2009 IEEE International Conference on Wireless and Mobile Computing, Networking and Communications*, Oct 2009, pp. 382–387.

[6] K. Mondal and P. S. Mandal, *Range-Free Mobile Node Localization Using Static Anchor*. Berlin, Heidelberg: Springer Berlin Heidelberg, 2013, pp. 269–284. [Online]. Available: http://dx.doi.org/10.1007/978-3-642-39701-1_23

[7] D. Pescaru and D.-I. Curiac, "Anchor node localization for wireless sensor networks using video and compass information fusion," *Sensors*, vol. 14, no. 3, pp. 4211–4224, 2014. [Online]. Available: http://www.mdpi.com/1424-8220/14/3/4211

[8] C. Miao, G. Dai, K. Ying, and Q. Chen, "Collaborative localization and location verification in wsns," *Sensors*, vol. 15, no. 5, pp. 10 631–10 649, 2015. [Online]. Available: http://www.mdpi.com/1424-8220/15/5/10631

[9] A. Alomari, F. Comeau, W. Phillips, and N. Aslam, "New path planning model for mobile anchor-assisted localization in wireless sensor networks," *Wireless Networks*, pp. 1–19, 2017. [Online]. Available: http://dx.doi.org/10.1007/s11276-017-1493-2

[10] A. Alomari, N. Aslam, W. Phillips, and F. Comeau, "Three-dimensional path planning model for mobile anchor-assisted localization in wireless sensor networks," in *2017 IEEE 30th Canadian Conference on Electrical and Computer Engineering (CCECE)*, April 2017, pp. 1–5.

[11] G. Han, H. Xu, J. Jiang, L. Shu, T. Hara, and S. Nishio, "Path planning using a mobile anchor node based on trilateration in wireless sensor networks," *Wireless Communications and Mobile Computing*, vol. 13, no. 14, pp. 1324–1336, 2013. [Online]. Available: http://dx.doi.org/10.1002/wcm.1192

[12] S. Y. Fu, L. W. Han, Y. Tian, and G. S. Yang, "Path planning for unmanned aerial vehicle based on genetic algorithm," in *2012 IEEE 11th International Conference on Cognitive Informatics and Cognitive Computing*, Aug 2012, pp. 140–144.

[13] K. Yao, J. Li, B. Sun, and J. Zhang, "An adaptive grid model based on mobility constraints for uav path planning," in *2016 2nd International Conference on Control Science and Systems Engineering (ICCSSE)*, July 2016, pp. 207–211.

[14] S. Ahmed, A. Mohamed, K. Harras, M. Kholief, and S. Mesbah, "Energy efficient path planning techniques for uav-based systems with space discretization," in *2016 IEEE Wireless Communications and Networking Conference*, April 2016, pp. 1–6.

[15] K. Hernandez, B. Bacca, and B. Posso, "Multi-goal path planning autonomous system for picking up and delivery tasks in mobile robotics," *IEEE Latin America Transactions*, vol. 15, no. 2, pp. 232–238, Feb 2017.

[16] P. Joshy and P. Supriya, "Implementation of robotic path planning using ant colony optimization algorithm," in *2016 International Conference on Inventive Computation Technologies (ICICT)*, vol. 1, Aug 2016, pp. 1–6.

[17] A. Alomari, N. Aslam, and F. Comeau, "Data collection using rendezvous points and mobile actor in wireless sensor networks," in *2012 IEEE International Conference on Communications (ICC)*, June 2012, pp. 7115–7119.

[18] A. Alomari, N. Aslam, W. Phillips, and F. Comeau, "A scheme for using closest rendezvous points and mobile elements for data gathering in wireless sensor networks," in *2014 IFIP Wireless Days (WD)*, Nov 2014, pp. 1–6.

[19] S. Mirjalili, S. M. Mirjalili, and A. Lewis, "Grey wolf optimizer," *Advances in Engineering Software*, vol. 69, pp. 46 – 61, 2014. [Online]. Available: http://www.sciencedirect.com/science/article/pii/S0965997813001853

[20] S. Mirjalili and A. Lewis, "The whale optimization algorithm," *Advances in Engineering Software*, vol. 95, pp. 51 – 67, 2016. [Online]. Available: http://www.sciencedirect.com/science/article/pii/S0965997816300163

[21] A. Alomari, W. Phillips, N. Aslam, and F. Comeau, "Dynamic fuzzy-logic based path planning for mobility-assisted localization in wireless sensor networks," *Sensors*, vol. 17, no. 8, 2017.

[22] ——, "Swarm intelligence optimization techniques for obstacle-avoidance mobility-assisted localization in wireless sensor networks," *IEEE Access*, pp. 1–19, 2017.

[23] R. R. Selmic, V. V. Phoha, and A. Serwadda, *Wireless Sensor Networks: Security, Coverage, and Localization*. Springer International Publishing, 2016.

[24] A. Alomari, "Energy efficient data collection scheme using rendezvous points and mobile actor in wireless sensor networks," Master's thesis, Dalhousie University, Canada, 2012.

[25] D. M. Kazem Sohraby and T. Znati, *Wireless Sensor Networks: Technology, Protocols, and Applications*. Hoboken, NJ: Wiley, mar 2007.

[26] N. Patwari, J. Ash, S. Kyperountas, A. Hero, R. Moses, and N. Correal, "Locating the nodes: cooperative localization in wireless sensor networks," *Signal Processing Magazine, IEEE*, vol. 22, no. 4, pp. 54–69, July 2005.

[27] G. Han, J. Jiang, C. Zhang, T. Q. Duong, M. Guizani, and G. K. Karagiannidis, "A survey on mobile anchor node assisted localization in wireless sensor networks," *IEEE Communications Surveys Tutorials*, vol. 18, no. 3, pp. 2220–2243, thirdquarter 2016.

[28] L. T. Nguyen, S. Kim, and B. Shim, "Localization in the internet of things network: A low-rank matrix completion approach," *arXiv preprint arXiv:1702.04054*, 2017.

[29] A. Ez-Zaidi and S. Rakrak, "A comparative study of target tracking approaches in wireless sensor networks," *Journal of Sensors*, vol. 2016, 2016.

[30] U. S. government. (2017) Gps: the global positioning system. [Online]. Available: https://www.gps.gov

[31] I. Amundson and X. D. Koutsoukos, *A Survey on Localization for Mobile Wireless Sensor Networks*. Berlin, Heidelberg: Springer Berlin Heidelberg, 2009, pp. 235–254. [Online]. Available: https://doi.org/10.1007/978-3-642-04385-7_16

[32] M. Khelifi, I. Benyahia, S. Moussaoui, and F. Nait-Abdesselam, "An overview of localization algorithms in mobile wireless sensor networks," in *Protocol Engineering (ICPE) and International Conference on New Technologies of Distributed Systems (NTDS), 2015 International Conference on*, July 2015, pp. 1–6.

[33] G. Han, J. Jiang, L. Shu, Y. Xu, and F. Wang, "Localization algorithms of underwater wireless sensor networks: A survey," *Sensors*, vol. 12, no. 2, p. 2026, 2012. [Online]. Available: http://www.mdpi.com/1424-8220/12/2/2026

[34] O. Cagirici, "Exploiting coplanar clusters to enhance 3d localization in wireless sensor networks," *CoRR*, vol. abs/1502.07790, 2015. [Online]. Available: http://arxiv.org/abs/1502.07790

[35] ——, "Exploiting coplanar clusters to enhance 3d localization in wireless sensor networks," *CoRR*, vol. abs/1502.07790, 2015. [Online]. Available: http://arxiv.org/abs/1502.07790

[36] D. Koutsonikolas, S. M. Das, and Y. C. Hu, "Path planning of mobile landmarks for localization in wireless sensor networks," *Comput. Commun.*, vol. 30, no. 13, pp. 2577–2592, Sep. 2007. [Online]. Available: http://dx.doi.org/10.1016/j.comcom.2007.05.048

[37] G. Han, C. Zhang, J. Lloret, L. Shu, and J. Rodrigues, "A mobile anchor assisted localization algorithm based on regular hexagon in wireless sensor networks," *The Scientific World Journal*, pp. 1–13, 2014.

[38] J. Rezazadeh, M. Moradi, A. Ismail, and E. Dutkiewicz, "Superior path planning mechanism for mobile beacon-assisted localization in wireless sensor networks," *Sensors Journal, IEEE*, vol. 14, no. 9, pp. 3052–3064, Sept 2014.

[39] "Confidence interval," https://www.investopedia.com/terms/c/confidenceinterval.asp, accessed: 2018-02-19.

[40] "Confidence interval: Definition, formula example," https://study.com/academy/lesson/confidence-interval-definition-formula-example.html, accessed: 2018-02-19.

[41] J. Rezazadeh, M. Moradi, A. S. Ismail, and E. Dutkiewicz, "Impact of static trajectories on localization in wireless sensor networks," *Wireless Networks*, vol. 21, no. 3, pp. 809–827, Apr 2015. [Online]. Available: https://doi.org/10.1007/s11276-014-0821-z

[42] R. M. Sandoval, A. J. Garcia-Sanchez, and J. Garcia-Haro, "Improving rssi-based path-loss models accuracy for critical infrastructures: a smart grid substation case-study," *IEEE Transactions on Industrial Informatics*, vol. PP, no. 99, pp. 1–1, 2017.

[43] H. P. Mistry and N. H. Mistry, "Rssi based localization scheme in wireless sensor networks: A survey," in *2015 Fifth International Conference on Advanced Computing Communication Technologies*, Feb 2015, pp. 647–652.

[44] J. Xu, W. Liu, F. Lang, Y. Zhang, and C. Wang, "Distance measurement model based on rssi in wsn," *Wireless Sensor Network*, vol. 2, no. 08, p. 606, 2010.

[45] Q. Dong and X. Xu, "A novel weighted centroid localization algorithm based on rssi for an outdoor environment, journal of communications," in *Journal of Communications*, Sep 2014, pp. 279–285.

[46] M. R. Gholami, "Positioning algorithms for wireless sensor networks," PhD dissertation, chalmersuniversityof technology, 2011.

[47] *Handbook of sensor networks : algorithms and architectures*. Hoboken, N.J.: Wiley, 2005.

[48] N. A. Alrajeh, M. Bashir, and B. Shams, "Localization techniques in wireless sensor networks," *International Journal of Distributed Sensor Networks*, vol. 9, no. 6, p. 304628, 2013. [Online]. Available: https://doi.org/10.1155/2013/304628

[49] J. Blumenthal, R. Grossmann, F. Golatowski, and D. Timmermann, "Weighted centroid localization in zigbee-based sensor networks," in *Intelligent Signal Processing, 2007. WISP 2007. IEEE International Symposium on*, Oct 2007, pp. 1–6.

[50] T. He, C. Huang, B. M. Blum, J. A. Stankovic, and T. Abdelzaher, "Range-free localization schemes for large scale sensor networks," in *Proceedings of the 9th Annual International Conference on Mobile Computing and Networking*, ser. MobiCom '03. New York, NY, USA: ACM, 2003, pp. 81–95. [Online]. Available: http://doi.acm.org/10.1145/938985.938995

[51] L. Lazos and R. Poovendran, "Hirloc: high-resolution robust localization for wireless sensor networks," *IEEE Journal on Selected Areas in Communications*, vol. 24, no. 2, pp. 233–246, Feb 2006.

[52] G. Han, H. Xu, T. Q. Duong, J. Jiang, and T. Hara, "Localization algorithms of wireless sensor networks: a survey," *Telecommunication Systems*, vol. 52, no. 4, pp. 2419–2436, Apr 2013. [Online]. Available: https://doi.org/10.1007/s11235-011-9564-7

[53] D. Niculescu and B. Nath, "Ad hoc positioning system (aps) using aoa," in *INFOCOM 2003. Twenty-Second Annual Joint Conference of the IEEE Computer and Communications. IEEE Societies*, vol. 3, March 2003, pp. 1734–1743 vol.3.

[54] K. Liu, S. Wang, F. Zhang, F. Hu, and C. Xu, "Efficient localized localization algorithm for wireless sensor networks," in *The Fifth International Conference on Computer and Information Technology (CIT'05)*, Sept 2005, pp. 517–523.

[55] A. Alomari, N. Aslam, W. Phillips, and F. Comeau, "Using the dv-hop technique to increase the localization ratio in static path planning models in wireless sensor networks," in *2016 10th International Symposium on Communication Systems, Networks and Digital Signal Processing (CSNDSP)*, July 2016, pp. 1–6.

[56] H. Chen, K. Sezaki, P. Deng, and H. C. So, "An improved dv-hop localization algorithm for wireless sensor networks," in *2008 3rd IEEE Conference on Industrial Electronics and Applications*, June 2008, pp. 1557–1561.

[57] Z. Zhong, "Range -free localization and tracking in wireless sensor networks," Ph.D. dissertation, 2010, copyright - Database copyright ProQuest LLC; ProQuest does not claim copyright in the individual underlying works; Last updated - 2016-03-10. [Online]. Available: http://ezproxy.library.dal.ca/login?url=https://search.proquest.com/docview/762746322?accountid=10406

[58] K. Römer, "The lighthouse location system for smart dust," in *Proceedings of the 1st International Conference on Mobile Systems, Applications and Services*, ser. MobiSys '03. New York, NY, USA: ACM, 2003, pp. 15–30. [Online]. Available: http://doi.acm.org/10.1145/1066116.1189036

[59] R. Stoleru, T. He, J. A. Stankovic, and D. Luebke, "A high-accuracy, low-cost localization system for wireless sensor networks," in *Proceedings of the 3rd International Conference on Embedded Networked Sensor Systems*, ser. SenSys '05. New York, NY, USA: ACM, 2005, pp. 13–26. [Online]. Available: http://doi.acm.org/10.1145/1098918.1098921

[60] A. Nasipuri and R. el Najjar, "Experimental evaluation of an angle based indoor localization system," in *2006 4th International Symposium on Modeling and Optimization in Mobile, Ad Hoc and Wireless Networks*, April 2006, pp. 1–9.

[61] R. C. Luo, O. Chen, and S. H. Pan, "Mobile user localization in wireless sensor network using grey prediction method," in *31st Annual Conference of IEEE Industrial Electronics Society, 2005. IECON 2005.*, Nov 2005, pp. 6 pp.–.

[62] J. P. Sheu, W. K. Hu, and J. C. Lin, "Distributed localization scheme for mobile sensor networks," *IEEE Transactions on Mobile Computing*, vol. 9, no. 4, pp. 516–526, April 2010.

[63] B. Neuwinger, U. Witkowski, and U. Rückert, *Ad-Hoc Communication and Localization System for Mobile Robots*. Berlin, Heidelberg: Springer Berlin Heidelberg, 2009, pp. 220–229. [Online]. Available: https://doi.org/10.1007/978-3-642-03983-6_26

[64] W. Wang and Q. Zhu, "Sequential monte carlo localization in mobile sensor networks," *Wirel. Netw.*, vol. 15, no. 4, pp. 481–495, May 2009. [Online]. Available: http://dx.doi.org/10.1007/s11276-007-0064-3

[65] G. Han, J. Chao, C. Zhang, L. Shu, and Q. Li, "The impacts of mobility models on dv-hop based localization in mobile wireless sensor networks," *Journal of Network and Computer Applications*, vol. 42, pp. 70 – 79, 2014.

[66] E. M. Royer, P. M. Melliar-Smith, and L. E. Moser, "An analysis of the optimum node density for ad hoc mobile networks," in *Communications, 2001. ICC 2001. IEEE International Conference on*, vol. 3, 2001, pp. 857–861 vol.3.

[67] Z. ZHONG, D.-Y. LUO, S.-Q. LIU, X.-P. FAN, and Z.-H. QU, "An adaptive localization approach for wireless sensor networks based on gauss-markov mobility model," *Acta Automatica Sinica*, vol. 36, no. 11, pp. 1557 – 1568, 2010. [Online]. Available: http://www.sciencedirect.com/science/article/pii/S1874102909600628

[68] R. Huang and G. V. Zaruba, "Static path planning for mobile beacons to localize sensor networks," in *Pervasive Computing and Communications Workshops, 2007. PerCom Workshops '07. Fifth Annual IEEE International Conference on*, March 2007, pp. 323–330.

[69] S. Li, D. Lowe, X. Kong, and R. Braun, "Wireless sensor network localization algorithm using dynamic path of mobile beacon," in *The 17th Asia Pacific Conference on Communications*, Oct 2011, pp. 344–349.

[70] H. Li, J. Wang, X. Li, and H. Ma, "Real-time path planning of mobile anchor node in localization for wireless sensor networks," in *2008 International Conference on Information and Automation*, June 2008, pp. 384–389.

[71] X. Li, N. Mitton, I. Simplot-Ryl, and D. Simplot-Ryl, "Mobile-beacon assisted sensor localization with dynamic beacon mobility scheduling," in *Mobile Ad-hoc and Sensor Systems (MASS), 2011 IEEE 8th International Conference on*, Oct 2011, pp. 490–499.

[72] S. M. Mazinani and F. Farnia, "Localization in wireless sensor network using a mobile anchor in obstacle environment," *International Journal of Computer and Communication Engineering*, vol. 2, no. 4, p. 438, 2013.

[73] Y. Chen, S. Lu, J. Chen, and T. Ren, "Node localization algorithm of wireless sensor networks with mobile beacon node," *Peer-to-Peer Networking and Applications*, vol. 10, no. 3, pp. 795–807, 2017. [Online]. Available: http://dx.doi.org/10.1007/s12083-016-0522-8

[74] H. Cui and Y. Wang, "Four-mobile-beacon assisted localization in three-dimensional wireless sensor networks," *Computers Electrical Engineering*, vol. 38, no. 3, pp. 652 – 661, 2012, the Design and Analysis of Wireless Systems and Emerging Computing Architectures and Systems. [Online]. Available: http://www.sciencedirect.com/science/article/pii/S0045790611001625

[75] H. Cui, Y. Wang, and J. Lv, "Path planning of mobile anchor in three-dimensional wireless sensor networks for localization," vol. 9, pp. 2203–2210, 08 2012.

[76] L. Liu, H. Zhang, X. Geng, and X. Shu, "Hexahedral localization (hl): A three-dimensional hexahedron localization based on mobile beacons," *The Scientific World Journal*, vol. 2013, 2013.

[77] Chipcon, *CC1100, Low-Power Sub- 1 GHz RF Transceiver*, Texas Insturments, 2014.

[78] J. Rezazadeh, M. Moradi, A. S. Ismail, and E. Dutkiewicz, "Impact of static trajectories on localization in wireless sensor networks," *Wirel. Netw.*, vol. 21, no. 3, pp. 809–827, Apr. 2015. [Online]. Available: http://dx.doi.org/10.1007/s11276-014-0821-z

[79] H. Chen, Q. Shi, R. Tan, H. V. Poor, and K. Sezaki, "Mobile element assisted cooperative localization for wireless sensor networks with obstacles," *IEEE Transactions on Wireless Communications*, vol. 9, no. 3, pp. 956–963, March 2010.

[80] G. Tan, H. Jiang, S. Zhang, Z. Yin, and A.-M. Kermarrec, "Connectivity-based and anchor-free localization in large-scale 2d/3d sensor networks," *ACM Trans. Sen. Netw.*, vol. 10, no. 1, pp. 6:1–6:21, Dec. 2013. [Online]. Available: http://doi.acm.org/10.1145/2529976

[81] *Fuzzy Logic Toolbox^{TM} User's Guide*, ser. 2.2.25. Natick, MA: MathWorks, 2017, vol. 2017a.

[82] B. Shah, F. Iqbal, A. Abbas, and K.-I. Kim, "Fuzzy logic-based guaranteed lifetime protocol for real-time wireless sensor networks," *Sensors*, vol. 15, no. 8, pp. 20 373–20 391, 2015. [Online]. Available: http://www.mdpi.com/1424-8220/15/8/20373

[83] Q. Wang, E. Kulla, G. Mino, and L. Barolli, "Prediction of sensor lifetime in wireless sensor networks using fuzzy logic," in *2014 IEEE 28th International Conference on Advanced Information Networking and Applications*, May 2014, pp. 1127–1131.

[84] Y. K. Tamandani and M. U. Bokhari, "Sepfl routing protocol based on fuzzy logic control to extend the lifetime and throughput of the wireless sensor network," *Wireless Networks*, vol. 22, no. 2, pp. 647–653, 2016. [Online]. Available: http://dx.doi.org/10.1007/s11276-015-0997-x

[85] R. Mhemed, N. Aslam, W. Phillips, and F. Comeau, "An energy efficient fuzzy logic cluster formation protocol in wireless sensor networks," *Procedia Computer Science*, vol. 10, pp. 255 – 262, 2012. [Online]. Available: http://www.sciencedirect.com/science/article/pii/S1877050912003924

[86] R. Logambigai and A. Kannan, "Fuzzy logic based unequal clustering for wireless sensor networks," *Wireless Networks*, vol. 22, no. 3, pp. 945–957, 2016. [Online]. Available: http://dx.doi.org/10.1007/s11276-015-1013-1

[87] P. Nayak and A. Devulapalli, "A fuzzy logic-based clustering algorithm for wsn to extend the network lifetime," *IEEE Sensors Journal*, vol. 16, no. 1, pp. 137–144, Jan 2016.

[88] M. Mirzaie and S. M. Mazinani, "Mcfl: an energy efficient multi-clustering algorithm using fuzzy logic in wireless sensor network," *Wireless Networks*, pp. 1–16, 2017. [Online]. Available: http://dx.doi.org/10.1007/s11276-017-1466-5

[89] Y. Zhang, J. Wang, D. Han, H. Wu, and R. Zhou, "Fuzzy-logic based distributed energy-efficient clustering algorithm for wireless sensor networks," *Sensors*, vol. 17, no. 7, 2017.

[90] M. Collotta, L. L. Bello, and G. Pau, "A novel approach for dynamic traffic lights management based on wireless sensor networks and multiple fuzzy logic controllers," *Expert Systems with Applications*, vol. 42, no. 13, pp. 5403 – 5415, 2015. [Online]. Available: http://www.sciencedirect.com/science/article/pii/S0957417415001104

[91] A. Messaoudi, R. Elkamel, A. Helali, and R. Bouallegue, "Distributed fuzzy logic based routing protocol for wireless sensor networks," in *2016 24th International Conference on Software, Telecommunications and Computer Networks (SoftCOM)*, Sept 2016, pp. 1–7.

[92] E. Ahvar, A. M. Ortiz, and N. Crespi, "Improving decision-making for fuzzy logic-based routing in wireless sensor networks," in *2013 IEEE 10th International Conference on Ubiquitous Intelligence and Computing and 2013 IEEE 10th International Conference on Autonomic and Trusted Computing*, Dec 2013, pp. 583–588.

[93] A. M. Ortiz, F. Royo, T. Olivares, J. C. Castillo, L. Orozco-Barbosa, and P. J. Marron, "Fuzzy-logic based routing for dense wireless sensor networks," *Telecommunication Systems*, vol. 52, no. 4, pp. 2687–2697, 2013. [Online]. Available: http://dx.doi.org/10.1007/s11235-011-9597-y

[94] H. Jiang, Y. Sun, R. Sun, and H. Xu, "Fuzzy-logic-based energy optimized routing for wireless sensor networks," *International Journal of Distributed Sensor Networks*, vol. 9, no. 8, p. 216561, 2013. [Online]. Available: http://dx.doi.org/10.1155/2013/216561

[95] K. Mondal, A. Karmakar, and P. S. Mandal, "Path planning algorithms for mobile anchors towards range-free localization," *Journal of Parallel and Distributed Computing*, vol. 97, pp. 35 – 46, 2016. [Online]. Available: http://www.sciencedirect.com/science/article/pii/S0743731516300661

[96] "Understanding rssi," http://www.metageek.com/training/resources/understanding-rssi.html, accessed: 2017-05-30.

[97] P. Parwekar and R. Reddy, "An efficient fuzzy localization approach in wireless sensor networks," in *2013 IEEE International Conference on Fuzzy Systems (FUZZ-IEEE)*, July 2013, pp. 1–6.

[98] A. Barua, L. Mudunuri, , and O. Kosheleva, "Why trapezoidal and triangular membership functions work so well: Towards a theoretical explanation," *Journal of Uncertain Systems*, vol. 8, pp. 164–168, 2014.

[99] L. Bianchi, M. Dorigo, L. M. Gambardella, and W. J. Gutjahr, "A survey on metaheuristics for stochastic combinatorial optimization," *Natural Computing*, vol. 8, no. 2, pp. 239–287, Jun 2009. [Online]. Available: https://doi.org/10.1007/s11047-008-9098-4

[100] J. H. Holland, "Genetic algorithms," *Scientific American*, vol. 267, no. 1, pp. 66–73, 1992. [Online]. Available: http://www.jstor.org/stable/24939139

[101] S. Kirkpatrick, C. Gelatt Jr., and M. Vecchi, "Optimization by simulated annealing," *Science*, vol. 220, no. 4598, pp. 671–680, 1983, cited By 21902. [Online]. Available: https://www.scopus.com/inward/record.uri?eid=2-s2.0-26444479778&partnerID=40&md5=d90f6f0271cad18bc63145c671398950

[102] J. Kennedy and R. Eberhart, "Particle swarm optimization," in *Neural Networks, 1995. Proceedings., IEEE International Conference on*, vol. 4, Nov 1995, pp. 1942–1948 vol.4.

[103] M. Dorigo and T. Stützle, *Ant Colony Optimization*. Scituate, MA, USA: Bradford Company, 2004.

[104] D. Karaboga and B. Basturk, "A powerful and efficient algorithm for numerical function optimization: artificial bee colony (abc) algorithm," *Journal of Global Optimization*, vol. 39, no. 3, pp. 459–471, Nov 2007. [Online]. Available: https://doi.org/10.1007/s10898-007-9149-x

[105] G. Abbas, J. Gu, U. Farooq, M. U. Asad, and M. El-Hawary, "Solution of an economic dispatch problem through particle swarm optimization: A detailed survey - part i," *IEEE Access*, vol. 5, pp. 15 105–15 141, 2017.

[106] M. Saleem, G. A. D. Caro, and M. Farooq, "Swarm intelligence based routing protocol for wireless sensor networks: Survey and future directions," *Information Sciences*, vol. 181, no. 20, pp. 4597 – 4624, 2011, special Issue on Interpretable Fuzzy Systems. [Online]. Available: http://www.sciencedirect.com/science/article/pii/S0020025510003233

[107] A. M. Zungeru, L.-M. Ang, and K. P. Seng, "Classical and swarm intelligence based routing protocols for wireless sensor networks: A survey and comparison," *Journal of Network and Computer Applications*, vol. 35, no. 5, pp. 1508 – 1536, 2012, service Delivery Management in Broadband Networks. [Online]. Available: http://www.sciencedirect.com/science/article/pii/S1084804512000719

[108] R. Kumar and D. Kumar, "Hybrid swarm intelligence energy efficient clustered routing algorithm for wireless sensor networks," *Journal of Sensors*, vol. 2016, pp. 1 – 19, 2016. [Online]. Available: http://dx.doi.org/10.1155/2016/5836913

[109] P. C. S. Rao, P. K. Jana, and H. Banka, "A particle swarm optimization based energy efficient cluster head selection algorithm for wireless sensor networks," *Wireless Networks*, Apr 2016. [Online]. Available: https://doi.org/10.1007/s11276-016-1270-7

[110] Y. Zhou, N. Wang, and W. Xiang, "Clustering hierarchy protocol in wireless sensor networks using an improved pso algorithm," *IEEE Access*, vol. 5, pp. 2241–2253, 2017.

[111] D. S. Deif and Y. Gadallah, "An ant colony optimization approach for the deployment of reliable wireless sensor networks," *IEEE Access*, vol. 5, pp. 10 744–10 756, 2017.

[112] D. Lavanya and S. K. Udgata, *Swarm Intelligence Based Localization in Wireless Sensor Networks*. Berlin, Heidelberg: Springer Berlin Heidelberg, 2011, pp. 317–328. [Online]. Available: https://doi.org/10.1007/978-3-642-25725-4_28

[113] Z. Sun, L. Tao, X. Wang, and Z. Zhou, "Localization algorithm in wireless sensor networks based on multiobjective particle swarm optimization," *International Journal of Distributed Sensor Networks*, vol. 11, no. 8, p. 716291, 2015. [Online]. Available: https://doi.org/10.1155/2015/716291

[114] Y. Zhang, J. Liang, S. Jiang, and W. Chen, "A localization method for underwater wireless sensor networks based on mobility prediction and particle swarm optimization algorithms," *Sensors*, vol. 16, no. 2, 2016.

[115] M. M. Fouad, A. I. Hafez, A. E. Hassanien, and V. Snasel, "Grey wolves optimizer-based localization approach in wsns," in *2015 11th International Computer Engineering Conference (ICENCO)*, Dec 2015, pp. 256–260.

[116] N. A. Al-Aboody and H. S. Al-Raweshidy, "Grey wolf optimization-based energy-efficient routing protocol for heterogeneous wireless sensor networks," in *2016 4th International Symposium on Computational and Business Intelligence (ISCBI)*, Sept 2016, pp. 101–107.

[117] M. Sharawi and E. Emary, "Impact of grey wolf optimization on wsn cluster formation and lifetime expansion," in *2017 Ninth International Conference on Advanced Computational Intelligence (ICACI)*, Feb 2017, pp. 157–162.

[118] M. M. Ahmed, E. H. Houssein, A. E. Hassanien, A. Taha, and E. Hassanien, *Maximizing Lifetime of Wireless Sensor Networks Based on Whale Optimization*

Algorithm. Cham: Springer International Publishing, 2018, pp. 724–733. [Online]. Available: https://doi.org/10.1007/978-3-319-64861-3_68

[119] R. Ismail, Z. Omar, and S. Suaibun, "Obstacle-avoiding robot with ir and pir motion sensors," *IOP Conference Series: Materials Science and Engineering*, vol. 152, no. 1, p. 012064, 2016. [Online]. Available: http://stacks.iop.org/1757-899X/152/i=1/a=012064

[120] M. Collotta, G. Pau, and V. Maniscalco, "A fuzzy logic approach by using particle swarm optimization for effective energy management in iwsns," *IEEE Transactions on Industrial Electronics*, vol. PP, no. 99, pp. 1–10, 2017.

[121] Z. Yu, L. Xiao, H. Li, X. Zhu, and R. Huai, "Model parameter identification for lithium batteries using the coevolutionary particle swarm optimization method," *IEEE Transactions on Industrial Electronics*, vol. 64, no. 7, pp. 5690–5700, July 2017.

[122] W. T. Elsayed, Y. G. Hegazy, M. S. El-bages, and F. M. Bendary, "Improved random drift particle swarm optimization with self-adaptive mechanism for solving the power economic dispatch problem," *IEEE Transactions on Industrial Informatics*, vol. 13, no. 3, pp. 1017–1026, June 2017.

Appendix A

Copyright Permission Letters

Title: A scheme for using closest rendezvous points and Mobile Elements for data gathering in wireless sensor networks

Conference Proceedings: Wireless Days (WD), 2014 IFIP

Author: Abdullah Alomari

Publisher: IEEE

Date: Nov. 2014

LOGIN

If you're a copyright.com user, you can login to RightsLink using your copyright.com credentials. Already **a RightsLink user** or want to learn more?

Thesis / Dissertation Reuse

The IEEE does not require individuals working on a thesis to obtain a formal reuse license, however, you may print out this statement to be used as a permission grant:

Requirements to be followed when using any portion (e.g., figure, graph, table, or textual material) of an IEEE copyrighted paper in a thesis:

1) In the case of textual material (e.g., using short quotes or referring to the work within these papers) users must give full credit to the original source (author, paper, publication) followed by the IEEE copyright line © 2011 IEEE.
2) In the case of illustrations or tabular material, we require that the copyright line © [Year of original publication] IEEE appear prominently with each reprinted figure and/or table.
3) If a substantial portion of the original paper is to be used, and if you are not the senior author, also obtain the senior author's approval.

Requirements to be followed when using an entire IEEE copyrighted paper in a thesis:

1) The following IEEE copyright/ credit notice should be placed prominently in the references: © [year of original publication] IEEE. Reprinted, with permission, from [author names, paper title, IEEE publication title, and month/year of publication]
2) Only the accepted version of an IEEE copyrighted paper can be used when posting the paper or your thesis on-line.
3) In placing the thesis on the author's university website, please display the following message in a prominent place on the website: In reference to IEEE copyrighted material which is used with permission in this thesis, the IEEE does not endorse any of [university/educational entity's name goes here]'s products or services. Internal or personal use of this material is permitted. If interested in reprinting/republishing IEEE copyrighted material for advertising or promotional purposes or for creating new collective works for resale or redistribution, please go to http://www.ieee.org/publications_standards/publications/rights/rights_link.html to learn how to obtain a License from RightsLink.

If applicable, University Microfilms and/or ProQuest Library, or the Archives of Canada may supply single copies of the dissertation.

BACK CLOSE WINDOW

SPRINGER LICENSE
TERMS AND CONDITIONS

Nov 07, 2017

This Agreement between Mr. Abdullah Alomari ("You") and Springer ("Springer") consists of your license details and the terms and conditions provided by Springer and Copyright Clearance Center.

License Number	4223951079012
License date	Nov 07, 2017
Licensed Content Publisher	Springer
Licensed Content Publication	Wireless Networks
Licensed Content Title	New path planning model for mobile anchor-assisted localization in wireless sensor networks
Licensed Content Author	Abdullah Alomari, Frank Comeau, William Phillips et al
Licensed Content Date	Jan 1, 2017
Type of Use	Thesis/Dissertation
Portion	Full text
Number of copies	1
Author of this Springer article	Yes and you are the sole author of the new work
Order reference number	
Title of your thesis / dissertation	Path planning models for mobile anchor-assisted localization in wireless sensor networks
Expected completion date	Feb 2018
Estimated size(pages)	180
Requestor Location	Mr. Abdullah Alomari 302-650 Washmill Lake Drive Halifax, NS B3S0H8 Canada Attn: Mr. Abdullah Alomari
Billing Type	Invoice
Billing Address	Mr. Abdullah Alomari 302-650 Washmill Lake Drive Halifax, NS B3S0H8 Canada Attn: Mr. Abdullah Alomari
Total	0.00 CAD
Terms and Conditions	

Introduction
The publisher for this copyrighted material is Springer. By clicking "accept" in connection with completing this licensing transaction, you agree that the following terms and conditions apply to this transaction (along with the Billing and Payment terms and conditions

established by Copyright Clearance Center, Inc. ("CCC"), at the time that you opened your Rightslink account and that are available at any time at http://myaccount.copyright.com).

Limited License

With reference to your request to reuse material on which Springer controls the copyright, permission is granted for the use indicated in your enquiry under the following conditions:

- Licenses are for one-time use only with a maximum distribution equal to the number stated in your request.
- Springer material represents original material which does not carry references to other sources. If the material in question appears with a credit to another source, this permission is not valid and authorization has to be obtained from the original copyright holder.
- This permission
• is non-exclusive
• is only valid if no personal rights, trademarks, or competitive products are infringed.
• explicitly excludes the right for derivatives.
- Springer does not supply original artwork or content.
- According to the format which you have selected, the following conditions apply accordingly:
• **Print and Electronic:** This License include use in electronic form provided it is password protected, on intranet, or CD-Rom/DVD or E-book/E-journal. It may not be republished in electronic open access.
• **Print:** This License excludes use in electronic form.
• **Electronic:** This License only pertains to use in electronic form provided it is password protected, on intranet, or CD-Rom/DVD or E-book/E-journal. It may not be republished in electronic open access.

For any electronic use not mentioned, please contact Springer at permissions.springer@spi-global.com.

- Although Springer controls the copyright to the material and is entitled to negotiate on rights, this license is only valid subject to courtesy information to the author (address is given in the article/chapter).
- If you are an STM Signatory or your work will be published by an STM Signatory and you are requesting to reuse figures/tables/illustrations or single text extracts, permission is granted according to STM Permissions Guidelines: http://www.stm-assoc.org/permissions-guidelines/

For any electronic use not mentioned in the Guidelines, please contact Springer at permissions.springer@spi-global.com. If you request to reuse more content than stipulated in the STM Permissions Guidelines, you will be charged a permission fee for the excess content.

Permission is valid upon payment of the fee as indicated in the licensing process. If permission is granted free of charge on this occasion, that does not prejudice any rights we might have to charge for reproduction of our copyrighted material in the future.

-If your request is for reuse in a Thesis, permission is granted free of charge under the following conditions:

This license is valid for one-time use only for the purpose of defending your thesis and with a maximum of 100 extra copies in paper. If the thesis is going to be published, permission needs to be reobtained.

- includes use in an electronic form, provided it is an author-created version of the thesis on his/her own website and his/her university's repository, including UMI (according to the definition on the Sherpa website: http://www.sherpa.ac.uk/romeo/);
- is subject to courtesy information to the co-author or corresponding author.

Geographic Rights: Scope

Licenses may be exercised anywhere in the world.

Altering/Modifying Material: Not Permitted

Figures, tables, and illustrations may be altered minimally to serve your work. You may not

alter or modify text in any manner. Abbreviations, additions, deletions and/or any other alterations shall be made only with prior written authorization of the author(s).

Reservation of Rights

Springer reserves all rights not specifically granted in the combination of (i) the license details provided by you and accepted in the course of this licensing transaction and (ii) these terms and conditions and (iii) CCC's Billing and Payment terms and conditions.

License Contingent on Payment

While you may exercise the rights licensed immediately upon issuance of the license at the end of the licensing process for the transaction, provided that you have disclosed complete and accurate details of your proposed use, no license is finally effective unless and until full payment is received from you (either by Springer or by CCC) as provided in CCC's Billing and Payment terms and conditions. If full payment is not received by the date due, then any license preliminarily granted shall be deemed automatically revoked and shall be void as if never granted. Further, in the event that you breach any of these terms and conditions or any of CCC's Billing and Payment terms and conditions, the license is automatically revoked and shall be void as if never granted. Use of materials as described in a revoked license, as well as any use of the materials beyond the scope of an unrevoked license, may constitute copyright infringement and Springer reserves the right to take any and all action to protect its copyright in the materials.

Copyright Notice: Disclaimer

You must include the following copyright and permission notice in connection with any reproduction of the licensed material:

"Springer book/journal title, chapter/article title, volume, year of publication, page, name(s) of author(s), (original copyright notice as given in the publication in which the material was originally published) "With permission of Springer"

In case of use of a graph or illustration, the caption of the graph or illustration must be included, as it is indicated in the original publication.

Warranties: None

Springer makes no representations or warranties with respect to the licensed material and adopts on its own behalf the limitations and disclaimers established by CCC on its behalf in its Billing and Payment terms and conditions for this licensing transaction.

Indemnity

You hereby indemnify and agree to hold harmless Springer and CCC, and their respective officers, directors, employees and agents, from and against any and all claims arising out of your use of the licensed material other than as specifically authorized pursuant to this license.

No Transfer of License

This license is personal to you and may not be sublicensed, assigned, or transferred by you without Springer's written permission.

No Amendment Except in Writing

This license may not be amended except in a writing signed by both parties (or, in the case of Springer, by CCC on Springer's behalf).

Objection to Contrary Terms

Springer hereby objects to any terms contained in any purchase order, acknowledgment, check endorsement or other writing prepared by you, which terms are inconsistent with these terms and conditions or CCC's Billing and Payment terms and conditions. These terms and conditions, together with CCC's Billing and Payment terms and conditions (which are incorporated herein), comprise the entire agreement between you and Springer (and CCC) concerning this licensing transaction. In the event of any conflict between your obligations established by these terms and conditions and those established by CCC's Billing and Payment terms and conditions, these terms and conditions shall control.

Jurisdiction

All disputes that may arise in connection with this present License, or the breach thereof,

shall be settled exclusively by arbitration, to be held in the Federal Republic of Germany, in accordance with German law.

Other conditions:

V 12AUG2015

ELSEVIER LICENSE
TERMS AND CONDITIONS

Nov 21, 2017

This Agreement between Mr. Abdullah Alomari ("You") and Elsevier ("Elsevier") consists of your license details and the terms and conditions provided by Elsevier and Copyright Clearance Center.

License Number	4233960457644
License date	Nov 21, 2017
Licensed Content Publisher	Elsevier
Licensed Content Publication	Journal of Network and Computer Applications
Licensed Content Title	A survey on mobility-assisted localization techniques in wireless sensor networks
Licensed Content Author	Subir Halder,Amrita Ghosal
Licensed Content Date	Jan 1, 2016
Licensed Content Volume	60
Licensed Content Issue	n/a
Licensed Content Pages	13
Start Page	82
End Page	94
Type of Use	reuse in a thesis/dissertation
Portion	figures/tables/illustrations
Number of figures/tables/illustrations	2
Format	electronic
Are you the author of this Elsevier article?	No
Will you be translating?	No
Original figure numbers	Figures 2 and 3
Title of your thesis/dissertation	Path planning models for mobile anchor-assisted localization in wireless sensor networks
Expected completion date	Feb 2018
Estimated size (number of pages)	180
Requestor Location	Mr. Abdullah Alomari 302-650 Washmill Lake Drive Halifax, NS B3S0H8 Canada Attn: Mr. Abdullah Alomari
Total	0.00 CAD
Terms and Conditions	

INTRODUCTION

1. The publisher for this copyrighted material is Elsevier. By clicking "accept" in connection with completing this licensing transaction, you agree that the following terms and conditions apply to this transaction (along with the Billing and Payment terms and conditions established by Copyright Clearance Center, Inc. ("CCC"), at the time that you opened your Rightslink account and that are available at any time at http://myaccount.copyright.com).

GENERAL TERMS

2. Elsevier hereby grants you permission to reproduce the aforementioned material subject to the terms and conditions indicated.
3. Acknowledgement: If any part of the material to be used (for example, figures) has appeared in our publication with credit or acknowledgement to another source, permission must also be sought from that source. If such permission is not obtained then that material may not be included in your publication/copies. Suitable acknowledgement to the source must be made, either as a footnote or in a reference list at the end of your publication, as follows:
"Reprinted from Publication title, Vol /edition number, Author(s), Title of article / title of chapter, Pages No., Copyright (Year), with permission from Elsevier [OR APPLICABLE SOCIETY COPYRIGHT OWNER]." Also Lancet special credit - "Reprinted from The Lancet, Vol. number, Author(s), Title of article, Pages No., Copyright (Year), with permission from Elsevier."
4. Reproduction of this material is confined to the purpose and/or media for which permission is hereby given.
5. Altering/Modifying Material: Not Permitted. However figures and illustrations may be altered/adapted minimally to serve your work. Any other abbreviations, additions, deletions and/or any other alterations shall be made only with prior written authorization of Elsevier Ltd. (Please contact Elsevier at permissions@elsevier.com). No modifications can be made to any Lancet figures/tables and they must be reproduced in full.
6. If the permission fee for the requested use of our material is waived in this instance, please be advised that your future requests for Elsevier materials may attract a fee.
7. Reservation of Rights: Publisher reserves all rights not specifically granted in the combination of (i) the license details provided by you and accepted in the course of this licensing transaction, (ii) these terms and conditions and (iii) CCC's Billing and Payment terms and conditions.
8. License Contingent Upon Payment: While you may exercise the rights licensed immediately upon issuance of the license at the end of the licensing process for the transaction, provided that you have disclosed complete and accurate details of your proposed use, no license is finally effective unless and until full payment is received from you (either by publisher or by CCC) as provided in CCC's Billing and Payment terms and conditions. If full payment is not received on a timely basis, then any license preliminarily granted shall be deemed automatically revoked and shall be void as if never granted. Further, in the event that you breach any of these terms and conditions or any of CCC's Billing and Payment terms and conditions, the license is automatically revoked and shall be void as if never granted. Use of materials as described in a revoked license, as well as any use of the materials beyond the scope of an unrevoked license, may constitute copyright infringement and publisher reserves the right to take any and all action to protect its copyright in the materials.
9. Warranties: Publisher makes no representations or warranties with respect to the licensed material.
10. Indemnity: You hereby indemnify and agree to hold harmless publisher and CCC, and their respective officers, directors, employees and agents, from and against any and all claims arising out of your use of the licensed material other than as specifically authorized pursuant to this license.
11. No Transfer of License: This license is personal to you and may not be sublicensed, assigned, or transferred by you to any other person without publisher's written permission.

12. No Amendment Except in Writing: This license may not be amended except in a writing signed by both parties (or, in the case of publisher, by CCC on publisher's behalf).
13. Objection to Contrary Terms: Publisher hereby objects to any terms contained in any purchase order, acknowledgment, check endorsement or other writing prepared by you, which terms are inconsistent with these terms and conditions or CCC's Billing and Payment terms and conditions. These terms and conditions, together with CCC's Billing and Payment terms and conditions (which are incorporated herein), comprise the entire agreement between you and publisher (and CCC) concerning this licensing transaction. In the event of any conflict between your obligations established by these terms and conditions and those established by CCC's Billing and Payment terms and conditions, these terms and conditions shall control.
14. Revocation: Elsevier or Copyright Clearance Center may deny the permissions described in this License at their sole discretion, for any reason or no reason, with a full refund payable to you. Notice of such denial will be made using the contact information provided by you. Failure to receive such notice will not alter or invalidate the denial. In no event will Elsevier or Copyright Clearance Center be responsible or liable for any costs, expenses or damage incurred by you as a result of a denial of your permission request, other than a refund of the amount(s) paid by you to Elsevier and/or Copyright Clearance Center for denied permissions.

LIMITED LICENSE

The following terms and conditions apply only to specific license types:
15. **Translation**: This permission is granted for non-exclusive world **English** rights only unless your license was granted for translation rights. If you licensed translation rights you may only translate this content into the languages you requested. A professional translator must perform all translations and reproduce the content word for word preserving the integrity of the article.
16. **Posting licensed content on any Website**: The following terms and conditions apply as follows: Licensing material from an Elsevier journal: All content posted to the web site must maintain the copyright information line on the bottom of each image; A hyper-text must be included to the Homepage of the journal from which you are licensing at http://www.sciencedirect.com/science/journal/xxxxx or the Elsevier homepage for books at http://www.elsevier.com; Central Storage: This license does not include permission for a scanned version of the material to be stored in a central repository such as that provided by Heron/XanEdu.
Licensing material from an Elsevier book: A hyper-text link must be included to the Elsevier homepage at http://www.elsevier.com . All content posted to the web site must maintain the copyright information line on the bottom of each image.

Posting licensed content on Electronic reserve: In addition to the above the following clauses are applicable: The web site must be password-protected and made available only to bona fide students registered on a relevant course. This permission is granted for 1 year only. You may obtain a new license for future website posting.
17. **For journal authors:** the following clauses are applicable in addition to the above:
Preprints:
A preprint is an author's own write-up of research results and analysis, it has not been peer-reviewed, nor has it had any other value added to it by a publisher (such as formatting, copyright, technical enhancement etc.).
Authors can share their preprints anywhere at any time. Preprints should not be added to or enhanced in any way in order to appear more like, or to substitute for, the final versions of articles however authors can update their preprints on arXiv or RePEc with their Accepted Author Manuscript (see below).
If accepted for publication, we encourage authors to link from the preprint to their formal publication via its DOI. Millions of researchers have access to the formal publications on ScienceDirect, and so links will help users to find, access, cite and use the best available

version. Please note that Cell Press, The Lancet and some society-owned have different preprint policies. Information on these policies is available on the journal homepage.
Accepted Author Manuscripts: An accepted author manuscript is the manuscript of an article that has been accepted for publication and which typically includes author-incorporated changes suggested during submission, peer review and editor-author communications.
Authors can share their accepted author manuscript:

- immediately
  - via their non-commercial person homepage or blog
  - by updating a preprint in arXiv or RePEc with the accepted manuscript
  - via their research institute or institutional repository for internal institutional uses or as part of an invitation-only research collaboration work-group
  - directly by providing copies to their students or to research collaborators for their personal use
  - for private scholarly sharing as part of an invitation-only work group on commercial sites with which Elsevier has an agreement
- After the embargo period
  - via non-commercial hosting platforms such as their institutional repository
  - via commercial sites with which Elsevier has an agreement

In all cases accepted manuscripts should:

- link to the formal publication via its DOI
- bear a CC-BY-NC-ND license - this is easy to do
- if aggregated with other manuscripts, for example in a repository or other site, be shared in alignment with our hosting policy not be added to or enhanced in any way to appear more like, or to substitute for, the published journal article.

Published journal article (JPA): A published journal article (PJA) is the definitive final record of published research that appears or will appear in the journal and embodies all value-adding publishing activities including peer review co-ordination, copy-editing, formatting, (if relevant) pagination and online enrichment.
Policies for sharing publishing journal articles differ for subscription and gold open access articles:
Subscription Articles: If you are an author, please share a link to your article rather than the full-text. Millions of researchers have access to the formal publications on ScienceDirect, and so links will help your users to find, access, cite, and use the best available version.
Theses and dissertations which contain embedded PJAs as part of the formal submission can be posted publicly by the awarding institution with DOI links back to the formal publications on ScienceDirect.
If you are affiliated with a library that subscribes to ScienceDirect you have additional private sharing rights for others' research accessed under that agreement. This includes use for classroom teaching and internal training at the institution (including use in course packs and courseware programs), and inclusion of the article for grant funding purposes.
Gold Open Access Articles: May be shared according to the author-selected end-user license and should contain a CrossMark logo, the end user license, and a DOI link to the formal publication on ScienceDirect.
Please refer to Elsevier's posting policy for further information.
18. **For book authors** the following clauses are applicable in addition to the above:
Authors are permitted to place a brief summary of their work online only. You are not allowed to download and post the published electronic version of your chapter, nor may you scan the printed edition to create an electronic version. **Posting to a repository:** Authors are permitted to post a summary of their chapter only in their institution's repository.

19. **Thesis/Dissertation**: If your license is for use in a thesis/dissertation your thesis may be submitted to your institution in either print or electronic form. Should your thesis be published commercially, please reapply for permission. These requirements include permission for the Library and Archives of Canada to supply single copies, on demand, of the complete thesis and include permission for Proquest/UMI to supply single copies, on demand, of the complete thesis. Should your thesis be published commercially, please reapply for permission. Theses and dissertations which contain embedded PJAs as part of the formal submission can be posted publicly by the awarding institution with DOI links back to the formal publications on ScienceDirect.

Elsevier Open Access Terms and Conditions

You can publish open access with Elsevier in hundreds of open access journals or in nearly 2000 established subscription journals that support open access publishing. Permitted third party re-use of these open access articles is defined by the author's choice of Creative Commons user license. See our open access license policy for more information.

Terms & Conditions applicable to all Open Access articles published with Elsevier:

Any reuse of the article must not represent the author as endorsing the adaptation of the article nor should the article be modified in such a way as to damage the author's honour or reputation. If any changes have been made, such changes must be clearly indicated.

The author(s) must be appropriately credited and we ask that you include the end user license and a DOI link to the formal publication on ScienceDirect.

If any part of the material to be used (for example, figures) has appeared in our publication with credit or acknowledgement to another source it is the responsibility of the user to ensure their reuse complies with the terms and conditions determined by the rights holder.

Additional Terms & Conditions applicable to each Creative Commons user license:

CC BY: The CC-BY license allows users to copy, to create extracts, abstracts and new works from the Article, to alter and revise the Article and to make commercial use of the Article (including reuse and/or resale of the Article by commercial entities), provided the user gives appropriate credit (with a link to the formal publication through the relevant DOI), provides a link to the license, indicates if changes were made and the licensor is not represented as endorsing the use made of the work. The full details of the license are available at http://creativecommons.org/licenses/by/4.0.

CC BY NC SA: The CC BY-NC-SA license allows users to copy, to create extracts, abstracts and new works from the Article, to alter and revise the Article, provided this is not done for commercial purposes, and that the user gives appropriate credit (with a link to the formal publication through the relevant DOI), provides a link to the license, indicates if changes were made and the licensor is not represented as endorsing the use made of the work. Further, any new works must be made available on the same conditions. The full details of the license are available at http://creativecommons.org/licenses/by-nc-sa/4.0.

CC BY NC ND: The CC BY-NC-ND license allows users to copy and distribute the Article, provided this is not done for commercial purposes and further does not permit distribution of the Article if it is changed or edited in any way, and provided the user gives appropriate credit (with a link to the formal publication through the relevant DOI), provides a link to the license, and that the licensor is not represented as endorsing the use made of the work. The full details of the license are available at http://creativecommons.org/licenses/by-nc-nd/4.0.

Any commercial reuse of Open Access articles published with a CC BY NC SA or CC BY NC ND license requires permission from Elsevier and will be subject to a fee.

Commercial reuse includes:

- Associating advertising with the full text of the Article
- Charging fees for document delivery or access
- Article aggregation
- Systematic distribution via e-mail lists or share buttons

Posting or linking by commercial companies for use by customers of those companies.

20. **Other Conditions**:

v1.9

Questions? customercare@copyright.com or +1-855-239-3415 (toll free in the US) or +1-978-646-2777.

JOHN WILEY AND SONS LICENSE TERMS AND CONDITIONS

Nov 23, 2017

This Agreement between Mr. Abdullah Alomari ("You") and John Wiley and Sons ("John Wiley and Sons") consists of your license details and the terms and conditions provided by John Wiley and Sons and Copyright Clearance Center.

License Number	4235030060040
License date	Nov 23, 2017
Licensed Content Publisher	John Wiley and Sons
Licensed Content Publication	Wiley Books
Licensed Content Title	Protocols and Architectures for Wireless Sensor Networks
Licensed Content Author	Holger Karl, Andreas Willig
Licensed Content Date	May 1, 2005
Licensed Content Pages	526
Type of use	Dissertation/Thesis
Requestor type	University/Academic
Format	Print and electronic
Portion	Figure/table
Number of figures/tables	2
Original Wiley figure/table number(s)	Figures 9.2 and 9.4
Will you be translating?	No
Title of your thesis / dissertation	Path planning models for mobile anchor-assisted localization in wireless sensor networks
Expected completion date	Feb 2018
Expected size (number of pages)	180
Requestor Location	Mr. Abdullah Alomari 302-650 Washmill Lake Drive Halifax, NS B3S0H8 Canada Attn: Mr. Abdullah Alomari
Publisher Tax ID	EU826007151
Billing Type	Invoice
Billing Address	Mr. Abdullah Alomari 302-650 Washmill Lake Drive Halifax, NS B3S0H8 Canada Attn: Mr. Abdullah Alomari
Total	0.00 CAD
Terms and Conditions	

TERMS AND CONDITIONS

This copyrighted material is owned by or exclusively licensed to John Wiley & Sons, Inc. or one of its group companies (each a"Wiley Company") or handled on behalf of a society with which a Wiley Company has exclusive publishing rights in relation to a particular work (collectively "WILEY"). By clicking "accept" in connection with completing this licensing transaction, you agree that the following terms and conditions apply to this transaction (along with the billing and payment terms and conditions established by the Copyright Clearance Center Inc., ("CCC's Billing and Payment terms and conditions"), at the time that you opened your RightsLink account (these are available at any time at http://myaccount.copyright.com).

Terms and Conditions

- The materials you have requested permission to reproduce or reuse (the "Wiley Materials") are protected by copyright.

- You are hereby granted a personal, non-exclusive, non-sub licensable (on a stand-alone basis), non-transferable, worldwide, limited license to reproduce the Wiley Materials for the purpose specified in the licensing process. This license, **and any CONTENT (PDF or image file) purchased as part of your order,** is for a one-time use only and limited to any maximum distribution number specified in the license. The first instance of republication or reuse granted by this license must be completed within two years of the date of the grant of this license (although copies prepared before the end date may be distributed thereafter). The Wiley Materials shall not be used in any other manner or for any other purpose, beyond what is granted in the license. Permission is granted subject to an appropriate acknowledgement given to the author, title of the material/book/journal and the publisher. You shall also duplicate the copyright notice that appears in the Wiley publication in your use of the Wiley Material. Permission is also granted on the understanding that nowhere in the text is a previously published source acknowledged for all or part of this Wiley Material. Any third party content is expressly excluded from this permission.

- With respect to the Wiley Materials, all rights are reserved. Except as expressly granted by the terms of the license, no part of the Wiley Materials may be copied, modified, adapted (except for minor reformatting required by the new Publication), translated, reproduced, transferred or distributed, in any form or by any means, and no derivative works may be made based on the Wiley Materials without the prior permission of the respective copyright owner.**For STM Signatory Publishers clearing permission under the terms of the STM Permissions Guidelines only, the terms of the license are extended to include subsequent editions and for editions in other languages, provided such editions are for the work as a whole in situ and does not involve the separate exploitation of the permitted figures or extracts,** You may not alter, remove or suppress in any manner any copyright, trademark or other notices displayed by the Wiley Materials. You may not license, rent, sell, loan, lease, pledge, offer as security, transfer or assign the Wiley Materials on a stand-alone basis, or any of the rights granted to you hereunder to any other person.

- The Wiley Materials and all of the intellectual property rights therein shall at all times remain the exclusive property of John Wiley & Sons Inc, the Wiley Companies, or their respective licensors, and your interest therein is only that of having possession of and the right to reproduce the Wiley Materials pursuant to Section 2 herein during the continuance of this Agreement. You agree that you own no right, title or interest in or to the Wiley Materials or any of the intellectual property rights therein. You shall have no rights hereunder other than the license as provided for above in Section 2. No right,

license or interest to any trademark, trade name, service mark or other branding ("Marks") of WILEY or its licensors is granted hereunder, and you agree that you shall not assert any such right, license or interest with respect thereto

- NEITHER WILEY NOR ITS LICENSORS MAKES ANY WARRANTY OR REPRESENTATION OF ANY KIND TO YOU OR ANY THIRD PARTY, EXPRESS, IMPLIED OR STATUTORY, WITH RESPECT TO THE MATERIALS OR THE ACCURACY OF ANY INFORMATION CONTAINED IN THE MATERIALS, INCLUDING, WITHOUT LIMITATION, ANY IMPLIED WARRANTY OF MERCHANTABILITY, ACCURACY, SATISFACTORY QUALITY, FITNESS FOR A PARTICULAR PURPOSE, USABILITY, INTEGRATION OR NON-INFRINGEMENT AND ALL SUCH WARRANTIES ARE HEREBY EXCLUDED BY WILEY AND ITS LICENSORS AND WAIVED BY YOU.

- WILEY shall have the right to terminate this Agreement immediately upon breach of this Agreement by you.

- You shall indemnify, defend and hold harmless WILEY, its Licensors and their respective directors, officers, agents and employees, from and against any actual or threatened claims, demands, causes of action or proceedings arising from any breach of this Agreement by you.

- IN NO EVENT SHALL WILEY OR ITS LICENSORS BE LIABLE TO YOU OR ANY OTHER PARTY OR ANY OTHER PERSON OR ENTITY FOR ANY SPECIAL, CONSEQUENTIAL, INCIDENTAL, INDIRECT, EXEMPLARY OR PUNITIVE DAMAGES, HOWEVER CAUSED, ARISING OUT OF OR IN CONNECTION WITH THE DOWNLOADING, PROVISIONING, VIEWING OR USE OF THE MATERIALS REGARDLESS OF THE FORM OF ACTION, WHETHER FOR BREACH OF CONTRACT, BREACH OF WARRANTY, TORT, NEGLIGENCE, INFRINGEMENT OR OTHERWISE (INCLUDING, WITHOUT LIMITATION, DAMAGES BASED ON LOSS OF PROFITS, DATA, FILES, USE, BUSINESS OPPORTUNITY OR CLAIMS OF THIRD PARTIES), AND WHETHER OR NOT THE PARTY HAS BEEN ADVISED OF THE POSSIBILITY OF SUCH DAMAGES. THIS LIMITATION SHALL APPLY NOTWITHSTANDING ANY FAILURE OF ESSENTIAL PURPOSE OF ANY LIMITED REMEDY PROVIDED HEREIN.

- Should any provision of this Agreement be held by a court of competent jurisdiction to be illegal, invalid, or unenforceable, that provision shall be deemed amended to achieve as nearly as possible the same economic effect as the original provision, and the legality, validity and enforceability of the remaining provisions of this Agreement shall not be affected or impaired thereby.

- The failure of either party to enforce any term or condition of this Agreement shall not constitute a waiver of either party's right to enforce each and every term and condition of this Agreement. No breach under this agreement shall be deemed waived or excused by either party unless such waiver or consent is in writing signed by the party granting such waiver or consent. The waiver by or consent of a party to a breach of any provision of this Agreement shall not operate or be construed as a waiver of or consent to any other or subsequent breach by such other party.

- This Agreement may not be assigned (including by operation of law or otherwise) by you without WILEY's prior written consent.

- Any fee required for this permission shall be non-refundable after thirty (30) days from receipt by the CCC.

- These terms and conditions together with CCC's Billing and Payment terms and conditions (which are incorporated herein) form the entire agreement between you and WILEY concerning this licensing transaction and (in the absence of fraud) supersedes all prior agreements and representations of the parties, oral or written. This Agreement may not be amended except in writing signed by both parties. This Agreement shall be binding upon and inure to the benefit of the parties' successors, legal representatives, and authorized assigns.

- In the event of any conflict between your obligations established by these terms and conditions and those established by CCC's Billing and Payment terms and conditions, these terms and conditions shall prevail.

- WILEY expressly reserves all rights not specifically granted in the combination of (i) the license details provided by you and accepted in the course of this licensing transaction, (ii) these terms and conditions and (iii) CCC's Billing and Payment terms and conditions.

- This Agreement will be void if the Type of Use, Format, Circulation, or Requestor Type was misrepresented during the licensing process.

- This Agreement shall be governed by and construed in accordance with the laws of the State of New York, USA, without regards to such state's conflict of law rules. Any legal action, suit or proceeding arising out of or relating to these Terms and Conditions or the breach thereof shall be instituted in a court of competent jurisdiction in New York County in the State of New York in the United States of America and each party hereby consents and submits to the personal jurisdiction of such court, waives any objection to venue in such court and consents to service of process by registered or certified mail, return receipt requested, at the last known address of such party.

WILEY OPEN ACCESS TERMS AND CONDITIONS

Wiley Publishes Open Access Articles in fully Open Access Journals and in Subscription journals offering Online Open. Although most of the fully Open Access journals publish open access articles under the terms of the Creative Commons Attribution (CC BY) License only, the subscription journals and a few of the Open Access Journals offer a choice of Creative Commons Licenses. The license type is clearly identified on the article.

The Creative Commons Attribution License

The Creative Commons Attribution License (CC-BY) allows users to copy, distribute and transmit an article, adapt the article and make commercial use of the article. The CC-BY license permits commercial and non-

Creative Commons Attribution Non-Commercial License

The Creative Commons Attribution Non-Commercial (CC-BY-NC)License permits use, distribution and reproduction in any medium, provided the original work is properly cited and is not used for commercial purposes.(see below)

Creative Commons Attribution-Non-Commercial-NoDerivs License

The Creative Commons Attribution Non-Commercial-NoDerivs License (CC-BY-NC-ND) permits use, distribution and reproduction in any medium, provided the original work is properly cited, is not used for commercial purposes and no modifications or adaptations are made. (see below)

Use by commercial "for-profit" organizations
Use of Wiley Open Access articles for commercial, promotional, or marketing purposes requires further explicit permission from Wiley and will be subject to a fee.
Further details can be found on Wiley Online Library
http://olabout.wiley.com/WileyCDA/Section/id-410895.html

Other Terms and Conditions:

v1.10 Last updated September 2015

Questions? customercare@copyright.com or +1-855-239-3415 (toll free in the US) or +1-978-646-2777.

Title: Swarm Intelligence Optimization Techniques for Obstacle-Avoidance Mobility-Assisted Localization in Wireless Sensor Networks

Author: Abdullah Alomari

Publication: IEEE Access

Publisher: IEEE

Date: Dec 31, 1969

Thesis / Dissertation Reuse

The IEEE does not require individuals working on a thesis to obtain a formal reuse license, however, you may print out this statement to be used as a permission grant:

Requirements to be followed when using any portion (e.g., figure, graph, table, or textual material) of an IEEE copyrighted paper in a thesis:

1) In the case of textual material (e.g., using short quotes or referring to the work within these papers) users must give full credit to the original source (author, paper, publication) followed by the IEEE copyright line © 2011 IEEE.
2) In the case of illustrations or tabular material, we require that the copyright line © [Year of original publication] IEEE appear prominently with each reprinted figure and/or table.
3) If a substantial portion of the original paper is to be used, and if you are not the senior author, also obtain the senior author's approval.

Requirements to be followed when using an entire IEEE copyrighted paper in a thesis:

1) The following IEEE copyright/ credit notice should be placed prominently in the references: © [year of original publication] IEEE. Reprinted, with permission, from [author names, paper title, IEEE publication title, and month/year of publication]
2) Only the accepted version of an IEEE copyrighted paper can be used when posting the paper or your thesis on-line.
3) In placing the thesis on the author's university website, please display the following message in a prominent place on the website: In reference to IEEE copyrighted material which is used with permission in this thesis, the IEEE does not endorse any of [university/educational entity's name goes here]'s products or services. Internal or personal use of this material is permitted. If interested in reprinting/republishing IEEE copyrighted material for advertising or promotional purposes or for creating new collective works for resale or redistribution, please go to http://www.ieee.org/publications_standards/publications/rights/rights_link.html to learn how to obtain a License from RightsLink.

If applicable, University Microfilms and/or ProQuest Library, or the Archives of Canada may supply single copies of the dissertation.

BACK CLOSE WINDOW